

I

THE CRYSTAL STRUCTURE OF OXAMIDE

II

THE CRYSTAL STRUCTURE OF
15,15'-DEHYDRO- β -CAROTENE

Thesis by

William Glenn Sly

In Partial Fulfillment of the Requirements
for the Degree of
Doctor of Philosophy

California Institute of Technology
Pasadena, California

1955

ACKNOWLEDGEMENTS

The author wishes to express his appreciation to Professor J. H. Sturdivant, who directed the work described in this thesis, for his continued interest, encouragement, and helpful criticism throughout; to Professor Verner Schomaker and Dr. Richard E. Marsh for helpful discussions; to Professor H. H. Inhoffen and Professor L. Zechmeister for the sample of 15,15'-dehydro- β -carotene; to Dr. Sheldon C. Crane for his help with the X-ray equipment and the cold-room; to Mrs. L. Hendrix and Mrs. M. Thompson for the preparation of some of the drawings; to the California Institute of Technology, the Dupont Company, and the National Science Foundation for generous fellowships; and finally to all of the many professors, students, and other friends too numerous to mention who have made the years at the California Institute both pleasant and rewarding.

ABSTRACT

I

A two-dimensional trial structure has been determined for oxamide by means of a Patterson projection. The analysis, which was the reinvestigation of a previous preliminary survey that had reported a slightly wavy planar structure with a 1.65 Å. C-C bond, was interrupted by the publication of an apparently satisfactory structure by Romers. The present study and two recent publications are in agreement both as to the parameters and space group of the triclinic unit cell, and the configuration of the molecule. The oxamide molecules are centered and they are hydrogen bonded into an essentially planar sheet which is parallel to the almost perfect cleavage plane exhibited by the crystals. The dimensions indicate that the C-C bond is a pure single bond and that the C-N bond has about 50% double-bond character as a result of resonance in the amide group. Oxamide, like oxalic acid and a few other related substances, is planar although the C-C bond apparently has no double-bond character.

II

The crystal structure of 15,15'-dehydro- β -carotene has been determined; this analysis represents the first conclu-

sive study of any carotenoid. The analysis was accomplished through the use of a three-dimensional Patterson coupled with trial and error methods, and has been carried to a moderate state of refinement with Fourier projections, two-dimensional least squares, and a three-dimensional Fourier. The monoclinic unit cell has the parameters $a_1 = 8.145 \text{ \AA.}$, $a_2 = 31.87 \text{ \AA.}$, $a_3 = 8.465 \text{ \AA.}$, and $\alpha_2 = 128^\circ 18.8'$; the space group is uniquely determined to be $C_{2h}^5 - P2_1/c$, which requires that the two molecules in the unit cell be centered. Except for the cyclohexene rings, the molecule is essentially plane with bond lengths and angles in general agreement with those predicted by theory and experiment. The chains are packed together almost unaffected by the cyclohexene rings. Each ring has the cis orientation about the single bond from ring to chain; the molecule is otherwise all trans. The molecules are efficiently packed, but the arrangement has resulted in a loss of resonance energy since the rings are not coplanar with the chain. The hypersymmetry of the molecules accounts for the deviation of the intensities from a normal statistical distribution.

A brief discussion of some of the IBM techniques used in the refinement of this structure has been included in the appendix.

TABLE OF CONTENTS

I.	THE CRYSTAL STRUCTURE OF OXAMIDE	
A.	Introduction	1
B.	The Determination of the Structure . . .	5
C.	The Description of the Structure	19
II.	THE CRYSTAL STRUCTURE OF 15,15'-DEHYDRO- β -CAROTENE	
A.	Introduction	29
B.	Preliminary Investigation	41
C.	The Collection and Correlation of Three-Dimensional Data	52
D.	The Three-Dimensional Patterson Function	65
E.	The Solution of a Projection of the Structure and Its Refinement	77
F.	Three-Dimensional Refinement	86
G.	Description of the Structure	95
H.	Discussion of the Structure	113
I.	Appendix I--Structure Factor Data . . .	134
J.	Appendix II--IBM Calculations	184
III.	REFERENCES	190
IV.	PROPOSITIONS	201

I

THE CRYSTAL STRUCTURE OF
OXAMIDE

A. Introduction

The molecular and crystal structures of oxamide have attracted the interest of structural chemists to such an extent that four independent crystal structure determinations have now been reported. The first of these, by van der Wyk and Misch (1), is incorrect. The second, published only as a preliminary report by Romers (2), interrupted the concurrent work which is described in this section of the present thesis. The fourth and most complete report was published by Ayerst and Duke (3). The last three determinations, and particularly the last two, agree well.

The interest in oxamide is stimulated by a number of factors. The unusually high melting point, $417-9^{\circ}\text{C.}$, and relatively high density, 1.667 gm./cm.^3 , indicate a compact structure which is strongly hydrogen bonded. A comparison with the somewhat anomalous structures of oxalic acid proves informative. The α and β forms of anhydrous oxalic acid (4,5) and oxalic acid dihydrate (6) were found to be planar with no apparent conjugation across the C-C bond. The carbon-carbon bonds of lengths 1.560 \AA. , 1.59 \AA. (not an accurate determination by present day standards), and 1.529 \AA. , found in the α anhydrous,

anhydrous, and dihydrated oxalic acids, respectively, are all seemingly single bonds. The space groups of these crystals require centered and hence planar molecules, although the bond system does not restrict the rotation of the carboxyl groups. The oxalate ion, on the other hand, as found in ammonium oxalate (7) is not planar. The planes of the COO^- groups make an angle of 28 degrees. The C-C bond of 1.56 Å. is, within limits of error, a single bond, and free rotation is expected. The planarity of oxalic acid in its three crystalline forms and of other molecules containing similar groups of atoms has been discussed by Cox, Dougill, and Jeffrey (4) and has been cited by Jeffrey and Parry (8) as evidence for intramolecular electrostatic attraction between hydroxyl and carbonyl oxygen atoms. Oxamide turns out to have a structure much like oxalic acid with an apparently single carbon-carbon bond and a planar structure. It is probably reasonable to assume that amine-carbonyl attraction is a factor contributing to the planarity of the oxamide molecule.

Protein chemists also find interest in the configuration and dimensions of the extensive peptide linkages that are found in the oxamide structure.

An early crystal structure investigation of oxamide was made by van der Wyk and Misch in 1938 (1). They reported a

slightly wavy planar molecule with a carbon-carbon bond of 1.65 $\overset{\text{O}}{\text{\AA}}$. In view of the structures reported for oxalic acid and the oxalate ion it seemed possible that a somewhat long C-C distance might have been correct for oxamide. A value as large as 1.65 $\overset{\text{O}}{\text{\AA}}$., however, appeared excessive. These workers gave an untenable explanation for the long bond length. The structure reported by van der Wyk and Misch was derived entirely from two-dimensional Patterson series and was really in the nature of a preliminary investigation since no atomic parameters were given.

Romers (2) published a preliminary report of an apparently satisfactory structure in 1953 and indicated that three-dimensional refinement was in progress. Romers' communication described a completely planar structure with a C-C distance of 1.49 $\overset{\text{O}}{\text{\AA}}$., which is short enough to indicate some π bond character.

Very recently Ayerst and Duke (3) have published their results for a completely refined structure of oxamide. Their structure is in substantial agreement with Romers' but indicates slight changes in molecular dimensions. They report the C-C distance to be 1.542 $\overset{\text{O}}{\text{\AA}}$., with a standard deviation of 0.006 $\overset{\text{O}}{\text{\AA}}$., an apparently single bond.

Prior to the last two publications, a reinvestigation of the structure of oxamide was undertaken by the present author to clarify several points of uncertainty left by the preliminary study of van der Wyk and Misch. Is the structure really planar? What is the nature of the C-C bond? What are the factors contributing to the planarity of the molecule? The following paragraphs describe the progress of the structural analysis of oxamide up until its interruption by Romers' short communication. The work reported, although finished after Romers' publication, was an entirely independent investigation. Pertinent information from both of the recent articles will be included for comparison.

B. The Determination of the Structure

Oxamide is readily available as a finely divided white crystalline powder. Some difficulty was encountered in obtaining suitable crystals since it is relatively insoluble in all solvents. Small but usable crystals were finally grown from saturated solutions in either water or formamide. They grow as transparent colorless needles with a considerable tendency toward overgrowths and twinning. The cleavage plane, (010), across the needle is almost perfect. X-ray investigation shows the needle axis to be a short crystallographic direction with a periodicity of 3.625 Å. X-ray photographs using Laue, rotation, and Weissenberg cameras fail to reveal any symmetry. The unit cell is therefore triclinic. Cell dimensions were calculated by the method of least squares using data obtained from the zero layers about all three axes. The X-ray rotation photographs used were taken in a camera of 50 mm. radius, and each film was calibrated by superimposing single-crystal sodium chloride reflections upon the desired orders from single crystals of oxamide. In all, twenty-three separate observational equations were used to calculate the lattice constants shown in the second column below.

	Sly	Romers (2)	Ayerst (3) & Duke
a_1	5.179 Å.	3.61 Å.	3.625 Å.
a_2	3.625 Å.	5.17 Å.	5.188 Å.
a_3	5.654 Å.	5.62 Å.	5.658 Å.
α_1	114° 4.8'	83° 50'	83.7°
α_2	83° 45.9'	113° 54'	114.1°
α_3	114° 55.7'	115°	115.1°

The density assuming one molecule per unit cell is

Sly	Romers	Ayerst & Duke
1.668 ₆ gm./cm. ³	1.687 gm./cm. ³	1.667 gm./cm. ³
Observed density 1.667 gm./cm. ³		

The primitive unit cell obviously contains just one molecule of oxamide. Since the molecule can be centered the space group may be either C_1^1 or C_i^1 .

The short axis with its associated cleavage plane support the hypothesis of a layer structure with the molecule contained approximately in the ac plane. Accordingly most of the features of the structure can be obtained by a study of (h0l) reflections. Careful visual estimates of intensities were made of the (h0l) reflections using intensity strips as standard. In all, five separate estimates were made on three separate sets of multiple-film

Weissenberg photographs exposed with the unfiltered X-radiation from a copper target. Correlation between films and the rechecking of those intensities in serious disagreement led to the average relative intensities listed in Table I, page 25.* Multiplication of these values by $2\sin 2\theta/(1+\cos^2 2\theta)$ corrected them for Lorentz and polarization factors and gave the reduced intensities, I^{red} .

Since no atomic parameters were given by van der Wyk and Misch in their publication, a trial structure had to be found before refinement could be undertaken. Inasmuch as two-dimensional Patterson series were used in the former investigation they were adopted here to facilitate comparison with the earlier structure.

A Patterson series with the peaks sharpened and with the peak at the origin removed requires both absolute intensities and a temperature factor for correction of atomic form factors (9). Statistical methods would not be expected to prove very satisfactory when applied to this structure, since there are so few atoms in general positions (10). There are only three if the structure is centered, neglecting hydrogens, and six if it is not centered. In addition, the zone of data at hand contains only 60 possible reflections, and part of these are in the region of low $\sin\theta$ where

*Other pertinent data pertaining to these intensities are also found in Table I, although no further reference will be made thereto.

statistical methods are less applicable (10, 11). For these reasons it was intended that absolute intensities would ultimately be obtained from powder samples in an X-ray spectrometer. Meanwhile, Wilson's method, in spite of its expected limitations, was applied to obtain a scale factor and an isotropic temperature factor (10, 12). This method assumes the following expression,

$$aI_{(hkl)}^{\text{red}} = F_{(hkl)}^2 = e^{-\frac{2B\sin^2\theta}{\lambda^2}} \left[\sum_1^n f_i^2 + \sum_2^n \sum_1^{n-1} 2f_i f_j \cos 2\pi(hu_{ij} + kv_{ij} + lw_{ij}) \right]$$

$i \neq j \quad i > j$

where I^{red} is the observed relative intensity corrected for Lorentz and polarization factors, a is the scale factor for conversion of I^{red} to absolute F^2 , f_i is the atomic form factor (13) of the i th atom, B is the isotropic temperature factor, and u_{ij} , v_{ij} , and w_{ij} are the coordinates in Patterson space of the atomic interaction between the i th and j th atom, viz., $u_{ij} = (x_i - x_j)$, $v_{ij} = (y_i - y_j)$, and $w_{ij} = (z_i - z_j)$. If the intensities of the reflections within a small interval of $\sin^2\theta/\lambda^2$ are averaged, the cosine term will be negative as often as positive and will average nearly zero, and we may write as an approximation,

$$a\bar{I} = e^{-2B \frac{\overline{\sin^2\theta}}{\lambda^2}} \sum_1^n \bar{f}_i^2$$

where $\overline{\sin^2\theta}/\lambda^2$ in this equation is the mean value of $\sin^2\theta/\lambda^2$ in the interval of the average. Taking the logarithm of this equation and rearranging terms gives the following usable expression,

$$\log \frac{\sum_1^n \overline{f_i^2}}{\overline{I}} = \log a + \frac{2B(\log e)\overline{\sin^2\theta}}{\lambda^2}$$

A straight line graph of $\log(\sum \overline{f_i^2}/\overline{I})$ against $\overline{\sin^2\theta}$ will have $\log(a)$ as an intercept and $2B(\log e)/\lambda^2$ as slope. The graph of $\log(\sum \overline{f_i^2}/\overline{I})$ versus $\overline{\sin^2\theta}$ for oxamide is shown in Fig. 1. The plotted values, as expected, do not lie exactly on a straight line and accordingly no great reliance is placed in either the absolute intensities or the temperature factor. The scale and temperature factor calculated from the intercept and slope have the values 0.310 and 2.18 respectively. The absolute F^2 values obtained with this scale factor, multiplied by 10, are listed in Table I under the heading $10F^2$.

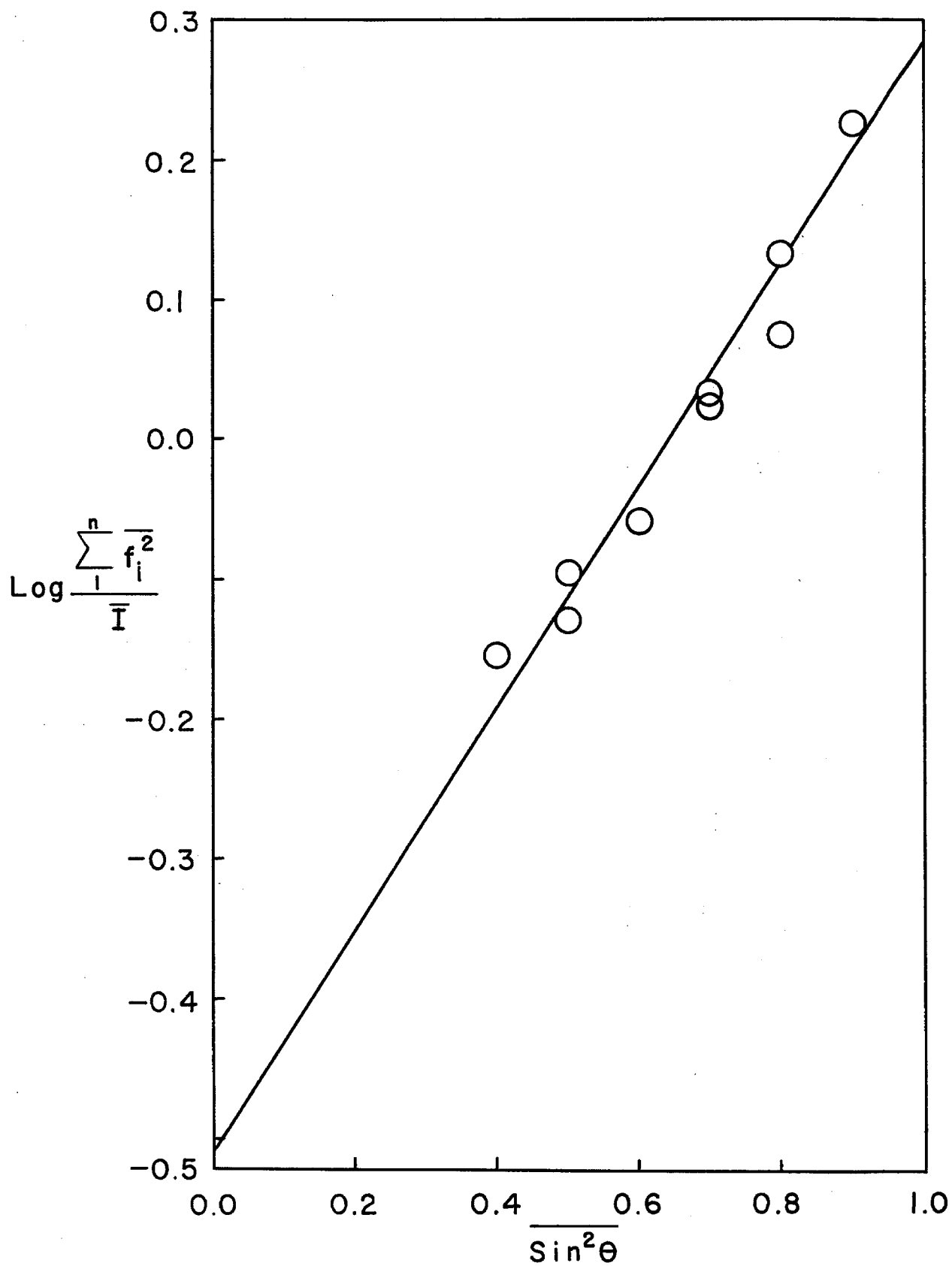


FIGURE I.

To remove the peak at the origin and to sharpen the interatomic interactions the coefficients of the two-dimensional Patterson series were modified by the equation,

$$\hat{F}_{(hkl)}^2 = \frac{(Z_N^2)(F_{(hkl)}^2 - \sum_1^n f_i^2 e^{-\frac{2B \sin^2 \theta}{\lambda^2}})}{f_N^2 e^{-\frac{2B \sin^2 \theta}{\lambda^2}}}$$

where Z_N and f_N are respectively the atomic number and atomic form factor for nitrogen. This modification of Patterson's peak sharpening factor (9) assumes the following as an approximation,

$$\frac{(\sum_1^n f_i)^2 e^{-\frac{2B \sin^2 \theta}{\lambda^2}}}{(\sum_1^n Z_i)^2} = \frac{f_N^2 e^{-\frac{2B \sin^2 \theta}{\lambda^2}}}{Z_N^2}$$

where Z_i is the atomic number of the i th atom and all other symbols are as previously defined. This sets the mean scattering per electron for all atoms in the structure, C, N, and O in equal numbers, the same as that for the nitrogen atom; the hydrogens are neglected. The Patterson series was then calculated from the expression,

$$\begin{aligned} \bar{F}_{(uw)}^2 = & \sum_h^m 2\hat{F}_{(h00)}^2 \cos 2\pi(hu) + \sum_l^n 2\hat{F}_{(00l)}^2 \cos 2\pi(lw) + \\ & \sum_h^p \sum_l^r 2\hat{F}_{(h0l)}^2 \cos 2\pi(hu + lw) + \sum_h^s \sum_l^t 2\hat{F}_{(h0\bar{l})}^2 \cos 2\pi(hu - lw) \end{aligned}$$

Note that no factor $1/A$ for the area of the ac plane has been included in this summation. By the use of Beevers-Lipson strips the sum was evaluated in units of $1/60$ of the unit cell dimensions for 1800 points in the asymmetric half-cell projection. The Patterson function is shown as Fig. 2 with contour lines every hundred positive units in \bar{F}^2 . The Patterson peaks were located graphically.

The crystals were tested in a modified Giebe and Scheibe (14) apparatus for piezoelectric effect with negative results. This does not conclusively prove the presence of a center, since a very weak effect might not be detected. The statistical method of Wilson (10) was applied in the slightly modified form of Howells, Phillips, and Rogers (15,11).

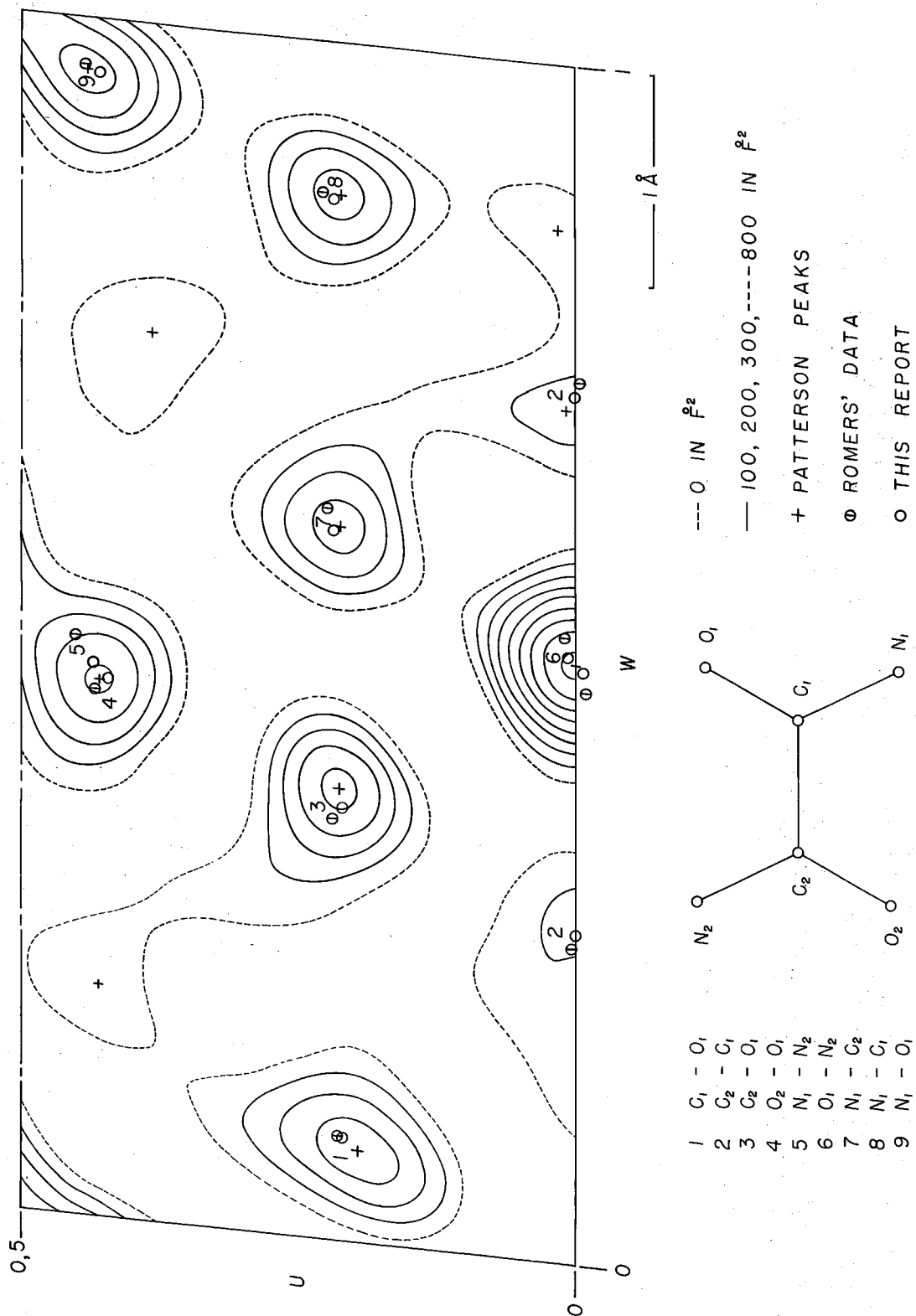


Figure 2.

PATTERSON PROJECTION ALONG THE 'B' AXIS (3.61 Å)

OF OXAMIDE

The graphs of ${}_1N(z) = 1 - e^{-z}$ and ${}_1N(z) = \text{erf}(\frac{1}{2}z)^{\frac{1}{2}}$ are shown in Fig. 3 along with the observed values of $N(z)$ vs. z for three overlapping groups of reflections taken in the region of moderate $\sin\theta$. The fit for the upper curve which corresponds to a centered projection is fairly good in spite of the unfavorable circumstances. All interpretations of the Patterson projection were accordingly based upon the space group C_i^1 , which require that the single molecule in the unit be centered and so by virtue of its bond configuration planar. The plane of the molecule is not, however, required to be in the plane (010).

A centered molecule can give, at most, nine independent interactions in a Patterson projection. There are eight clearly resolved peaks in Fig. 2 with an amplitude greater than 100, and seven of these have an amplitude greater than 300. If the eight peaks are assumed to represent atomic interactions then there are only two unresolved interatomic distances. The interpretation of the Patterson with the aid of expected bond lengths and use of relative peak heights was quite simple. The observed peak heights of a Patterson may be compared with the product $Z_i Z_j$ for the interaction involved. If the peaks are all resolved and roughly the same Gaussian shape, then peak height is proportional to the integral

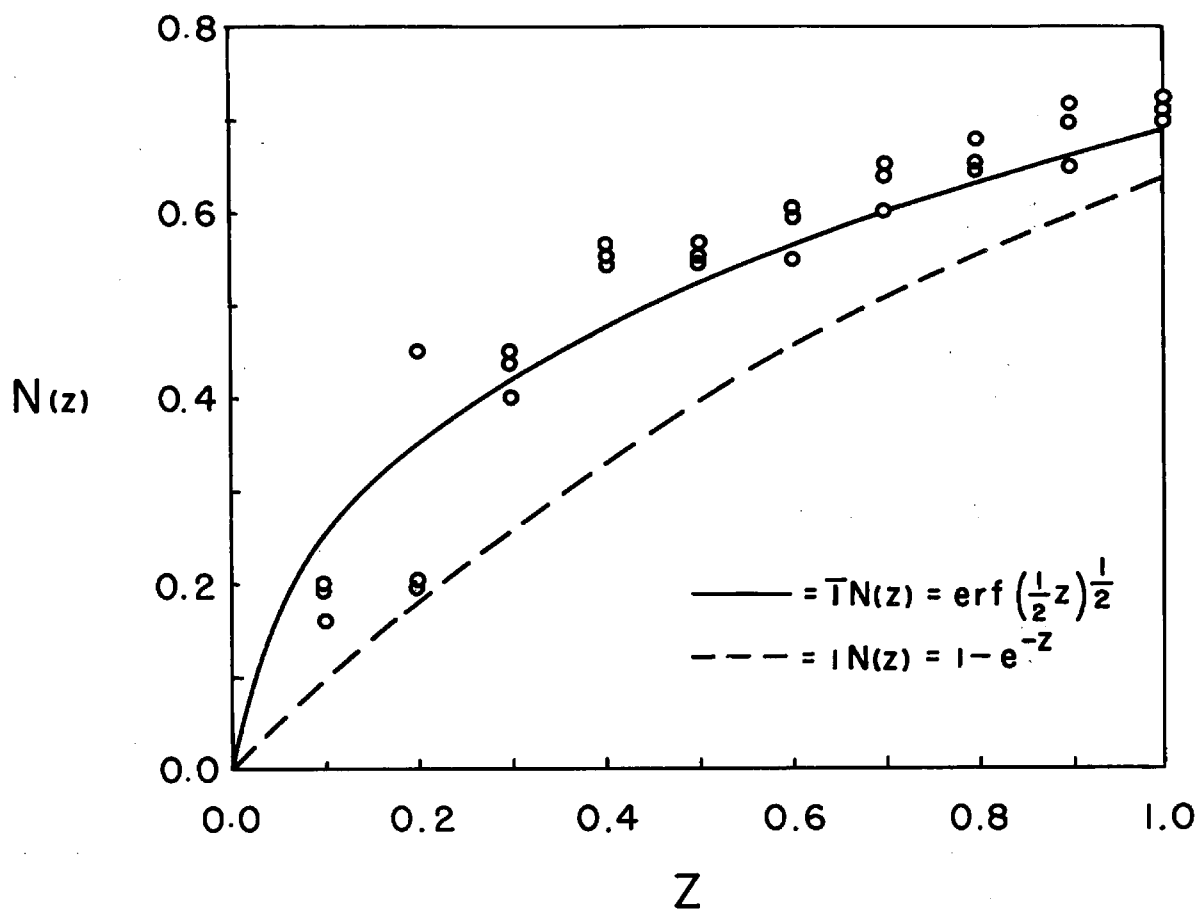


FIGURE 3

$$\int_{\text{peak}} \frac{\rho^2 F(s)}{A} ds$$

and thus to $Z_i Z_j$. Here $\rho^2 F(s)/A$ is "modified" electrons squared per unit area, ds is an area element, and the integration is to be carried out over the area of the peak. The following table lists the corresponding $Z_i Z_j$ values for the interactions in the Patterson.

Interaction	Peak Height x (0.256)		$Z_i Z_j$
$C_1 - C_2$	35	36	$Z_C Z_C$
$C_1 - O_1$	92	96	$2Z_C Z_O$
$C_2 - O_1$	109	96	$2Z_C Z_O$
$N_1 - C_1$	87	84	$2Z_N Z_C$
$N_1 - C_2$	86	84	$2Z_N Z_C$
$N_1 - O_1$	112	112	$2Z_O Z_N$
$O_1 - N_2$	210	224	$4Z_O Z_N$
$\left\{ \begin{array}{l} O_2 - O_1 \\ N_1 - N_2 \end{array} \right\}$	106	113	$Z_O Z_O + Z_N Z_N$

The two overlapping peaks $O_1 - N_2$ and $O_1 - O_2 + N_1 - N_2$ both come out lower than calculated, as might be expected from the addition of two peaks not exactly superimposed. The largest discrepancy is the $C_2 - O_1$ peak of 109 and it is only 15% in error. It is apparent that there is good corre-

lation between peak height and the assigned interactions.

The trial structure derived from the Patterson has the following bond system.

C-C	1.55 Å.	\angle C-C-O	119°
C-N	1.28 Å.	\angle C-C-N	119°
C=O	1.24 Å.	\angle O-C-N	122°

The C-C bond lies along the z axis. The C-N distance is perhaps shorter than expected, but the other values are quite reasonable. The parameters corresponding to this model are

	x	z
C	0.000	0.138
N	-0.218	0.270
O	0.211	0.224

The atomic interactions resulting from these coordinates are shown on the Patterson projection along with those from Romers' model.* The average distance between the Patterson peaks and the trial structure peaks is 0.063 Å.

*Fig. 2 was drawn before the recent publication by Ayerst and Duke. Their structure is substantially the same although it fits the Patterson slightly better than Romers'.

The corresponding parameters reported by Romers (2) and by Ayerst and Duke (3) are

	x		y		z	
	Romers	A.&D.*	Romers	A.&D.	Romers	A.&D.
C	0.000	0.0025	0.002	0.0060	0.132	0.1362
N	0.000	-0.0032	-0.226	-0.2230	0.259	0.2629
O	0.000	0.0061	0.217	0.2208	0.219	0.2168

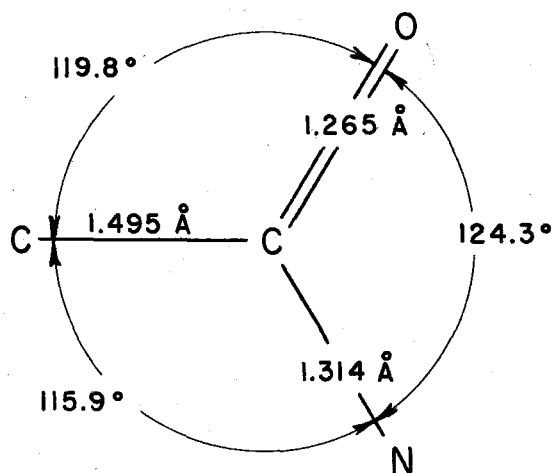
The average difference in the values of the parameters between the trial structure and the structure of Ayerst and Duke is 0.006.

It may be recalled that a $1.65 \overset{\circ}{\text{A}}$. carbon-carbon distance had been derived by van der Wyk and Misch from a study of Patterson projections. It is true that about the same degree of agreement between trial structure peaks and Patterson peaks could be obtained with a spacing of about $1.65 \overset{\circ}{\text{A}}$., but certainly no better. The ac projection of the earlier workers was made using 29 reflections while the author's series was based on 60 reflections only one of which was too weak to be estimated.

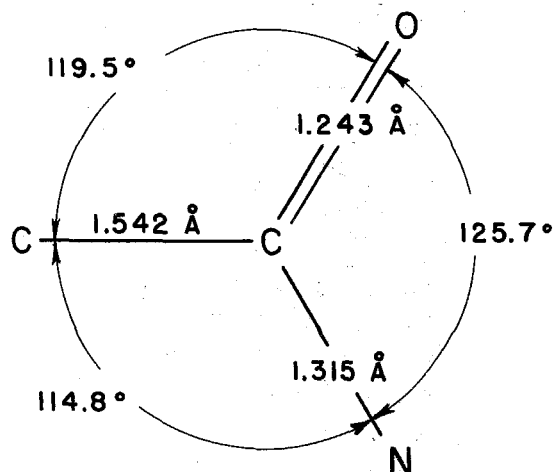
*The coordinates of Ayerst and Duke were based on the molecule centered at $(0\frac{1}{2}\frac{1}{2})$ and a transformation of coordinates gave the values listed.

C. The Description of the Structure

The configuration of the molecule as found by Romers,^{*} and by Ayerst and Duke is diagrammed below.



ROMERS



AYERST & DUKE

The structure may be described as an infinite layer of hydrogen-bonded molecules with van der Waals forces acting between layers. Two layers of the structure in vertical projection are shown in Fig. 4.^{**} The H-N-C angles and the N-H bonds have arbitrarily been assigned the values 125° and 1.00 \AA , respectively in this drawing. The skew b axis displaces successive layers to produce good packing of the atoms of the upper layer into the pockets of the lower. The vertical separation between layers is 3.007 \AA .

^{*}The distances and angles were calculated by the author since Romers' preliminary paper did not list bond angles.

^{**}Figure 4 was drawn before the recent publication of Ayerst and Duke and is based on Romers' parameters.

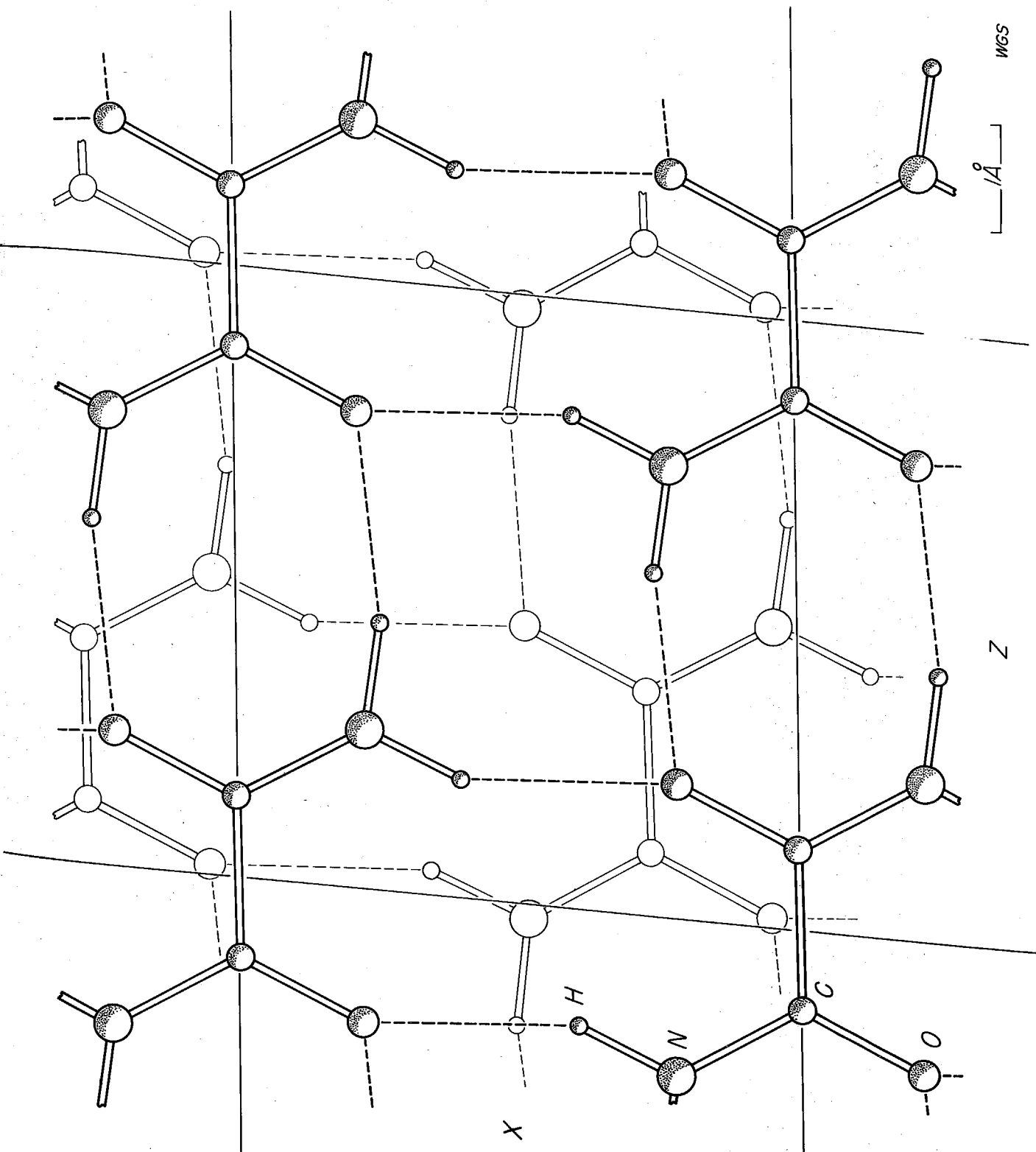
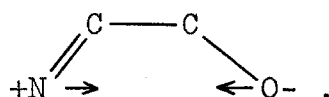


Figure 4.

Three things are significant about the completely planar structure. First, the C-C distance of 1.542 Å. is apparently a single bond with no π bond character. Second, the C-N distance is rather short. Short bonds are also found in cyanuric acid, 1.345 Å. (16,17), and urea, 1.335 Å. (18), and in similar structures (19). The shortening indicates considerable contribution by the structure $\text{C}-\text{C} \begin{smallmatrix} \text{O}^- \\ \diagup \\ \text{N}^+ \end{smallmatrix}$. The 1.315 Å. distance compared to the normal single bond of 1.47 Å. requires about 50% double bond character (20). The presence of this ionic resonance hybrid may be a factor contributing to the planarity of the molecule through intramolecular electrostatic attraction between N and O, viz.,



Third, the hydrogen bonds in different directions in the infinite layer are significantly different. The hydrogen bonds parallel to the \bar{a} axis are 2.93 Å. with an angle O----N-C of 143° while those in the \bar{c} direction are 2.96 Å. with an angle of 116° . The latter are approximately linear for an assumed angle of 120° for the H-N-C bond and accordingly must be regarded as relatively strong hydrogen bonds. The hydrogen bonds directed along the \bar{a} axis, however, are far from linear. Now Pauling and Corey (20) have assumed linear hydrogen bonds in their discussions of proteins and have considered certain proposed structures as unlikely be-

cause they require nonlinear hydrogen bonds. Elliot (21) has pointed out the sparsity of data pertaining to the angular dependence of hydrogen bond strength, but the following comments may still prove informative.

Newman and Badger (22) have found a H-N-C bond angle of $100^\circ \pm 10^\circ$ by means of polarized infrared studies on N-acetylglycine. The crystal structure of the same compound (23) gives 132° for the angle O----N-C, which is within the range of values reported by Donohue (19) for such hydrogen bonds. These combined studies indicate that the hydrogen bond O----N-C is non linear by about 45° ($180 - \text{angle O---H-N}$). N-acetylglycine represents an instance in which the hydrogen atom is displaced away from the position giving a linear hydrogen bond and away from the expected angle of about 120° . It is true, however, that the O-----N distance is $3.03 \overset{\text{O}}{\text{\AA}}$ and the hydrogen bond is accordingly regarded as weak. There is also a strong O----H-O hydrogen bond of $2.56 \overset{\text{O}}{\text{\AA}}$ linking the N-acetylglycine molecules into chains. The rather weak O----H-N bonds may thus be just the best available hydrogen bonds of a secondary nature linking the molecules into sheets. If Newman and Badger are correct the O----H-N hydrogen atom of N-acetylglycine is directed about midway between an oxygen atom of the same molecule and one of an adjacent molecule. There is apparently some attraction between the

highly polar $C=O$ group and the N-H group of the same molecule. The slight shortening of the C-C bond, 1.506 \AA , is attributed to hyperconjugation of the C-H bonds with the neighboring carbonyl group (23). Perhaps the hyperconjugation and the amine-carbonyl attraction are both factors contributing to the planarity of the N-acetylglycine molecule. Oxamide presents almost exactly the same structural possibilities. If the H-N-C angle for the hydrogen bonds directed along the \bar{a} axis is 103° , the hydrogen atom will lie along the line bisecting the $O'----N_1----O_1$ angle. This would make possible two interactions of hydrogen with unshared electrons of oxygen atoms. The intramolecular O----N distance is 2.70 \AA , while the intermolecular bond is 2.93 \AA . The two hydrogen bonds would be non-linear by a matter of 58° ($180^\circ - \text{angle } O----H-N$) and would accordingly be weak. If the H-N-C angle is assumed to be 120° , the departure from linearity for the single intermolecular hydrogen bond is 34° , and this is presumably a weak hydrogen bond. It might be best to state that the structure is composed of planar chains of oxamide molecules strongly hydrogen bonded along their length and weakly bonded into infinite sheets. The somewhat unfavorable hydrogen bond angles offer then the best arrangement available to the chains of molecules.

The foregoing paragraphs have not included any discussion of electrostatic attractions between molecules. Since ionic resonance hybrids make a considerable contribution to the molecular structure such forces must play some role in bonding the molecules into layers. From a polarized infrared study of oxamide, particularly in the region of the N-H stretching frequency, it might be possible to find out if the hydrogen atoms directed along the \bar{a} axis are displaced as in N-acetyl glycine. The intramolecular attraction supposed to exist in this case might be an additional factor contributing to the planarity of the oxamide molecule.

Table I

The intensities of the $h0l$ reflections for oxamide

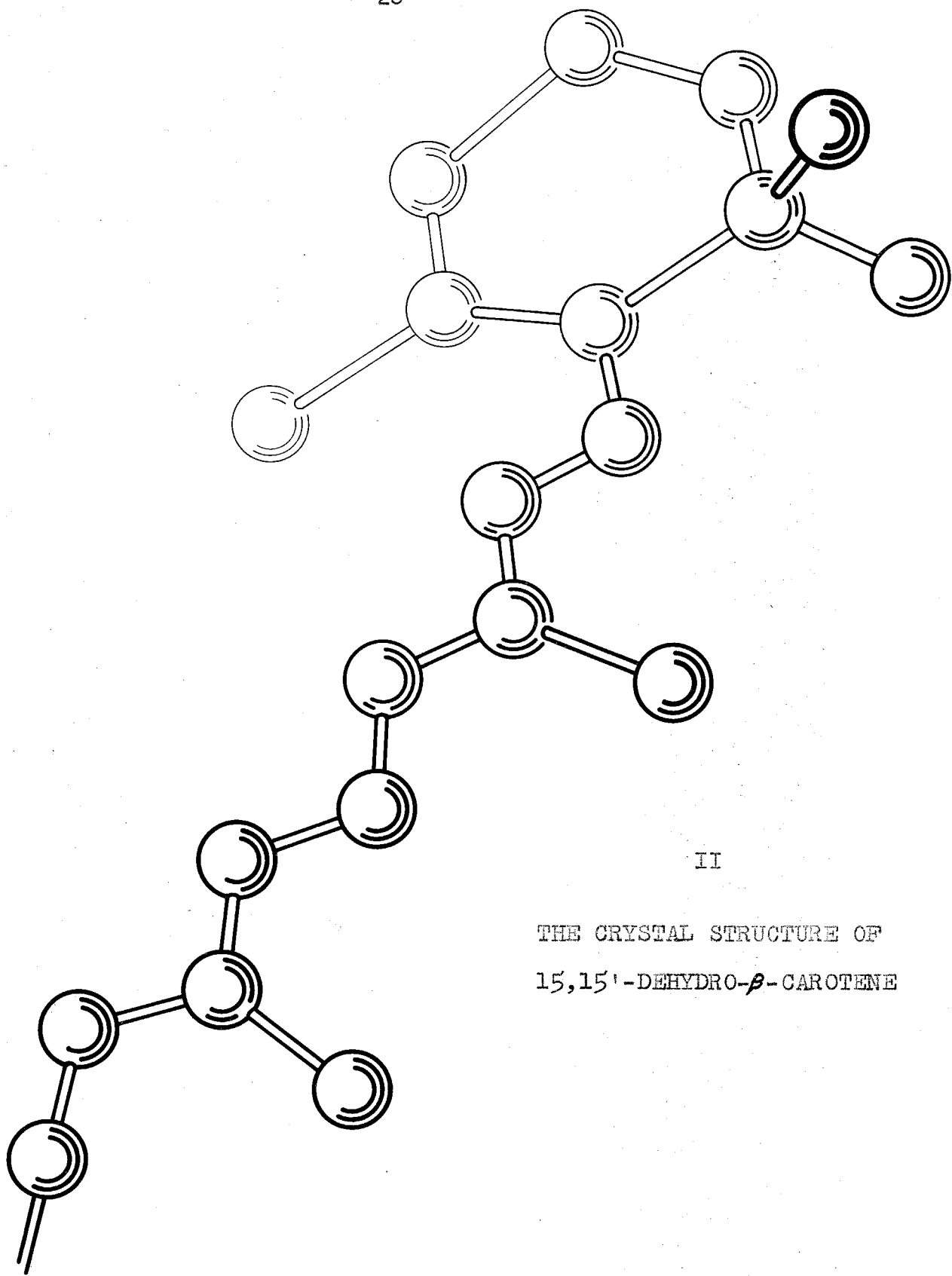
hkl	$\sin \theta$	$\sin^2 \theta$	1	Relative Intensity			5	Avg. Rel. Int.	I^{red}	$(10)F^2$	F^2
				2	3	4					
206	0.978	0.956		10.4	9.7		9.1	9.7	4.3	13.3	-15
106	0.923	0.852	9.8	10.4	9.7		9.1	9.8	9.3	28.8	-6
006	0.894	0.799	5.1	5.4				5.3	6.2	19.2	-16
10 $\bar{6}$	0.895	0.801	17.6	17.6	15.0	16.6	17.1	16.8	19.7	61.1	15
20 $\bar{6}$	0.925	0.856	33.0	36.0	33.2	35.6	35.6	34.7	32.4	100.4	56
305	0.926	0.857	5.9	5.6				5.8	5.4	16.7	-16
205	0.839	0.704	4.2	4.1				4.2	6.6	20.5	-19
105	0.776	0.602									-31
005	0.745	0.555		1.5				1.5	2.9	9.0	-28
10 $\bar{5}$	0.749	0.561	4.5	4.5				4.5	8.8	27.3	-21
20 $\bar{5}$	0.788	0.621	11.9	11.9			10.4	11.4	20.9	64.8	-2
30 $\bar{5}$	0.856	0.733		1.4				1.4	2.0	6.2	-27
404	0.921	0.848		1.2				1.2	1.2	3.7	-27
304	0.803	0.645	36.0	36.0	41.2	39.6	36.8	37.9	66.9	207.4	68
204	0.704	0.496	33.0	31.5	27.1	28.7	27.0	29.5	59.0	183.0	21
104	0.632	0.399	4.5	4.1				4.3	8.1	25.1	-27
004	0.597	0.356	17.4	16.3	15.8	14.6	16.3	16.1	28.5	88.4	-17
10 $\bar{4}$	0.607	0.368	34.5	34.0	32.3	37.2	34.9	34.6	62.3	193.1	2
20 $\bar{4}$	0.655	0.429	103.5	97.5	88.9	91.8	94.9	95.3	184.9	573.2	97

Table I (continued)

hkl	$\sin \theta$	$\sin^2 \theta$	1	2	3	4	5	Avg. Rel. Int.	I ^{red}	(10) F^2	F^2
304	0.738	0.545	5.9	5.6			5.5	5.7	11.3	35.0	-19
404	0.845	0.714	11.3	10.6			10.7	10.9	16.6	51.4	-1
504	0.968	0.937		1.8				1.8	1.0	3.1	-27
503	0.963	0.927		12.5	12.1		11.4	12.0	7.2	22.3	-7
403	0.822	0.676	8.4	8.4			8.6	8.5	14.2	44.0	-8
303	0.691	0.477	4.8	4.5			4.0	4.4	8.8	27.3	-24
203	0.576	0.332		1.1				1.1	1.9	5.9	-32
103	0.489	0.239	15.6	15.9	16.6	17.4	16.3	16.4	22.0	68.2	-26
003	0.448	0.201	79.5	76.0	77.2	75.2	78.4	77.3	91.4	283.3	-11
103	0.463	0.214	27.5	26.0	26.3	29.1	28.6	27.5	34.1	105.7	-23
203	0.531	0.282		1.4				1.4	2.1	6.5	-31
303	0.634	0.402	2.0	1.6				1.8	3.4	10.5	-30
403	0.759	0.576	5.9	5.4			6.0	5.8	11.2	34.7	-18
503	0.896	0.803	5.6	5.4			6.4	5.8	6.8	21.1	-15
502	0.892	0.796	21.6	20.6	23.4	23.4	23.0	22.4	26.8	83.1	30
402	0.740	0.548	11.4	11.9	13.3	12.1	12.6	12.3	24.3	75.4	-5
302	0.595	0.354	29.5	29.0	31.9	31.9	31.2	30.7	54.0	167.4	-5
202	0.461	0.213	93.0	93.0	97.0	97.0	100.8	96.2	118.1	366.1	-3
102	0.352	0.124	154.0	162.0	161.7	153.6	156.2	157.5	132.6	411.1	-13
002	0.298	0.089	765.0	730.0	723.6	741.8	739.0	739.9	501.7	1555.3	18
102	0.328	0.108	16.7	17.1	15.0	15.8	16.1	16.1	12.4	38.4	-29

Table I (continued)

hkℓ	$\sin \theta$	$\sin^2 \theta$	1	2	3	4	5	Avg. Rel. Int.	I ^{red}	(10)F ²	F ²
20 $\bar{2}$	0.423	0.179	287.0	287.0	278.9	295.1	308.2	291.2	316.8	982.1	32
30 $\bar{2}$	0.551	0.304	5.3	5.0			5.7	5.3	8.4	26.1	-29
40 $\bar{2}$	0.694	0.482	34.5	33.0	35.2	36.4	31.6	34.1	68.1	211.1	26
50 $\bar{2}$	0.844	0.712	6.2	7.5			7.1	6.9	10.6	32.8	-12
501	0.841	0.707		2.0				2.0	3.1	9.6	-25
401	0.682	0.465	5.4	5.9			5.4	5.6	11.1	34.4	-23
301	0.524	0.275	13.7	13.0	12.1	12.1	13.4	12.9	19.1	59.2	-25
201	0.370	0.137	5.3	4.7			5.0	5.0	4.5	14.0	-30
101	0.230	0.053	74.0	77.5	78.0	82.1	78.1	77.9	38.6	119.7	-28
001	0.149	0.022	360.0	360.0	335.5	359.8	353.9	353.8	109.0	337.9	-26
101	0.212	0.045	143.0	146.0	157.7	147.6	156.2	150.1	67.8	210.2	-26
20 $\bar{1}$	0.347	0.120	58.5	56.5	63.1	61.9	59.6	59.9	49.5	153.5	-24
30 $\bar{1}$	0.500	0.250	6.5	5.9			6.9	6.4	8.9	27.6	-29
40 $\bar{1}$	0.657	0.432	3.9	4.1			3.7	3.9	7.6	23.6	-26
50 $\bar{1}$	0.816	0.666	5.4	5.9			5.5	5.6	9.5	29.5	-15
100	0.163	0.027	775.0	775.0	762.0	762.0	739.0	762.6	259.3	803.8	-18
200	0.326	0.106	300.0	287.0	327.4	305.2	285.5	301.0	228.8	709.3	-5
300	0.490	0.240	5.3	5.0			5.7	5.3	7.1	22.0	-30
400	0.653	0.426			61.4	63.9	57.1	60.8	117.7	364.9	50
500	0.815	0.664	33.4	34.5	36.0	32.3	36.4	34.5	58.8	182.3	61



II

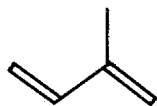
THE CRYSTAL STRUCTURE OF
15,15'-DEHYDRO- β -CAROTENE

THE HALF MOLECULE OF DHC.

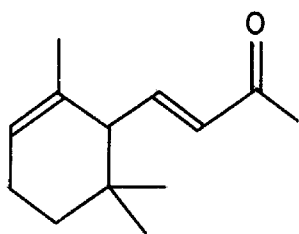
A. Introduction

The compound 15,15'-dehydro- β -carotene* is representative of many carotenoids both synthetic and natural. These highly colored substances form the pigments found in the fruits, flowers, and leaves of many plants, and they also occur in various animal organisms (24, 25, 26, 27). The naturally occurring carotenoids include aldehydes, acids, esters, alcohols, ketones, and epoxides as well as hydrocarbons; they are characterized structurally by the presence of isoprene groups, 2-methyl-1,3-butadiene, and often contain α or β -ionone rings, 4-(2,6,6-trimethyl-1 or 2-cyclohexenyl)-3-buten-2-one (24-28). Compare the structures of isoprene, α and β -ionone, and γ -carotene shown in Figure 5. Lycopene is an example of an open chain hydrocarbon, while α and β -carotene are terminated with rings at both ends. The α -carotene molecule has one ring of each of the two types shown in Figure 5, while β -carotene has both rings of the β form. Lycopene and the three carotenes are all structural isomers with the composition $C_{40}H_{56}$. Certain of the carotenoids are of considerable biochemical interest because they are related to vitamin A and are active as provitamins, for

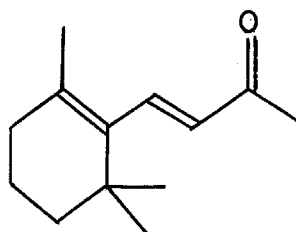
*The nomenclature used here is the accepted form proposed by P. Karrer (30, 31, 32). The compound has also been referred to as 9,9'-dehydro- β -carotene (60-64).



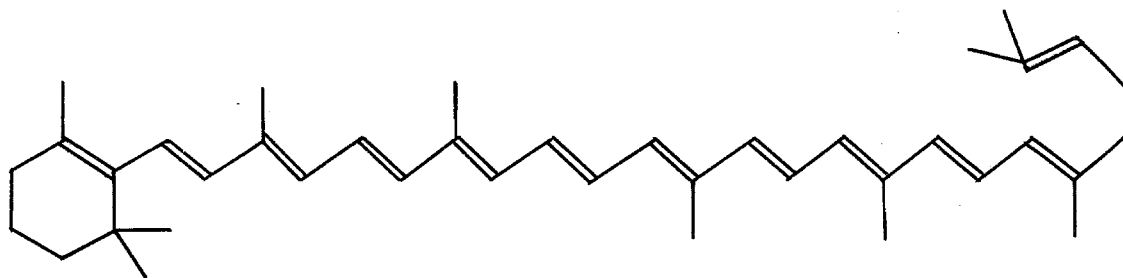
ISOPRENE



α -IONONE



β -IONONE



γ -CAROTENE

FIGURE 5. THE STRUCTURAL FORMULAS OF ISOPRENE, α -IONONE, β -IONONE, AND γ -CAROTENE.

example α -carotene, β -carotene, γ -carotene, and cryptoxanthin (29). Several synthetic methods have been devised for the preparation of β -carotene and related polyenes, notably those of Karrer et al. (33-48), and Inhoffen and co-workers (49-80). It will suffice here to say that the occurrence of these compounds is widespread in nature and that considerable work has been done in determining their structural formulas, in devising methods of synthesis, and in evaluating the role they play in metabolic processes.

The carotenoids, with from nine to thirteen double bonds in a linear chain, are among the most unsaturated compounds found in nature. This makes possible a great variety of cis-trans isomerism. The compound β -carotene, for example, is predicted to have twenty unhindered isomers of this type, of which thirteen have actually been observed (26, 29, 81, 82). Moreover Garbers, Eugster, and Karrer (43, 45, 46) have recently reported the preparation of some of the hindered cis isomers of β -carotene, lycopene, and phenylpolyenes; and Oroshnik, et al. (83) have prepared a similar form of retrovitamin A methyl ether.* The number of iso-

* In 1948, prior to these papers, Karrer, Schwyzer, and Neuwirth (84) reported the preparation of a hindered cis isomer of methyl muconic acid. Elvidge, Linstead, Sims, and Orkin (85, 86, 87) showed shortly thereafter that this was a cis-trans isomer and not the hindered cis-cis form. Pauling's further comment on hindered cis isomers (88), in answer to Karrer's paper, appeared in 1949.

meric forms is therefore large and many of them have not been assigned structures, for example the neodehydro- β -carotenes described by Wallcave (89). The isolation and analysis of the carotenoids, which often occur in rather minute quantities, have paralleled the development of the science of chromatography. A great deal has been accomplished by the organic chemists in isolating and characterizing the various isomers. The configurations of the all-trans forms, and of some of the central mono-cis carotenoids are apparently well established (26, 29, 82, 90-95). However, there are many compounds, and the multifarious problems connected with their structural analysis are of such complexity that the precise nature of these isomers will probably only be determined by X-ray investigation of their crystals, and this will certainly not be easy (82). The present report represents the first conclusive structure analysis of any of the carotenoids.*

The determination of the configuration of the carotenoid stereoisomers is just part of the structural problem of linearly conjugated systems in general. The concepts of resonance, as applied by Pauling and others, have led to many correct predictions about the bond lengths, bond

*Recently MacGillavry, Kreuger, and Eichhorn (114) have reported the structure of a compound related to part of one end of the β -carotene molecule, trans- β -ionylidene crotonic acid.

angles, and the planar configuration of conjugated functional groups and molecules (82, 96). Quantum mechanical calculations of the resonance energies, bond orders, and bond lengths of aromatic and linearly conjugated systems were made during the years 1933 to 1939, and especially from 1937 to 1939 (97-106). However, to date, no refined structural analysis has been reported for any highly conjugated linear molecule, and consequently we have no experimental data for comparison with the theoretical dimensions. Considerable effort has been directed toward the solution of the crystal structures of such systems. Hengstenberg and Kuhn (107) studied a series of diphenylpolyenes in 1930 and reported the general orientation of molecules described as planar and all-trans. The planes of a few strong reflections were used to locate the molecules but no intensities were measured or calculated, and no atomic parameters were reported. Although the configuration and orientation are very likely correct, the analysis was neither conclusive nor complete. The same may be said for the study made in 1932 by Waldmann and Brandenberger on methyl bixin (108, 109), an ester of a carotenoid acid with nine conjugated carbon-carbon bonds in a linear chain. Both of these investigations, inconclusive by present day standards, were carried out prior to the quantum mechanical treatment of conjugated systems; they

were followed by the X-ray study of β -carotene described in the following paragraphs.

In 1937, Taylor (110) published an inconclusive X-ray investigation of β -carotene, presumably the all-trans form. The monoclinic lattice was found to have the parameters,

$$\begin{array}{ll} a & 7.75 \text{ \AA.} \\ b & 9.5 \text{ \AA.} \\ c & 25.0 \text{ \AA.} \\ \beta & 105^\circ, \end{array}$$

with the space group probably $C_{2h}^5 - P2_1/c$. Density measurements require the unit cell to contain two molecules which must be centrosymmetric in this space group. The crystals were studied optically as well as with X-rays. Absolute intensities for the $h0l$ reflections were measured on a spectrometer and were used to evaluate a Patterson projection along the \bar{b} axis. The direction of high optical absorbance, the traces of the strong $h0l$ reflections, and the location of the peaks in the Patterson, although very poorly resolved, gave the general orientation of the molecule. A large number of trial structures were tested but none gave satisfactory agreement with all of the $h0l$ intensity data. Despite considerable effort Taylor was unable to complete the analysis.

Smare continued Taylor's investigation of β -carotene and reported the following results in a private communication to Dr. E. W. Hughes in 1949. Complete $hk\ell$ data were obtained by the visual estimation of intensities. Several sections of a three-dimensional Patterson function were evaluated which confirmed Taylor's general orientation of the molecule. Smare made a considerable number of trial \bar{b} -axis projections similar to those of Taylor but also without success; however his report contained a rather poorly resolved Fourier projection along the \bar{a} axis. In 1949 Smare expected to continue work on β -carotene by further refining the projection on (100), while at the same time attempting to obtain agreement with the $h0\ell$ data. As nearly as can be determined Smare found the projections along \bar{a} and \bar{b} impossible to refine with the available data and abandoned all work on β -carotene shortly thereafter. In any case no publications have appeared since Taylor's paper in 1937.

The crystal structure investigation of β -carotene was handicapped by three difficulties. 1) The data were insufficient. The high temperature factor resulted in the absence of all reflections with $\sin\theta > 0.70$, based on copper $K\alpha$ X-radiation. 2) The probable orientation of the molecule is such that the projections are not well resolved. 3) The space group is not known with certainty. Only a single order from (010), namely 020, was observed, and the

assumption that all odd orders of $0k0$ are systematically absent may not be valid.

The compound 15,15'-dehydro- β -carotene, hereinafter also referred to as DHC, differs from β -carotene only by the presence of a triple bond in the center rather than a double bond. The compound is the precursor of β -carotene in the total synthesis by Inhoffen (60-64). The final step in the synthesis is the selective reduction of the conjugated alkyne to an olefin by means of a lead-poisoned palladium catalyst described by Lindlar (111). The reduction gives almost quantitatively the 15,15'-mono-cis- β -carotene. Inhoffen was therefore interested in the configuration of DHC about the three collinear central bonds, since he felt that a knowledge of this would make possible a useful comparison of properties with those of the all-trans and the central mono-cis- β -carotenes, and might clarify the steric course of the catalytic reduction. Inhoffen accordingly offered a crystalline sample of DHC to Professor Zechmeister for X-ray analysis. These crystals were used in the structural determination described herein, and the author extends thanks to both Professor Inhoffen and Professor Zechmeister.

Before continuing with a detailed description of the crystal structure of DHC a brief discussion of the catalytic

reduction will be worth while. The structures of DHC and β -carotene in both extended trans and central 'V' forms are shown in Figure 6. There is currently available considerable evidence which indicates that the catalytic semireduction of a conjugated alkyne leads almost invariably to an ethylene group with the cis configuration regardless of the relative stability of the cis and trans isomers of the product (43, 45, 46, 59, 64, 83, 112, 113). The preparation of some of the hindered cis isomers previously mentioned depends upon just this reaction (43, 45, 46, 83, 112). The structure found for DHC is centrosymmetric and must be the trans isomer (a) shown in Fig. 6. Inhoffen in his published description of the preparation of the carotenes (59, 64) has shown DHC in the 'V' form about the three central bonds as drawn in Fig. 6(c). Apparently the fact that DHC is reduced to a cis form does not require a 'V' molecule, although it certainly does not preclude this possibility. If the molecules of DHC retain in solution the configuration they have in the crystal, the reduction to the mono cis form not only bends the molecule but rotates one end about the central bonds. This means that the course of the reduction is such that free rotation of one end of the molecule is possible at some intermediate stage. Alternatively DHC might be isomeric in solution with the two forms shown

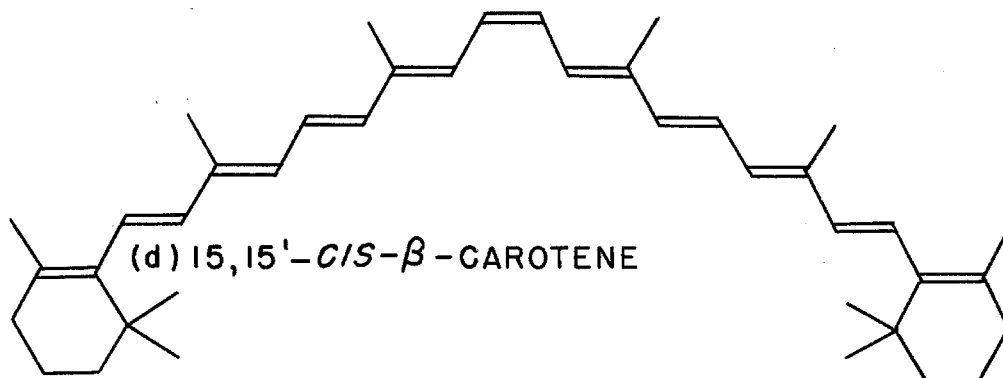
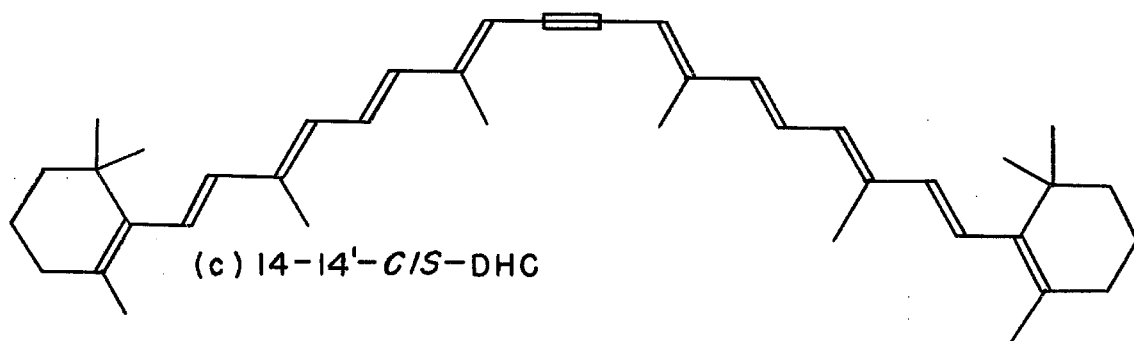
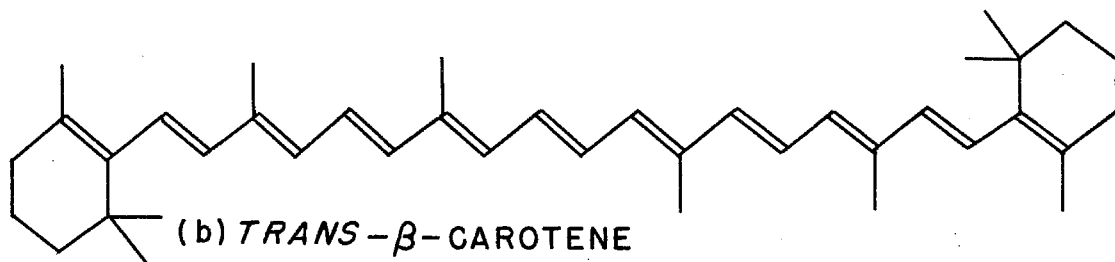
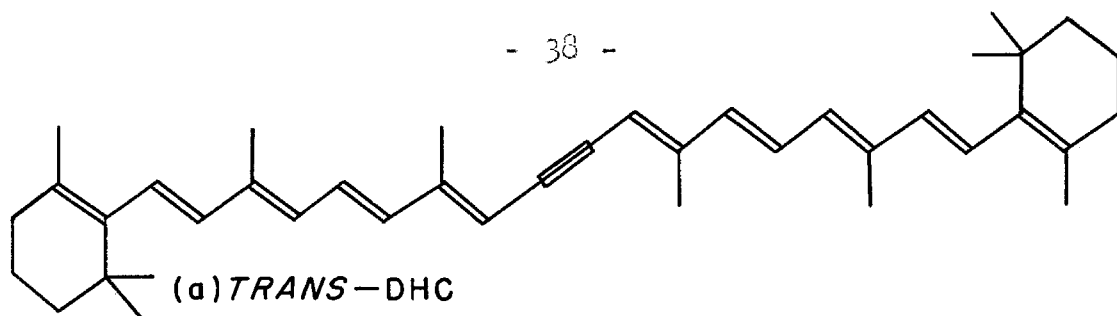


FIGURE 6. THE STRUCTURES OF THE ALL *TRANS* AND CENTRAL 'V' FORMS OF DHC AND β -CAROTENE.

in Fig. 6 (a) and (c).^{*} But if this were the case then the chromatographic separation of a solution prepared by dissolving crystalline DHC should yield more than one product. Inhoffen has apparently not carried out this experiment, but the former hypothesis is perhaps more tenable anyway. The catalytic reduction of DHC was carried out by Inhoffen at a temperature low enough to prevent the thermal isomerization of 15,15'-cis- β -carotene to the more stable trans form, that is, to prevent a rotation about a double bond of a highly conjugated molecule. The conversion of the trans form of DHC to the 'v' form of Fig. 6 would require a rotation around one of the three central bonds, either single or triple. Although these two cases, DHC and β -carotene, are doubtless not exactly equivalent one may argue that the single, double, and triple bonds all have the same amount of double-bond character in the center of a molecule having eleven conjugated multiple bonds, involving a total of twenty-one atoms. If this is true then the temperature of Inhoffen's reduction was probably also too low to isomerize the trans DHC to the presumably less stable cis form. The author is

^{*} There are possible resonance forms having the planes of the two halves of the molecule at right angles; however these forms have lower resonance energy and would probably have only a transitory existence.

inclined to believe that DHC can exist in solution in either the cis or the trans form but without appreciable interconversion at room temperature,* and that the conversion to a cis β -carotene occurs in the process of reduction. If this is true we have here evidence supporting the postulate that catalytic reduction gives the cis isomer regardless of the steric form of the initial compound.

*Some effort should be made to isolate the cis DHC since a comparison of the properties of all four compounds shown in Fig. 6 should be very illuminating, especially the spectra and the conditions for isomerization between pairs.

B. Preliminary Investigation

The compound 15,15'-dehydro- β -carotene, $C_{40}H_{54}$, Fig. 7, crystallizes in thin, orange, monoclinic rhomboids, platy on (010), with edges parallel to [100] and [001]. By transmitted polarized light the crystals are dark orange-red if the electric vector of the incident light is approximately parallel to $[\bar{1}01]$, but otherwise a pale yellow-green. At

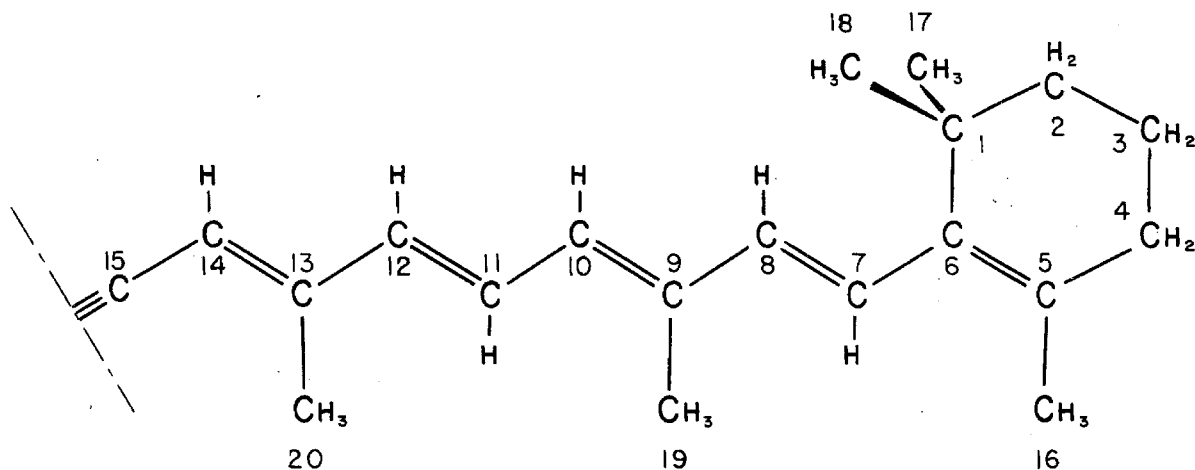


Figure 7. The structural formula of the half molecule of 15,15'-dehydro- β -carotene. The other half of the molecule is obtained by inversion through a center at the triple bond. The numbering is consistent with the atomic parameters listed in Table 2. Atoms 16 to 20 inclusive are numbered arbitrarily by the author; the others are numbered according to accepted carotene nomenclature (30, 31, 32).

a temperature of -20° C. the unit cell has the parameters,

$$\begin{array}{ll} a_1 & 8.14_5^{\circ} \text{ \AA.} \\ a_2 & 31.8_7^{\circ} \text{ \AA.} \\ a_3 & 8.46_5^{\circ} \text{ \AA.} \\ \alpha_2 & 128^{\circ}18.8'. \end{array}$$

From systematic absences the space group was uniquely determined to be $C_{2h}^5 - P2_1/c$. Rough measurements of density require the unit cell to contain two molecules of DHC, which accordingly must be centrosymmetric.

Preliminary Weissenberg photographs were taken at room temperature with copper $K\alpha$ X-radiation and with the crystals exposed to air. The high temperature factor made the exposure time of the order of five to ten days, and only a limited amount of data could be obtained. The crystals have a tendency to curl upon standing in air for moderate lengths of time, probably a result of oxidation. They accordingly give poor X-ray photographs after perhaps two weeks to a month depending upon their size, thickness, and original quality. The crystals scatter so poorly and are so thin that it was not considered feasible to enclose them in capillaries. A thoroughly refined analysis of any complicated crystal structure requires complete three-dimensional data. A compound such as DHC, where the intensities of the reflections are limited both in number and

accuracy by unfavorable experimental conditions, will require a major effort to obtain all possible data if the structure determination is to be successful. It was apparent after a few preliminary photographs that this would be a long and arduous task, even with improvements in technique that were designed to increase the coherent scattering of X-rays and to lower the rate of air oxidation. It was therefore deemed desirable to attempt to find a trial structure with the data available while complete X-ray photographs were being taken. The following paragraphs are devoted to a description of the methods and the results of this preliminary investigation.

From the method of synthesis the compound was expected to be all-trans with the possible exception of the configuration about the three collinear central bonds (60-64). Since the molecule is centered, it is trans about these bonds also, and the alternative 'V' model must be rejected. Upon the premise of an all-trans planar chain structure models of the asymmetric half molecule were constructed with bond lengths and angles selected on the basis of resonance considerations (96), of quantum mechanical calculations (97-106), and of all available experimental data. The bond lengths along the conjugated chain were expected to be almost equal near the center of the molecule and graded towards the ends into almost pure single and double

bonds. Thus the distances would vary from 1.39 \AA . to a value of 1.46 \AA . for single bonds and 1.36 \AA . for double. These limiting values have been set at the experimental lengths for butadiene (115) rather than the theoretical one hundred percent single and double bonds of 1.54 \AA . and 1.33 \AA ., respectively. The bond angles along a conjugated chain are predicted to have the value $125^{\circ} 16'$ (96, 82). However the benzene molecule has a very high resonance energy with bond angles of 120° , therefore we cannot exclude the possibility of bond angles between these two limits. The difficulty encountered in constructing the models was to determine how the angles and distances change along the chain. The calculations of quantum mechanics (97-106) were helpful but in the end the assignments were largely arbitrary. Both wire frame models and ball and stick models with spheres of van der Waals radii were built with the configuration shown in Figure 7.

Trial structures were sought that satisfied packing requirements, that were consistent with the observed dichroism, and that gave reasonable agreement with the intensities of the strong reflections observed in the zero layers about all three axes. The absolute F values for the strongest reflections in these layers are listed below.*

*In this preliminary work unitary structure factors were compared with very rough relative intensity measurements. The absolute F values listed were obtained subsequently by the application of Wilson's method (10, 12) to hk0 data as described in the following paragraphs.

hk l	F	hk l	F	hk l	F
100	70	120	45	021	62
002	69	130	50	031	51
10 $\bar{2}$	67	140	50	041	90
20 $\bar{2}$	43	150	60	051	137
30 $\bar{2}$	79	160	55	061	78
				022	70

Total electrons per unit cell 588.

The plane of the half molecule was oriented in the trial structures approximately parallel to (101). There are two reasons for this selection. First, that the hk0 and Ok l Weissenberg photographs are very similar indicates that the molecule should lie approximately parallel to the plane (101), or to the plane (10 $\bar{1}$); h0 l reflections where l is odd are systematically absent and could not be used to determine which was the better choice. Second, light is most strongly absorbed when the electric vector is approximately parallel to [10 $\bar{1}$]. The angle of the chain with the ac plane was chosen to give large values to the structure factors for 041 and 051, and accordingly to 140 and 150, and yet to give reasonable van der Waals contacts between the half molecules related by the c glide plane. F's were calculated for numerous orientations of the molecule varied slightly from these directions. No good agreement was ever obtained between observed and calculated F's

for all of the strong reflections although the results seemed promising. The calculated values for 051 were recurrently low, and those for 031 were always too large. Study of the coordinates suggested that the molecule should be tilted more toward the direction of the \bar{b} axis. This, however, created packing problems with the models used, and also led to low values for the structure factors 100 and 002.

The intensities of all $hk0$ reflections were estimated with the use of intensity strips and multiple film Weissenberg photographs exposed with the characteristic X-radiation from a copper target.* The observed intensities were corrected for Lorentz and polarization factors and then placed on an absolute scale by the method of Wilson (10, 12). The relative intensities of 62 reflections were obtained, up to a limiting value of $\sin\theta$ equal to 0.73. About 80 reflections were unobserved because of low scattering.** The high thermal motion present in this compound is indicated by the

*The reflection 020 has such a low value of $\sin\theta$ that it was obscured by the beam stop, and special techniques were later employed to estimate its intensity.

** This particular set of films was unfortunately rather poor. A later set of Weissenberg films taken under identical conditions but with a better crystal and with longer exposure have over 115 measurable reflections. Taylor reported the intensities of 50 out of 75 possible $h0l$ reflections in his study of β -carotene, and it appears that the yield from the later films compares favorably with Taylor's.

large exponent, $B=8.9$, in the isotropic temperature factor found in this preliminary determination. Correlation of the $hk0$ intensities with the rough estimates of a few reflections from the zero layers about \bar{a} and \bar{b} gave the observed $|F|$'s listed above.

It was suggested that some information about the angle of inclination of the chain relative to (010) might be obtained from a two-dimensional Patterson. The available $hk0$ data were therefore used to make a Patterson series, $P(u,v)$. Inasmuch as the normal Beevers-Lipson strips used in making summations of this kind are not available for values of h greater than 20, the functions $\cos 2\pi hx$ and $\sin 2\pi hx$ were calculated for x at intervals of $1/180$ and for h from 0 to 30. From these tabulations of the trigonometric functions Beevers-Lipson strips for the amplitudes needed were made for the summation over v . The summation over u was then carried out with the conventional strips in units of $1/60$. It was hoped that the Patterson would give some information about the distances in the chain which occur with high multiplicity and close to the origin in Patterson space. The summation was therefore carried out only for u from 0 to $\frac{1}{2}$ and for v from 0 to $\frac{1}{4}$; the asymmetric quarter cell extends from 0 to $\frac{1}{2}$ in both coordinates. The Patterson projection contained broad plateaus rather than sharply defined peaks and consequently

was of limited value. Among the various trial structures for which structure factors were calculated, those with the largest angle between the chain and the ac plane gave best agreement with the Patterson. The agreement would have been even better if the molecule had been more steeply inclined, as a study of the coordinates of these trial structures had previously indicated.

The problem still remained of finding a trial structure accurate enough to promise convergence to the correct structure. Trial and error methods using models were abandoned for two reasons. First, the configuration of the molecule was not known with certainty. Although a planar structure was expected for DHC, the chain is long enough to allow considerable departure from planarity and still maintain strong conjugation. It was not known how much reliability could be placed in the chemists' contention that the molecule is all-trans (60-64). The theoretical calculations (97-106) and what few experimental data were available (82, 96, 115) did not place very stringent limitations on the bond angles and bond lengths in a long conjugated chain. All of these factors served to make uncertain the configuration of the molecule, and particularly the location of the cyclohexene ring, since deviations from ideal parameters along the chain are apt to be cumulative. Second, the orientation

of the molecule had not been definitely established. Preliminary upper-layer data revealed that the 111 reflection was very strong, probably even stronger than 051. The interplanar spacing for 111 is 4.02 \AA , close to the thickness of a planar chain; e.g., the benzene ring is about 3.7 \AA thick. This seemed to indicate that the molecule is approximately planar and contained roughly in the plane (111). There remained the question of the angle between the basal plane ac and the chain of the molecule. The molecule might be steeply inclined or it might lie along the plane of maximum values for the structure factor 051; however, both orientations presented difficulties. If the molecule was inclined steeply, and it was perhaps reasonable to expect a molecule 30 \AA long to lie approximately along a 32 \AA axis, it was not obvious how 051 and 041 could have large F's. If the molecule was not steeply inclined, no way was apparent to obtain large F values for 100, 002, $10\bar{2}$, $20\bar{2}$, and $30\bar{2}$. If the chain was inclined to lie approximately along 051, the models could not be correct, because they would not pack in that orientation. A three-dimensional Patterson was adopted as the method most likely to give a suitable trial structure, since it does not require extensive knowledge of the structure.

Most of the foregoing paragraphs were contained in a report on the structure determination made prior to the

calculation of the three-dimensional Patterson and before the structure had been solved. In retrospection perhaps a few comments may be pertinent. Structure factors were calculated for small positional variations of all kinds from the location described as follows. The half molecule was oriented so that its projection onto the ac plane, looking along $-\bar{b}$, was a few degrees to the right of $[\bar{1}01]$. The mean length of the half molecule was inclined 20° upward from (010) and the molecule was twisted about its axis so that the double bonds, which were approximately parallel to the ac plane, projected onto (010) in the direction of the \bar{E} vector for maximum absorption of polarized light, viz. ca 5.5° to the left of $[\bar{1}01]$. This corresponded to the molecule roughly contained in the plane (111) and gave large positive values to the structure factor for 100. In its correct orientation the molecule proves to be projected to the left of $[\bar{1}01]$, inclined 27° to (010), and twisted to the left so that the double bonds remained projected as before. This orientation gives a negative structure factor for 100 and places the molecule in $(1\bar{1}1)$, which is crystallographically equivalent to (111). The general features of the configuration of the molecule in the unit cell, derived from very limited data, were correct, but the details were wrong. The models used were also incorrect in some features; principally in that the

half molecule turned out to be about $3/4 \text{ \AA}$. too long, and that the configuration of the ring relative to the chain had to be considerably altered. It is now the author's conviction that, with suitable improvements in technique, the correct solution could have been made using zero-layer data. This matter will be discussed in more detail after the description of the three-dimensional Patterson and the determination of the correct structure.

C. The Collection and Correlation of Three-Dimensional Data

Complete three-dimensional data were collected at -20° C. using equi-inclination Weissenberg techniques. Chromium $K\alpha$ X-radiation was used for the zero layers and iron $K\alpha$ for all others. The high temperature factor limits the data obtainable with copper X-radiation. The reduced temperature was used to lower the rate of air oxidation and to intensify the coherent scattering of X-rays. The intensities of all reflections were estimated visually by comparison with standard intensity strips. The film factors for both iron and chromium $K\alpha$ radiations are so high that multiple exposures were required rather than the multiple film techniques conventionally employed with the harder copper X-rays. This requires an experimental evaluation of the film factors between successive films of each layer, from three to five such determinations per layer. The diffraction spots resulting from the thin flat plates of DHC were poor for intensity work; they were not consistent in size or shape either from layer to layer or even within a given layer. As a result several intensity strips were used, having spots of different size and shape, the correlation between them being experimentally established. An additional problem was the rather high background of incoherent scattering over which all comparisons of intensity had to be made. The net result was a difficult and

time consuming process of intensity estimation that at very best could not be expected to give exceedingly accurate results. Many of the reflections were rechecked in the process of determining the film factors, and two of the higher layers were estimated twice, once with films exposed with chromium $K\alpha$ and once with photographs taken with iron X-radiation. Some quantitative estimate of the reliability of the intensity data will be made after the correlation of data is discussed.

Most of the calculations described in the following pages were carried out by straightforward operations with the Type 604 IBM electronic computer. For the most part the calculations are too simple to warrant any detailed discussion. The problems of crystallography require the evaluation of several standard functions, some of which cannot be expressed in closed form. A number of these functions have been evaluated for small intervals of some suitable variable and are stored in master decks from which they are gang punched onto detail cards when needed. Cards are thus available for the atomic form factors vs. $\sin\theta/\lambda$, for e^{-x} vs. x , for $\cos\theta/(1 + \cos^2 2\theta)$ vs. $\sin\theta$, etc. The sorting, collating, and gang punching procedures using these cards are but routine IBM operations and deserve no further mention. The same may be said for a number of standard calculate panels that are

available for evaluating the sines and cosines used to obtain structure factors and in least-squares refinements, and for taking square roots by successive application of Newton's method.

The observed relative intensities and indices were hand punched into IBM cards along with suitable code punches which indicated the axis of rotation, layer, and the radiation used. A separate card was used for each intensity measurement. The minimum estimated intensity was code punched into the cards for unobserved reflections, except for space group extinctions; this provided an upper limit to the intensity of these reflections. $\sin^2\theta$ values were then calculated from the following expression,

$$\begin{aligned} \sin^2\theta_{(hkl)} = & h^2(b_1^2\lambda^2/4) + k^2(b_2^2\lambda^2/4) + l^2(b_3^2\lambda^2/4) \\ & + hl(b_1b_3\lambda^2\cos\beta_2)/2 \end{aligned}$$

where θ is the Bragg angle, h , k , and l are the indices of the reflection, b_1 , b_2 , b_3 , and β_2 are the reciprocal lattice parameters, and λ is the wave length of the radiation used. Calculations of $\sin\theta$, $(\sin^2\theta - \sin^2\gamma)^{\frac{1}{2}}$, $\sin^2\theta/\lambda^2$, and $\sin\theta/\lambda$ were carried out. The reflection cards were then sorted on $\sin\theta$ and collated with the deck

containing $\cos\theta/(1 + \cos^2 2\theta)$, and a single operation with the 604 was sufficient to make the following calculation,

$$I^{\text{red}} = I_0 \sqrt{\sin^2 \theta - \sin^2 \gamma} \frac{\cos \theta}{1 + \cos^2 2\theta}$$

where γ is the equi-inclination angle. This corrected the observed relative intensities I_0 for Lorentz and polarization factors and gave the reduced intensities I^{red} .

Average scale factors for correlating the two layers of data taken both with iron and chromium radiations were calculated. The intensities were placed on the same scale, common reflections were averaged, and the resulting values were reproduced onto single cards. Minimum intensities were retained for the unobserved reflections.

The correlation of the various layers about the three axes was carried out by an iterative procedure that is essentially equivalent to the method of least squares. The majority of the intensity measurements were made on Weissenberg photographs taken about the shorter a and c axes. All layers with equi-inclination angles up to 45° were photographed for these axes. This included h and l

up to the fifth order. Only the zero and first layers were taken about the long b axis to complete the three-dimensional coverage. The ratios

$$R_{a_h^b k} \equiv \frac{I_{(hk\ell)}^b}{I_{(hk\ell)}^a} \equiv \frac{1}{R_{b_k^a h}}$$

were calculated for all multiply observed reflections, where a and b are the axes of rotation, h and k are the corresponding layers, and I^a and I^b are the reduced relative intensities. These ratios were averaged over the missing index, ℓ in the case above, to give mean values $\bar{R}_{a_h^b k}$. The very weak, and a few very strong reflections that were in serious disagreement with the mean were neglected in this averaging process.

The b axis layers contain only a relatively few reflections and thus the ratios $\bar{R}_{a_h^b k}$ and $\bar{R}_{b_k^c \ell}$ were multiplied to give $\bar{R}_{a_h^c \ell}$ values which were weighted proportionally to the number of reflections and averaged with the directly observed $\bar{R}_{a_h^c \ell}$ terms. The resulting mean values for the various layers of the a and c axes form an overdetermined group that must be made self-consistent. The following expression was used to calculate a set of best values for these ratios,

$$R_{a_i c_j}^1 = \frac{3n\bar{R}_{a_i c_j} + \sum_h \sum_k \frac{m + o + p}{3} \bar{R}_{a_i c_k} \bar{R}_{c_k a_h} \bar{R}_{a_h c_j}}{3n + \sum_h \sum_k \frac{m + o + p}{3}} ,$$

(k ≠ j)
(h ≠ i)

where n is the number of reflections included in $\bar{R}_{a_i c_j}$,

m	"	$\bar{R}_{a_i c_k}$
o	"	$\bar{R}_{c_k a_h}$
p	"	$\bar{R}_{a_h c_j}$

The $R_{a_i c_j}^1$ terms thus calculated were weighted unity and were made self-consistent by a successive evaluation of the expression,

$$R_{a_i c_j}^r = \frac{1}{26} \left(R_{a_i c_j}^{r-1} + \sum_h \sum_k R_{a_i c_k}^{r-1} R_{c_k a_h}^{r-1} R_{a_h c_j}^{r-1} \right)$$

(k ≠ j)
(h ≠ i)

By the third iteration of this equation, viz. r-4, the individual terms of this sum had a maximum deviation of less than 1% from the mean and an average variation of only about 0.25%. Two typical sets of terms from the

r= 4 iteration are listed below, along with the maximum and mean deviations,

ikhj	R^4		ikhj	R^4	
5--4	1.558	$= R_{54}^3$	0--2	0.622	$= R_{02}^3$
5004	1.566		0012	0.622	
5014	1.566		0022	0.620	
5024	1.569		0032	0.620	
5034	1.566		0042	0.619	
5044	1.566		0052	0.617	
5104	1.559		0112	0.622	
5114	1.557	$R_{54}^4 = 1.562$	0122	0.622	$R_{02}^4 = 0.620$
5124	1.565		0132	0.619	
5134	1.557		0142	0.621	
5144	1.564	$\text{Max. } \frac{\Delta R}{\bar{R}} = 0.58\%$	0152	0.620	$\text{Max. } \frac{\Delta R}{\bar{R}} = 0.65\%$
5204	1.554		0312	0.622	
5214	1.553		0322	0.621	
5224	1.561	$\text{Avg. } \frac{\Delta R}{\bar{R}} = 0.25\%$	0332	0.623	$\text{Avg. } \frac{\Delta R}{\bar{R}} = 0.25\%$
5234	1.560		0342	0.620	
5244	1.562	\bar{R}	0352	0.622	\bar{R}
5304	1.554		0412	0.622	
5314	1.553	Original	0422	0.619	Original
5324	1.559	Direct	0432	0.619	Direct
5334	1.562	Observation	0442	0.619	Observation
5344	1.558	1.581	0452	0.620	0.591
5504	1.570		0512	0.621	
5514	1.567		0522	0.616	
5524	1.562		0532	0.619	
5534	1.568		0542	0.616	
5544	1.563		0552	0.616	

No further iteration was deemed necessary in view of the consistency of the terms above. All of the intensities were placed on the scale of the zero layer of the a axis. The 36 numbers determined by the procedure outlined above gave directly or by simple calculation the ratios $R_{a_{ccl}}^*$ and $R_{a_{oh}}^*$ which are the reciprocals of the scale factors for reduction of the a and c axis data to a common basis. Reciprocal scale factors for the two b axis layers were calculated as follows,

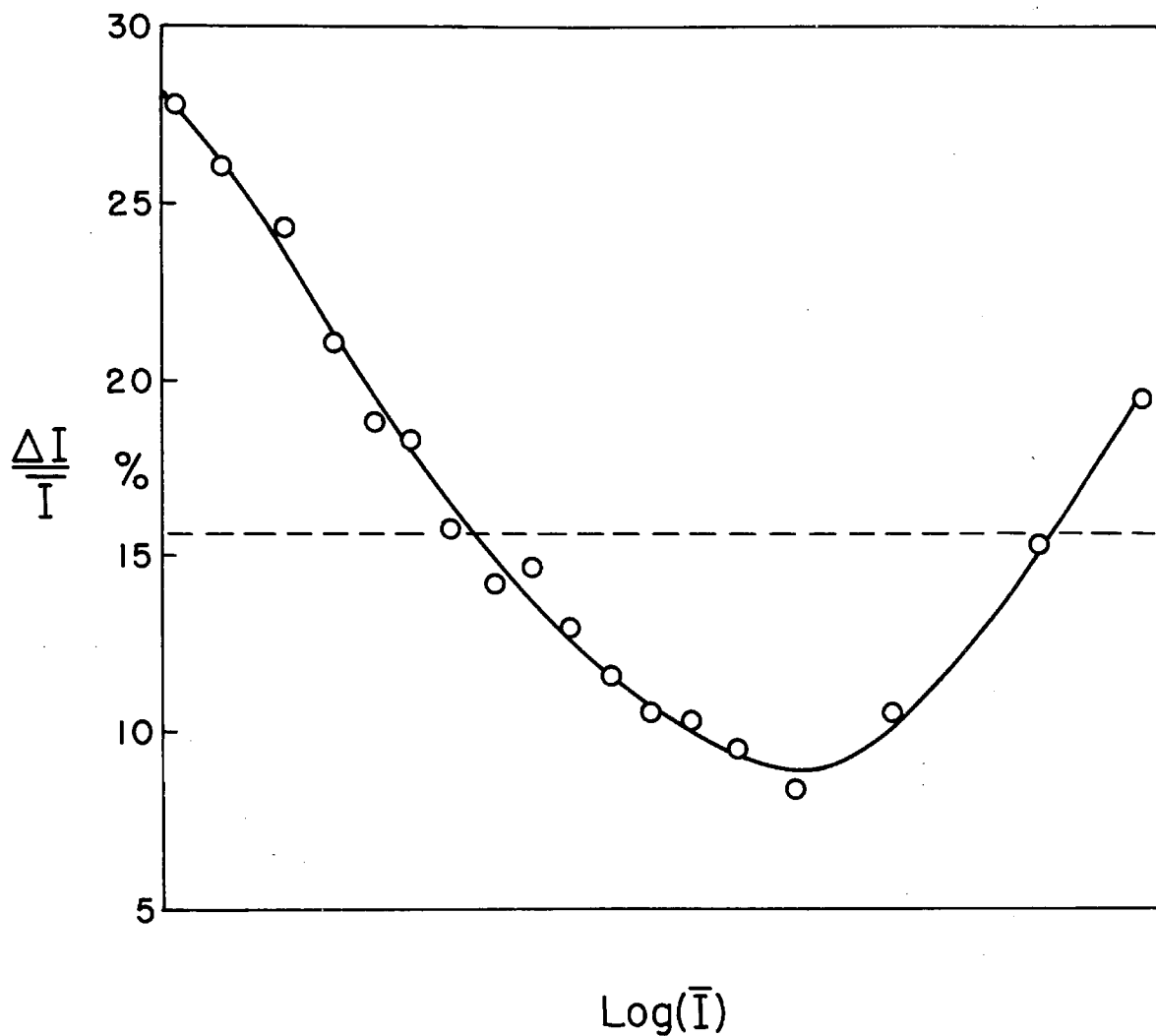
$$R_{a_0 b_k}^* = \frac{n \bar{R}_{a_0 b_k} + \sum_h m \bar{R}_{a_0 a_h}^* \bar{R}_{a_h b_k} + \sum_l p \bar{R}_{a_0 c_l}^* \bar{R}_{c_l b_k}}{n + \sum_h m + \sum_l p}$$

where n is now the number of reflections included in $\bar{R}_{a_0 b_k}$

m	"	$\bar{R}_{a_h b_k}$
p	"	$\bar{R}_{c_l b_k}$

The intensities of the reflections in the various layers were multiplied by the appropriate scale factors to bring all data to the same scale of relative intensity. The intensities of multiply-observed reflections were averaged, while the smallest I^{red} values were retained for the unobserved reflections.

A measure of the self-consistency of the data is given by the quantity $\Delta I / \bar{I}$, where ΔI is the difference in reduced relative intensity for two observations of the same reflection and \bar{I} is their mean value. Figure 8 shows a plot of the mean value of $\Delta I / \bar{I}$ vs. $\log (\bar{I}_{\text{avg.}})$ for two overlapping groups of the 829 multiply-observed reflections. Each point, except for the two at the ends of the curve, represents the mean of 100 reflections. The $\log(\bar{I})$ has no particular significance here but is merely used to reduce the scale of the drawing. The curve drawn in Fig. 8 is



PLOT OF $\frac{\Delta I}{I}$ VS. $\text{LOG}(\bar{I})$ FOR TWO OVERLAP-
PING GROUPS OF THE MULTIPLY OBSERVED
REFLECTIONS.

FIGURE 8.

typical of visual intensity data, with the poorest agreement found for very weak and for very strong reflections. The very weak reflections are inherently difficult to estimate and are thus subject to large absolute errors; as a rule they are only measured once on the most heavily exposed film so that there is no intralayer cross check of intensities. Very strong reflections are mostly of low $\sin\theta$ where the spots are badly distorted, especially on nonzero layers. Their relative intensities depend upon a number of experimentally evaluated film factors, and some of these may be based on only a very few common reflections. The intensities of medium and moderately strong reflections therefore have the greatest reliability as shown in Figure 8. The overall average value of $\Delta I/\bar{I}$ is 15.7%, marked by the dotted line of Figure 8, which indicates a well correlated set of data. The graph shown serves two useful purposes. First, it indicates an upper limit to the accuracy of the data; since most of the intensities were based on two readings, the standard deviations $\sigma I/\bar{I}$ are one-half of the values shown on the curve; there may be other errors which increase the standard deviation but the data alone have an average value of 8%.* Second,

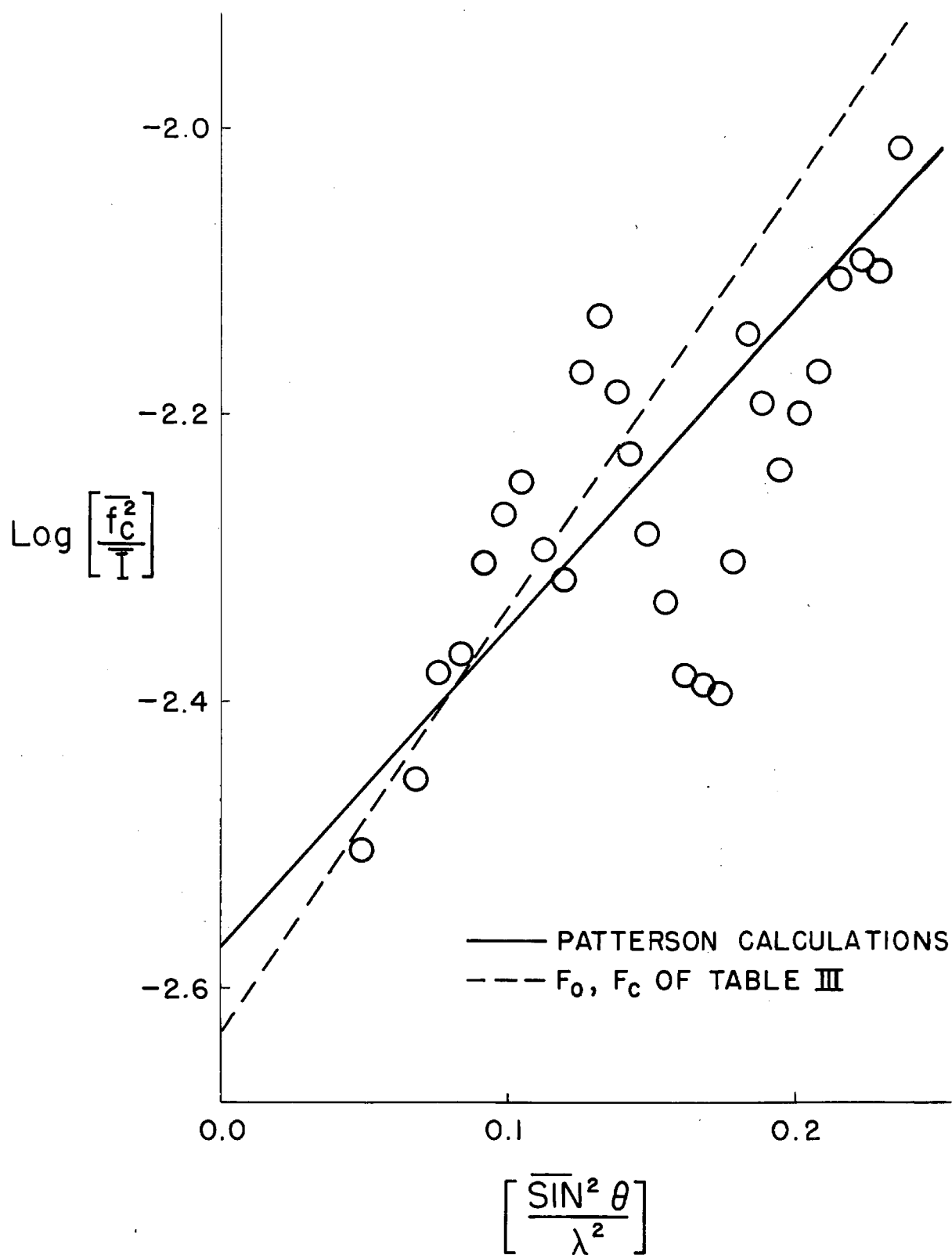
*Actually the data may even be better than indicated by this standard deviation. The majority of the multiply-observed reflections were estimated on \bar{a} and \bar{c} axis photographs, and most of the medium and moderately strong reflections were measured twice or three times in each layer so that \bar{I} is really the mean of from 4 to 6 measurements.

the graph provides a basis for weighting the $F_o - F_c$ terms in a least-squares refinement.

Wilson's method was employed in an effort to place the reduced relative intensities on an absolute scale and to obtain an isotropic temperature factor for use in calculating a three-dimensional Patterson with the inter-atomic interactions sharpened and with the peak at the origin removed. For DHC Wilson's method can be expressed in the equation.

$$\log \left[\frac{\overline{f_c^2}}{\overline{I}} \right] = \log (a/80) + 2B \frac{\overline{\sin^2 \theta}}{\lambda^2} (\log e)$$

where a is the scale factor to absolute F^2 , B is the isotropic temperature factor for correcting the atomic form factors, and f_c is the atomic form factor for carbon (116). This equation expresses the linear relation between $\overline{\sin^2 \theta / \lambda^2}$ and $\log(\overline{f_c^2 / I})$ when the quantities f_c^2 , I , and $\sin^2 \theta / \lambda^2$ are averaged over a small region of $\sin \theta$. The intercept of the straight line gives the scale factor a , and the slope the isotropic temperature factor B . Figure 9 shows the plotted values of the above expression for the DHC data. The reflections were arranged in order of increasing $\sin \theta$ and were averaged in intervals of one hundred reflections to give one group of values. The procedure was



PLOT OF WILSON'S METHOD FOR TWO OVERLAPPING GROUPS OF REFLECTIONS.

FIGURE 9.

repeated for a second group after removing the fifty reflections with lowest $\sin\theta$ so that this group overlapped the first. The deviation from linearity of Wilson's statistical method is apparent in the figure, and the reasons therefor will be discussed in the final section. The two straight lines drawn on the graph were derived in a rather arbitrary manner. The solid line, which has $a = 0.217$ and $B = 2.56$, represents the values of the scale and temperature factors used to calculate the three-dimensional Patterson. The dotted line, with $a = 0.1875$ and $B = 3.41$, corresponds to the values used to obtain the observed and calculated structure factors of Table III, in part I of the appendix. The value 3.41 for the exponent in the isotropic temperature factor is probably low, if we consider the high incoherent scattering from the DHC crystals, and the value for the completely refined structure may well be larger than this. The plot above gave only very general values for a and B , and the selection of these quantities for use in calculating the three-dimensional Patterson function will be considered in the following section.

D. The Three-Dimensional Patterson Function

A three-dimensional Patterson with the peak at the origin removed and with the interatomic interactions sharpened requires absolute F^2 values and the temperature factor. The Patterson function may be defined as follows,

$$P(uvw) = \frac{1}{V} \sum_{h=-\infty}^{\infty} \sum_{k=-\infty}^{\infty} \sum_{l=-\infty}^{\infty} |F_{(hkl)}|^2 \cos 2\pi(hu + kv + lw).$$

If the temperature factor is assumed to be isotropic,

$F_{(hkl)}$ may be written,

$$F_{(hkl)} = e^{-\frac{B \sin^2 \theta}{\lambda^2}} \sum_{i=1}^n f_i e^{2\pi i(hx_i + ky_i + lz_i)}.$$

Assuming the f 's to be real we may write,

$$|F_{(hkl)}|^2 = F_{(hkl)} F_{(hkl)}^* = e^{-\frac{2B \sin^2 \theta}{\lambda^2}} \left[\sum_{i=1}^n f_i^2 + \right.$$

$$\left. \sum_{\substack{i \neq j \\ i > j}}^n \sum_{j=1}^{n-1} 2f_i f_j \cos 2\pi(hu_{ij} + kv_{ij} + lw_{ij}) \right],$$

where, $u_{ij} = x_i - x_j$, $v_{ij} = y_i - y_j$, and $w_{ij} = z_i - z_j$. These are simply the coordinates of the vector between the i th and the j th atoms. Substituting the expression for $|F(hk\ell)|^2$ into $P(uvw)$ and rearranging terms gives

$$\begin{aligned}
 P(uvw) = & \frac{1}{V} |F(000)|^2 + \frac{1}{V} \sum_h \sum_{\substack{k \\ -\infty}}^{\infty} \sum_{\ell} [\exp(-2B \sin^2 \theta / \lambda^2)] \sum_i^n f_i^2 \cdot \\
 & [\cos 2\pi(hu + kv + \ell w)] + \frac{1}{V} \sum_h \sum_{\substack{k \\ -\infty}}^{\infty} \sum_{\ell} \exp(-2B \sin^2 \theta / \lambda^2) \sum_2^n \sum_{\substack{i \neq j \\ i > j}}^{n-1} f_i f_j \cdot \\
 & \left(\cos 2\pi[h(u - u_{ij}) + k(v - v_{ij}) + \ell(w - w_{ij})] + \right. \\
 & \left. \cos 2\pi[h(u + u_{ij}) + k(v + v_{ij}) + \ell(w + w_{ij})] \right).
 \end{aligned}$$

The second term of this expression gives the large peak at the origin of Patterson space. The third term gives the peaks at $\pm (u_{ij}, v_{ij}, w_{ij})$ corresponding to all interactions within the unit cell. Consider the contribution of the various terms of this expression at $u = v = w = 0$.

Wilson's statistical argument assumes that the average of the third term over a small range of $\sin \theta$ will be nearly zero. In the case of DHC this is found to be not valid. The question then remains, can the term be neglected if all reflections are totaled? If so we may write, omitting $F_{(000)}^2$,

$$VP'(000) = a \sum_h \sum_k \sum_{\ell}^{\infty} I_{(hk\ell)}^{\text{red}} = \sum_h \sum_k \sum_{\ell}^{\infty} \sum_l^n f_l^2 e^{-\frac{2B \sin^2 \theta}{\lambda^2}}$$

The assumption that the contribution from all of the interaction peaks to the peak at the origin is negligible may well be no more valid than the assumptions of Wilson's statistical argument. However, the above equation can be evaluated without difficulty or ambiguity, and although the a and B factors obtained may not be very accurate they can be used as approximate values. It is perhaps worth pointing out that this procedure cannot be used for two-dimensional data since peaks in Patterson space can project into the region of the origin. The method suffers from two further disadvantages: first, the effects of series termination are not known; this, however, may not be particularly serious; second, errors of large magnitude may occur in the intensity estimates of the strong reflections, and if these are not random, as well may be the case, they could introduce serious discrepancies. Despite the limitations the method was employed to obtain the scale factor of 0.217 and the exponent for the isotropic temperature factor of $B = 2.56$. The value of $B = 2.56$ was believed too low; however, this influences the Patter-

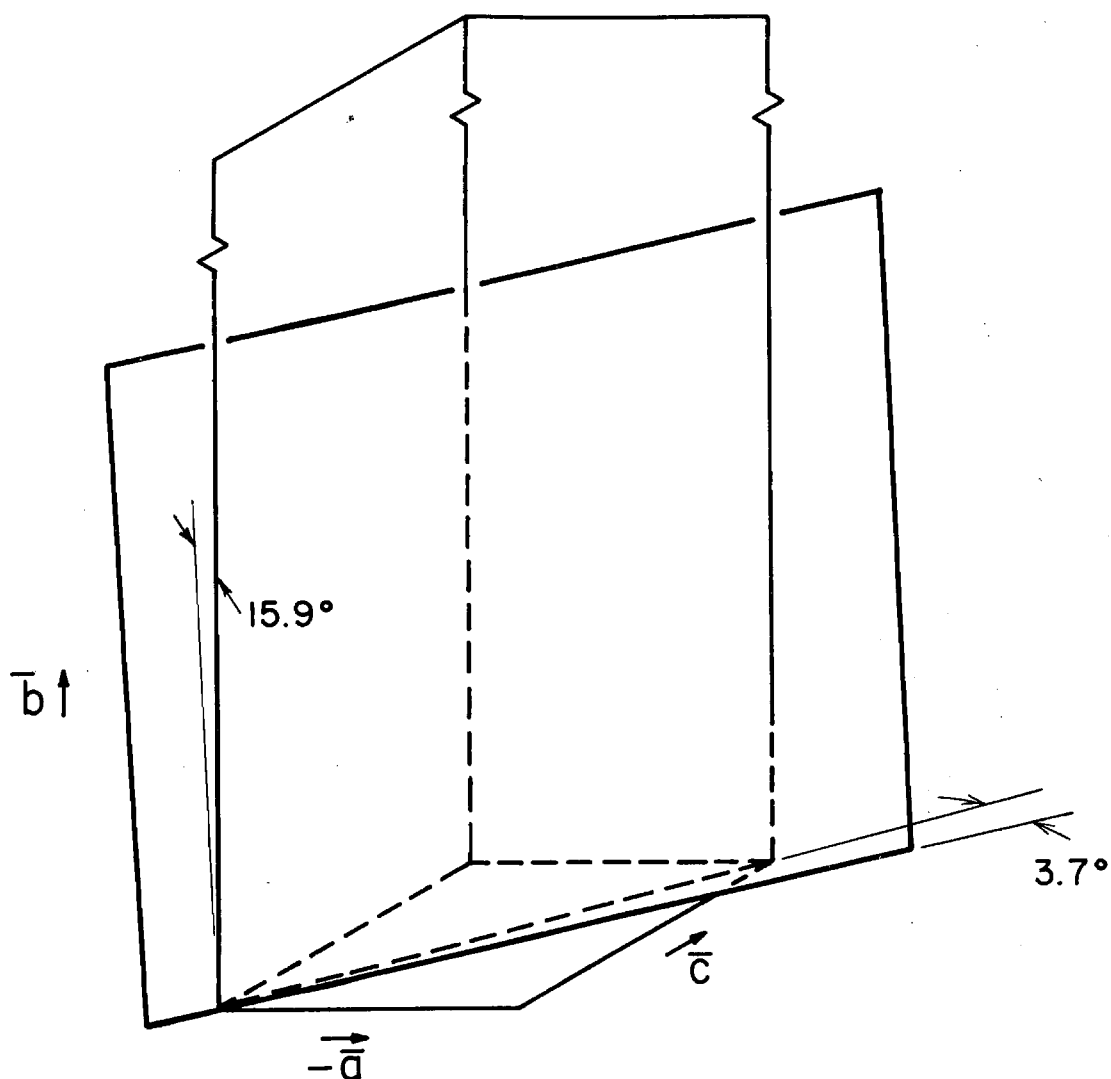
son principally in reducing the effect of peak sharpening and this was not regarded as particularly undesirable.

The modified terms $\hat{F}_{(hkl)}^2$ used in calculating the Patterson function were obtained from the following expression,

$$\hat{F}_{(hkl)}^2 = \frac{F_{(hkl)}^2 - (80 f_C^2 + 108 f_H^2) e^{-\frac{2B \sin^2 \theta}{\lambda^2}}}{f_C e^{-\frac{B \sin^2 \theta}{\lambda^2}}} .$$

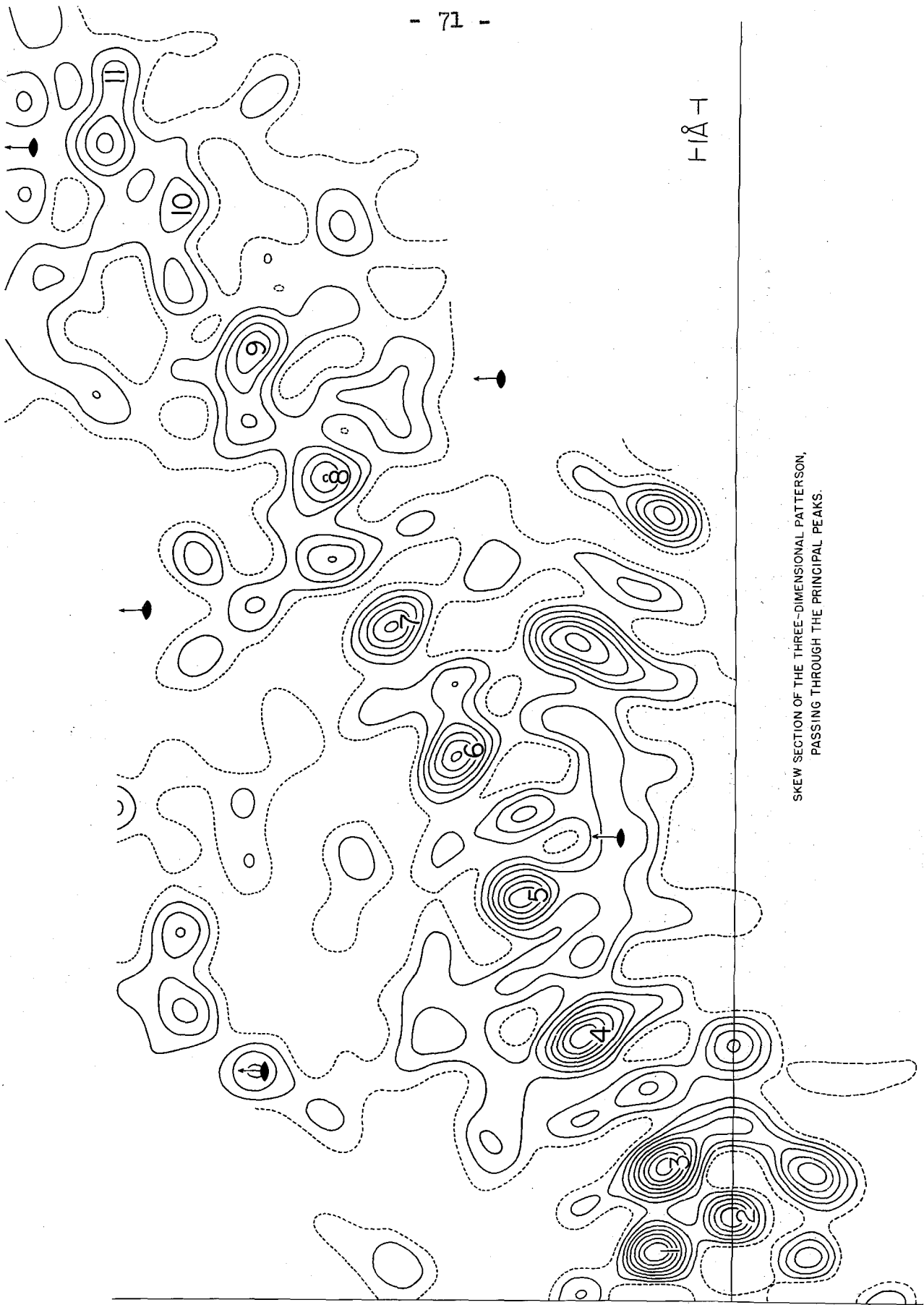
Throughout the calculation of reduced intensities and the correlation of data the lowest observable intensity was retained as an estimate for each missing reflection. This represents an upper limit for the square of the calculated structure factor. Missing reflections were included in the Patterson at half of this value. A modified M-card system was used to evaluate the Patterson in 180ths for *v* and 60ths for *u* and *w* over the asymmetric quarter cell which extends from *u* = 0 to 1, *v* = 0 to $\frac{1}{2}$, and *w* = 0 to $\frac{1}{2}$. The M-card system allows a systematic summation of the contributions from the 1811 reflections at each of the 162,000 points in Patterson space. Most of the values for these points were plotted on prepared grids 60 by 30 units parallel to the *ac* plane.

The Patterson contains a number of large, approximately coplanar peaks that can be assigned to the C-C bond, to the C=C bond, to the $\text{C}=\text{C}^{\nearrow}\text{C}$ distance, which we shall designate by the symbol Q, and to multiples of the latter distance. The plane passing through these peaks is inclined 15.9° to the b axis, and its intersection with the ac plane makes an angle of 3.7° with the direction $[\bar{1}01]$, as shown in Figure 10. This skew section of the three-dimensional Patterson is shown in Figure 11 with some of the important peaks numbered. The symmetry elements in this figure are two-fold axes which are inclined at an angle of 15.9° to the plane of the paper and pass up through the skew section; see Figure 10. A similar two-fold axis passes through the origin, which is also a center of symmetry. Peaks corresponding to the single bond, 1, the double bond, 2, and to the vector Q and multiples thereof, 3, 4, 5, - - -, are all clearly resolved in the section. The amplitudes of these peaks are in rough agreement with their expected multiplicities. The bond lengths of 1.46 \AA. for C-C, 1.37 \AA. for C=C, and 2.43 \AA. with a bond angle of 120° for Q are reasonable values for a conjugated system. The single bond-double bond combination Q, which describes the direction of the molecule is inclined 27° to the ac plane.



A DRAWING OF THE UNIT CELL OF DHC SHOWING THE ORIENTATION OF THE PLANE PASSING THROUGH THE PRINCIPAL PEAKS OF THE THREE-DIMENSIONAL PATTERSON.

FIGURE 10.



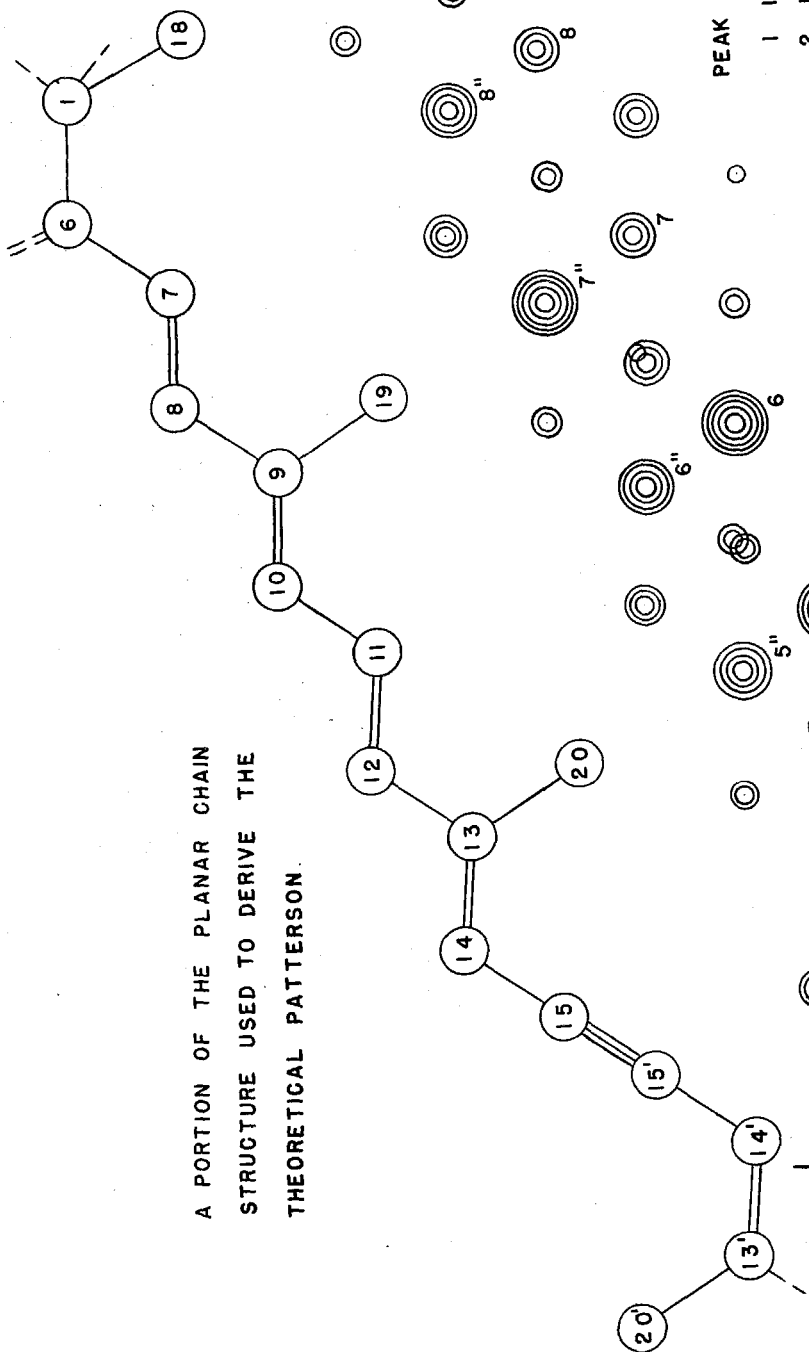
SKEW SECTION OF THE THREE-DIMENSIONAL PATTERSON,
PASSING THROUGH THE PRINCIPAL PEAKS.

Figure 11.

The Patterson function of a complicated molecule such as DHC, containing no heavy atoms, will exhibit only peaks resulting from the superposition of several interactions. The planar conjugated chain structure of DHC will have a number of similar distances giving rise to large peaks with the maxima located at some average position. Inter-molecular interatomic vectors will be much more randomly distributed in space, and most of the peaks of Figure 11 must be accounted for by the interactions within one molecule. Considerable departure from the average bond length and direction, as given by the location of the peaks, is possible for any specific interaction.

The general features of the Patterson are clearly shown in Figure 11, but a more detailed analysis of the section reveals that the superficial interpretation is not completely correct. Figure 12 shows a vector diagram of the coplanar chain atoms of a plausible molecule of DHC which has the Q vectors roughly collinear. This drawing, which is to the same scale as Figure 11, also shows part of the molecule used to derive the vector map and a list of representative interactions for some of the peaks. This illustration is very similar to Figure 11, especially in the region near the origin. For example, peaks 1 to 6 and a to h of Figure 12 can all be located in the observed Patterson. There are also features of disagreement. First,

A PORTION OF THE PLANAR CHAIN
STRUCTURE USED TO DERIVE THE
THEORETICAL PATTERSON.



PEAK INTER-
ACTION

PEAK INTER-
ACTION

PEAK INTER-
ACTION

8 14'-18
d 9-19
b 14-20
c 7-18
d 12-19
e 19-8
f {14'-15
20-11
g 20-10
h {13-10
13'-15
j 14-9

5" {20-7
14'-11
5 {13-7
20'-12
6" 14'-9
6 {20-18
15-7
20'-10
7" 14'-7
7 20'-8
8" 13'-6

1 11-10
2 12-11
3 12-10
4" {20-9
14'-13
13-9
20-19
4 {14-10
20'-14

H1A-T

A THEORETICAL PATTERSON OF THE COPLANAR CHAIN ATOMS
OF ONE MOLECULE OF DHC WITH APPROXIMATELY COLLINEAR
 $C \equiv C \rightarrow C$ BONDS. EACH CONTOUR REPRESENTS 4 INTERACTIONS

Figure 12.

Figure 12 shows a definite break in the line of strong peaks from 6 to 7". This step, which corresponds to the $C\equiv C-C$ distance, is not present in Figure 11. Second, Figure 12 has a pair of peaks of roughly equal amplitude derived from peaks 4, 5, 6, - - -, by the addition and subtraction of the $C=C$ distance, e.g., peaks h and j. The similar peaks of Figure 11 show considerable disparity.* The explanation of these discrepancies lies in what is perhaps the most striking point of similarity between the observed Patterson and the vector diagram, namely the periodic occurrence of peaks every 1.2 to 1.3 Å. along the mean direction of the molecule. If some angular variation is allowed in the interactions of Figure 12, the superposition of the "smeared" vectors can really lead to the Patterson of Figure 11. That is, the peaks of the observed Patterson result from the merging of the unprimed and double primed peaks of Figure 12, 6 with 6", 7 with 7", etc. That this is actually the case is evidenced by the elongated peak 4 of Figure 11. The angular spread of the large number of interactions involved in this peak is not enough

*These features of the Patterson were somewhat puzzling during the early stages of interpretation. The collinear group of peaks 3 to 11 would be typical of a molecule having no triple bond. Some form of asymmetry in peak amplitudes would be characteristic of a stepped molecule having the triple bond. The observed Patterson has some features of both types of structure and the DHC molecule satisfactorily explains the Patterson.

to allow resolution into two or more peaks but is sufficient to cause considerable distortion. The foregoing discussion means that the collinear peaks 3 to 11 of Figure 11 lie along the mean direction of the Q vectors and the interatomic vectors across the step due to the triple bond.

The Patterson yields quantitative information about the orientation of the molecule but does not give the coordinates of any specific interaction. The plane and average direction of the molecule are known, but the direction of the triple bond remains uncertain, and the location and orientation of the ring, which contains roughly half of the carbon atoms in the structure, is only approximately known. In summary it may be said that a great deal is known in general but almost nothing in detail.

With an angle of inclination of 27° from the ac plane one molecule will have little or no overlap with the molecule related by the c glide plane at $y = \frac{1}{4}$ when viewed normal to the \bar{b} axis. This coupled with the fact that the molecular plane is only slightly inclined to the \bar{b} axis mean that the projection of the molecule onto the plane (101) will be essentially resolved and relatively undistorted. Attention therefore turns in the next section to the projection along the zone [101], which is

only 2.9° from the normal to (101). The structural details of this two-dimensional projection will be sufficiently resolved to be capable of considerable refinement before recourse to three-dimensional data is necessary.

E. The Solution of a Projection of the Structure and
Its Refinement

A two-dimensional trial structure consistent with the Patterson was found by the projection of models onto (101) and by the use of $hk\bar{h}$ data with appropriate structure-factor maps. Certain of the $hk\bar{h}$ data were particularly useful in determining the preliminary structure. Within the limits of the three-dimensional Patterson some considerable leeway is available for the direction of the three collinear central bonds and consequently in the position of the cyclohexene ring. The very weak 020 reflection served to restrict the location of the ring to orientations where the atoms with the greatest y coordinate were below but very near to $y = \frac{1}{4}$. The direction and magnitude of the average $C = C \text{---} C$ vector as determined from the three-dimensional Patterson, and the structure factor maps for the strongest reflections of low order, $13\bar{1}$, $15\bar{1}$, $20\bar{2}$, $21\bar{2}$, and $24\bar{2}$, were sufficient to establish the length of the molecule in projection. With a knowledge of the molecular length and the y parameters of the ring atoms a compatible trial structure was constructed.

The three-dimensional Patterson confirmed the existence of an essentially planar structure with a number of nearly collinear atoms. The Fourier transform of such a regular array of atoms was expected to have peaks of large

amplitude in the region of high $\sin\bar{\theta}$ and consequently with small spacings. An examination of the intensities of the $hk\bar{h}$ data reveals a number of high order reflections with large unitary structure factors. Some of these reflections are listed in the table below.

h	k	Unitary structure factor	h	k	Unitary structure factor
5	15	51%	1	29	23%
5	10	28%	1	28	20%
5	12	28%	1	21	18%
5	16	26%	1	20	19%
4	13	23%	1	19	17%
4	17	18%	1	17	18%
4	25	22%	1	8	16%
3	17	19%	0	16	25%
2	29	16%	0	22	21%
2	25	22%	0	26	26%
2	19	15%			
2	17	27%			
2	13	22%			
2	12	28%			

Prof. Verner Schomaker suggested that the structure might be solved by an application of the mapping method first used by Lonsdale on hexamethylbenzene (117) and later by

White and Robertson on coronene (118). The method was tried, but proved to be of limited value because of the complexity of the line patterns that were obtained. An alternative procedure suggested itself, however; namely, that of using the method for refinement rather than as a means of directly determining the structure. After the fairly good trial structure had been obtained as outlined above, a modified mapping method was therefore used to refine the structure as follows. The projected structure, drawn on a transparent sheet, was superposed on the structure-factor maps of the high order hkh reflections which have large unitary structure factors. The probable signs were determined for as many of these reflections as possible; the chain atoms were given greater weight than those of the ring structure, because their positions were considered more reliable. A celluloid sheet was next placed over the structure-factor map for one of these reflections, and lines were roughly drawn with India ink along the 0.7 amplitude contour for the regions with correct sign. With the same celluloid sheet this procedure was repeated for each reflection whose sign could be established with reasonable certainty. Rectangles were drawn enclosing the entire areas of proper sign common to $5 \cdot 15 \cdot \bar{5}$ and $5 \cdot 16 \cdot \bar{5}$ with portions deleted as required by $0 \cdot 16 \cdot 0$. The drawing made in this manner is shown in Figure 13. The rectangular areas are shaded because of the

$\begin{matrix} \text{X}=\overline{1} \\ \text{Z}=\overline{1} \end{matrix}$

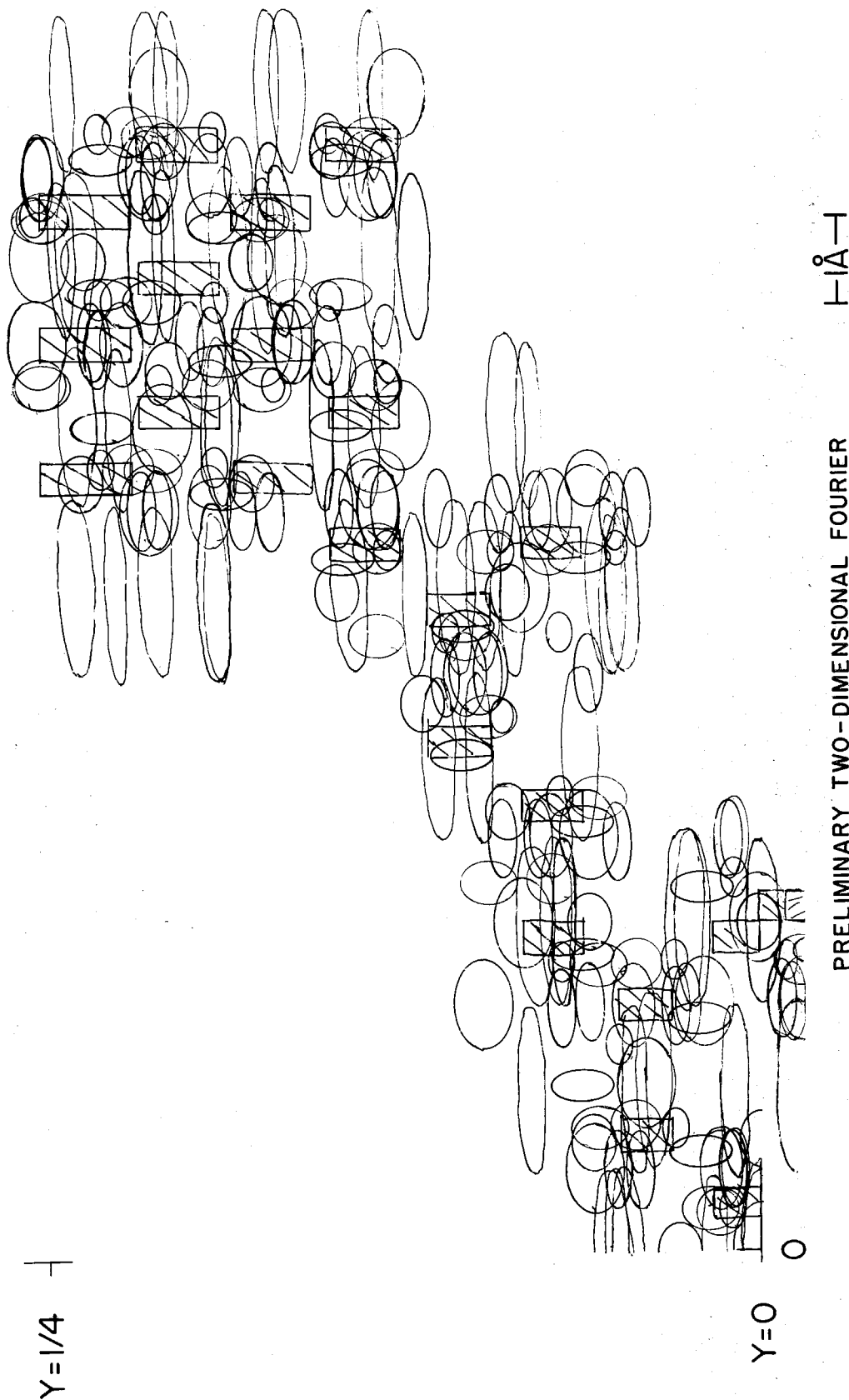


Figure 13.

extremely high unitary structure factor of $5.15\bar{5}$. On the composite map of Figure 13 the atoms are to be located within the maximum number of contours. The location of the peaks of this graphical summation may be compared with the refined atomic positions shown in Figure 15, page 84. The coordinates obtained from the map represent a high-order refinement of a structure that was presumed correct in its general features.

Further refinement of the projection was undertaken by the use of Fourier series. Several calculations of structure factors were made with variations in some of the ring and chain parameters. A number of Fouriers were evaluated with the resulting combinations of signs, and with permutations of the signs for some of the uncertain terms. In determining changes of parameters considerable use was made of the structure-factor maps of uncertain reflections. Chemical knowledge of expected bond lengths and angles was also applied when changes of atomic positions were necessary, particularly in smoothing out the bond lengths and angles along the chain by slight positional changes from the peaks of Fouriers. Chain atoms were well resolved in the Fouriers and their parameters were quickly refined. Certain of the atoms associated with the ring atoms, on the other hand, were very troublesome. The structure factors for most of the high order

reflections were in good agreement, but a few of the low order terms were not correct.

Throughout all of these stages of preliminary refinement, as in all earlier work, an all-trans chain structure was retained with the cyclohexene ring oriented in the trans configuration of Figure 14a. It soon became apparent that this orientation of the ring was impossible, and an inversion to the cis form of 14b was made. This was necessary to give correct values to $20\bar{2}$, 060, and 080

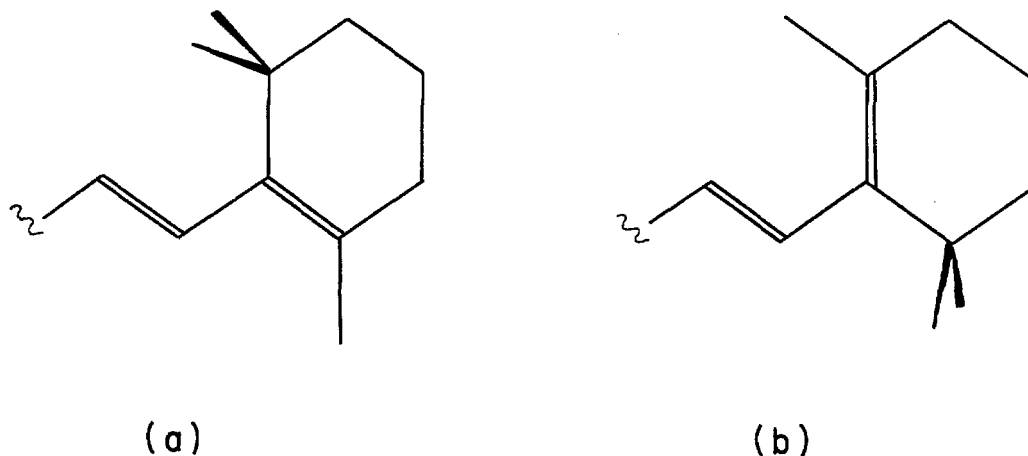


Figure 14. The configuration of the cyclohexene ring in (a) trans- β -ionylidene crotonic acid (114), (b) 15,15'-dehydro- β -carotene.

and a few other reflections of higher order. The inversion of the ring results primarily in the transposition of one atom; this brings about a marked improvement in the above low order reflections but does not affect the agreement already achieved for the high order terms. The trans ring orientation has recently been reported by MacGillavry, Kreuger and Eichhorn (114). This orientation of the ring was abandoned rather reluctantly, since some distortion of the ring and loss of conjugation will inevitably result. A plausible two-dimensional Fourier, similar to Figure 15 but with the ring inverted, can indeed be calculated if five or six structure factors are left out of the summation, but this only demonstrates the limitations of two-dimensional methods.

The change to the cis ring orientation was sufficient to reduce the two-dimensional reliability factor, R, where

$$R \equiv \frac{\sum_{hkl} \left| |F_o| - |F_c| \right|}{\sum_{hkl} |F_o|} = \frac{\sum_{hkl} |\Delta F|}{\sum_{hkl} |F_o|}$$

from 37% to 29%. Convergence thereafter was rapid, and Fourier refinement followed by two least-squares calculations sufficed to reduce the R factor to 19.9%.

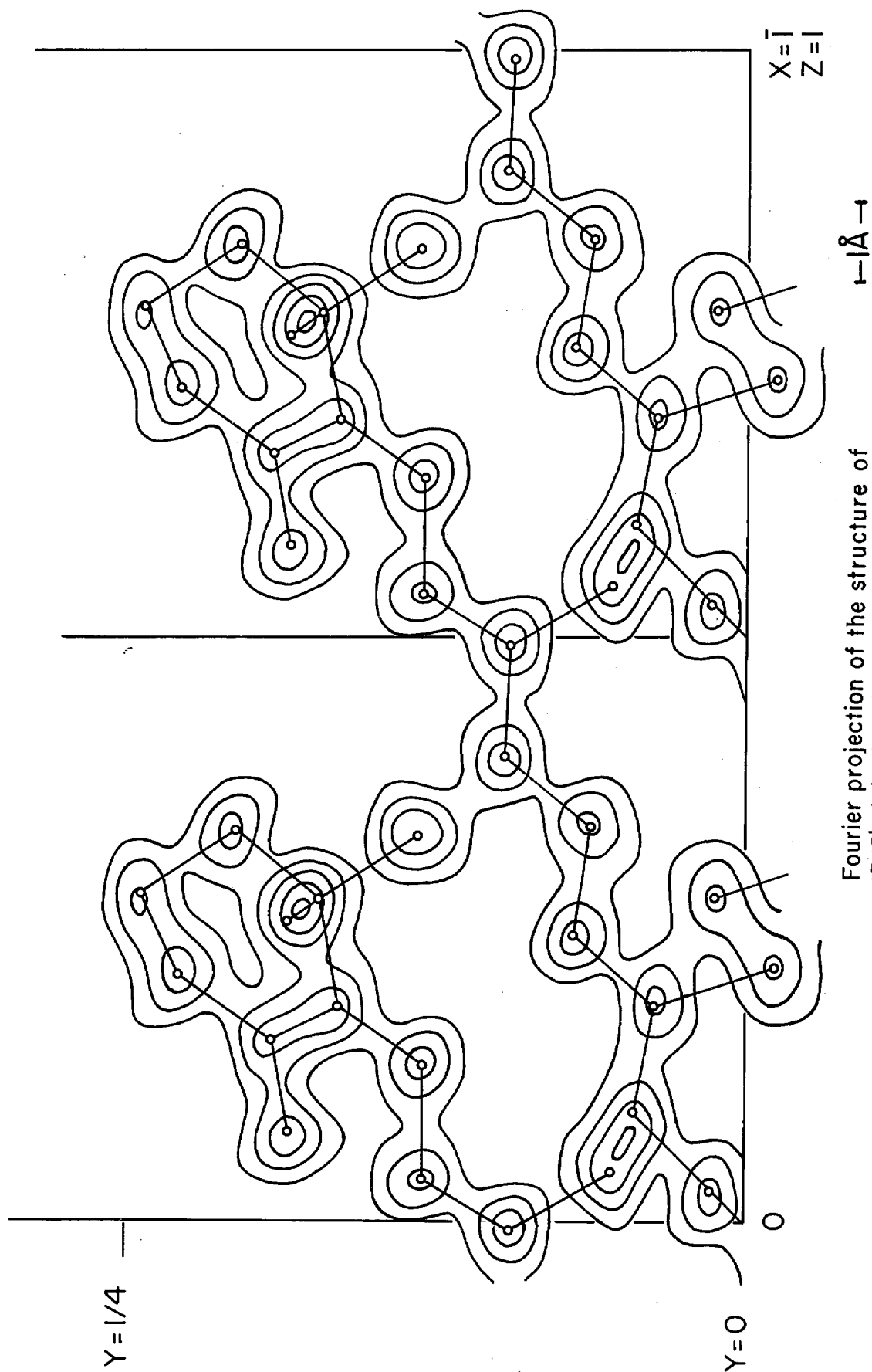


Figure 15.

The final Fourier projection along $[101]$ onto (101) is shown in Figure 15, with a superimposed drawing of the structure determined by least-squares refinement. The Fourier is very well resolved and the peak heights are all very nearly the same. No atomic coordinates y and r , where $r = z - x$, will be listed here but the parameters given in Table II, of the next section, obtained from a three-dimensional Fourier, are only very slightly different from those derived by the two-dimensional least squares. The results of further refinement with hkh data were not deemed commensurate with the time required, especially since a complete structure analysis will necessitate a three-dimensional Fourier or least squares treatment or both. Two-dimensional methods using hkh data were therefore abandoned at this point.

Part II of the appendix, page 184, contains a description of some of the IBM procedures used to calculate structure factors, least squares, and two-dimensional Fourier projections. This rather specialized information is specifically concerned with the refinement carried out in this section but it has more general application and was therefore not included in the text.

F. Three-Dimensional Refinement

Given the refined projection, since y and $z - x$ are known, the determination of a three-dimensional structure becomes principally a one-dimensional problem, that of finding $z + x$. The plane of the molecule must be assumed nearly coincident with the plane of the three-dimensional Patterson section described in Section D. Approximate three-dimensional parameters for the chain atoms were therefore obtained by back projection along $[101]$ from (101) to the plane shown in Figure 10, page 70. The cyclohexene ring shown in the $[101]$ projection of Figure 15 cannot be coplanar with the chain and the ring is also obviously puckered. Back projection could not be used for these atoms, and their coordinates were obtained from a special model constructed for this purpose of the ring structure and the last two atoms of the chain. This model was made with wires strung in the direction $[101]$ and located at the correct y and r coordinates. Lead beads were fixed on the wires so that they could be slid in the $[101]$ direction. The positions of the atoms were varied until a satisfactory set of bond lengths were obtained, and measurements of the positions projected along y were sufficient to give x and z for these atoms.

Refinement of this first set of three-dimensional coordinates by means of a and c axis projections proved to be of limited value. The R factor for the $hk0$, $h0l$, and $Ok1$ data was reduced from 42 to 37% by use of one set of a and c axis projections. These projections suffer from a lack of resolution because the molecule is considerably foreshortened in both, and because the zero layers were both photographed with chromium $K\alpha$ X-radiation and could not possibly give a resolution greater than $\lambda(0.61/2) = 0.69 \overset{0}{\text{\AA}}$. (119). The $h0l$, $Ok1$, and $hk0$ structure factors were calculated for two other structures having only moderate changes in ring and chain parameters in the $x + z$ direction. Both gave R factors of the order of 50.

Further refinement by means of a one-dimensional least squares calculation was considered, but abandoned in favor of a three-dimensional Fourier. The Fourier has the advantage over least squares procedures of showing that a structure is wrong while also giving some indication of the correct structure. With an R factor no lower than 37% for zero layer data the structure could still be wrong in some essential and the Fourier was judged most likely to expose the error.

A three-dimensional Fourier was calculated by straight-

forward application of M card techniques with y in 120ths and x and z in 60ths. The asymmetric unit extends from $y = 0$ to $\frac{1}{2}$, from $x = 0$ to 1, and from $z = 0$ to 1. The Fourier was plotted only in the positive regions, and $F(000)$ was left out of the summation. The results are summarized in the table on the following page which lists peak heights E and half-amplitude diameters A , B , and C for the twenty atoms of the structure. The diameters have been listed in terms of y , r , and $z + x$, since the major corrections in atomic position are expected in the last coordinate. Except in the regions associated with the atomic peaks the electron density was everywhere less than 1.1 electrons per \AA^3 .

The table also includes the corrections to the $z + x$ parameters obtained from the Fourier. These corrections were derived from the preliminary coordinates used to calculate the Fourier, and from the Fourier peaks as follows,

$$\Delta(z + x)_i = 1.2[(z + x)_i^F - (z + x)_i^P]$$

where $(z + x)_i^F$ is the $(z + x)$ coordinate of the Fourier peak of the i th atom, and $(z + x)_i^P$ is the preliminary $(z + x)$ coordinate of the i th atom. Also listed in the table are the products S of the three diameters and the peak height. If the peak height is proportional to the

Atom No.	Peak Height	Half Amplitude Diameters				
	E $e/\text{\AA}^3$	A $z - x$ $\text{\AA}.$	B $z + x$ $\text{\AA}.$	C y $\text{\AA}.$	$\Delta(x + z)$ $\text{\AA}.$	S (ABCE)
1	6.9	0.87	0.93	0.81	0.08	4.52
2	5.8	0.91	0.98	0.81	0.14	4.19
3	6.1	1.01	0.95	0.86	0.00	5.03
4	6.5	0.89	0.88	0.87	0.12	4.43
5	6.3	0.95	0.93	0.85	0.18	4.73
6	6.5	0.87	0.95	0.85	0.25	4.57
7	5.8	0.88	1.12	0.89	0.27	5.09
8	6.0	0.89	0.99	0.86	0.09	4.55
9	6.5	0.85	0.91	0.86	0.05	4.32
10	6.1	0.85	0.95	0.87	-0.05	4.29
11	6.3	0.85	0.93	0.87	-0.02	4.33
12	6.3	0.88	0.95	0.83	-0.08	4.37
13	6.5	0.89	0.91	0.84	-0.02	4.42
14	6.3	0.88	0.90	0.84	-0.10	4.19
15	6.2	0.88	0.89	0.86	-0.02	4.18
16	6.4	0.95	0.88	0.89	0.03	4.76
17	6.0	0.96	0.88	0.93	-0.20	4.71
18	6.3	0.92	0.97	0.88	0.11	4.95
19	6.0	0.92	0.97	0.87	0.04	4.66
20	<u>5.9</u>	<u>0.94</u>	<u>1.00</u>	<u>0.87</u>	<u>0.23</u>	4.83
Avg. X	6.23	0.902 $\text{\AA}.$	0.944 $\text{\AA}.$	0.861 $\text{\AA}.$	0.10 $\text{\AA}.$	

Mean value of S for atoms 1 - 15 inclusive 4.48 ± 0.21 (avg.)
for groups 16- 20 inclusive 4.76 ± 0.12 (avg.)

mean density within the volume of the peak, and with all of the peaks well resolved this is a reasonable assumption, this product will be proportional to a density integration. The magnitude of S is perhaps more significant than peak height in the present instance where the structure is not well refined. The mean value of S is 4.48 with an average deviation of 0.21 for the 15 carbon atoms of the chain and ring, and 4.76 with an average deviation of 0.12 for the 5 methyl groups. The difference between these two values may not be significant in view of the large deviations. The table illustrates the lack of refinement in the $x + z$ parameters, since the average diameter of the peaks in this direction is greater than along either r or y . The greatest difference is usually associated with the largest correction terms, for example atoms 7, 6, 2, and 8. A notable exception is atom 17, but this is one of the few atoms where the Fourier also indicated a change of $z - x$ parameter. The y and r coordinates were only half corrected from their original positions because significant refinement had already been made in these coordinates.

It is difficult to make more than qualitative comments on many of the features of a Fourier at this stage of refinement. Series termination effects, incorrect signs of structure factors, and anisotropic vibrations

are going to influence the Fourier in a not altogether predictable way. For example details such as the shape of the peak associated with atom 3 may be significant. The peak is 0.06 \AA wider in diameter in the $z - x$ direction than in the $z + x$, even though no correction in any parameter was made for this atom. The larger diameter is in about the direction causing the ring to pucker in the opposite configuration and larger vibrations might be expected in this direction. It is doubtful, however, if the present state of refinement warrants such considerations.

Structure factors were calculated for the 1758 observable reflections, excluding space group extinctions, both before and after the Fourier refinement. The R factor broken down into groups of negative and positive λ is informative.

	First three-dimensional calculation	Second three-dimensional calculation
687 terms with $\lambda \geq 0$	43.3%	27.1%
1071 terms with $\lambda < 0$	32.9%	24.7%
Overall average	37.2%	25.7%

This is exactly what is expected from data where the $z - x = r$ parameters are more refined. Reflections with negative λ values, especially when h and λ are nearly the same, must have much better agreement than those with

positive λ . The reduction in R factor by this stage of refinement has been considerable, especially in the structure factors with positive λ indices, 16%.

The structure factors calculated from the refined parameters are listed in Table III, Appendix I, page 134. The observed structure factors and the values of $||F_o| - |F_c|| = |\Delta F|$ are also listed in this table. A number of reflections, some with large ΔF values, have changed sign as a result of the Fourier refinement; these are indicated in Table III with an asterisk after the ΔF terms. There were 182 sign changes, roughly 10% of the data; the following breakdown is about as expected.

	negative λ	positive λ	Total
Total sign changes	85	97	182
Unobserved reflections	42	28	70
Reflections with $ F_o > 10.0$	9	20	29

In almost every instance the new F_c values are in better agreement with F_o than the first calculated. The R factor, the changes of sign, and a detailed comparison of observed and calculated structure factors all serve to illustrate the degree of refinement. There have been enough changes in sign almost to invalidate any detailed analysis of the three-dimensional Fourier.

The parameters derived from the Fourier are listed in Table II on the following page. It is doubtful if the resulting atomic positions differ from their true locations by more than $0.03 \overset{\circ}{\text{\AA}}$ on the average, and the maximum error will probably not exceed the average change just made, namely $0.10 \overset{\circ}{\text{\AA}}$. Three-dimensional least squares can certainly be applied to the structure in this stage of refinement with almost certain assurance of convergence to the correct structure.

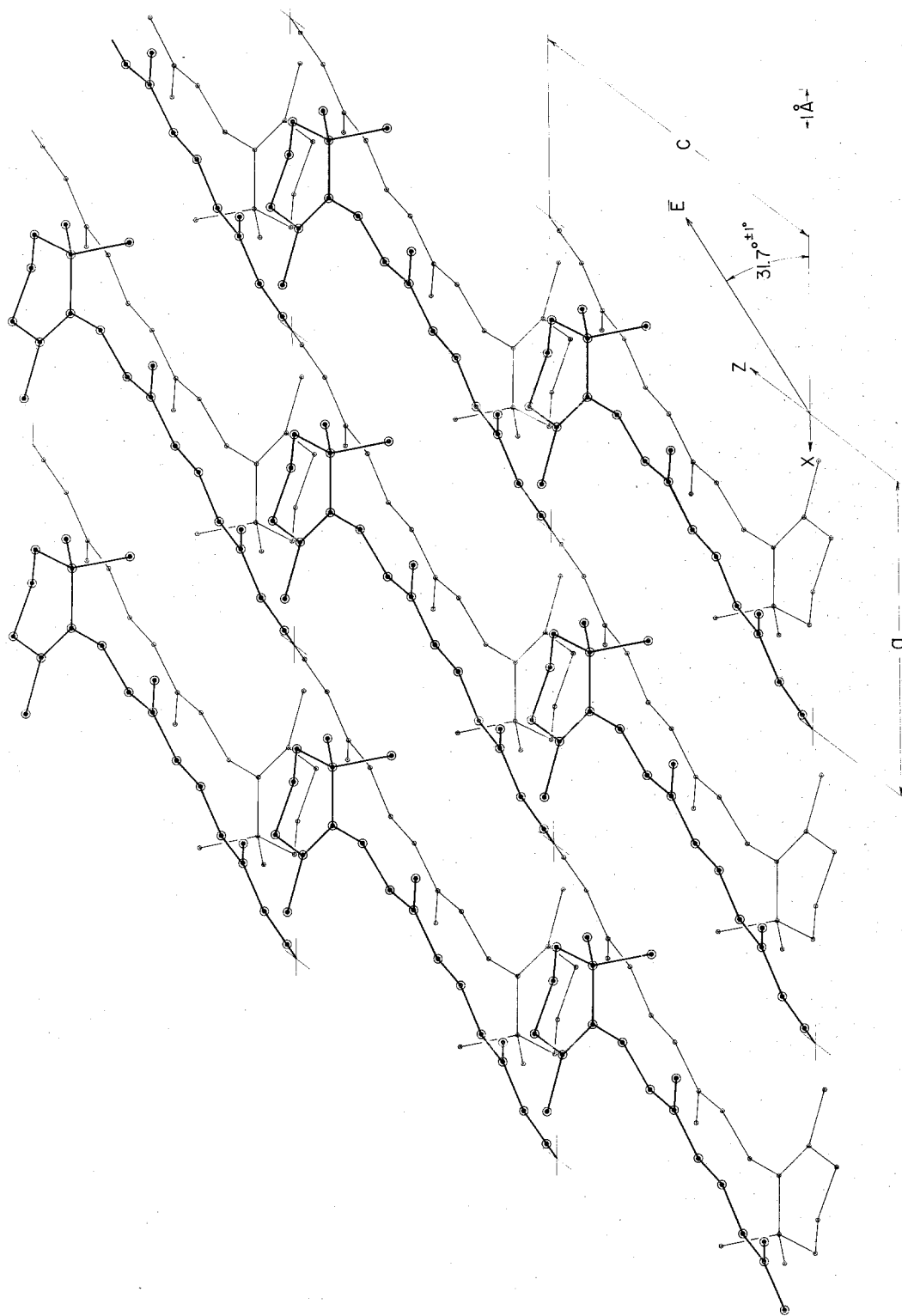
Table II. Coordinates of the carbon atoms of 15,15'-
dehydro- β -carotene.

Atom Number	x	y	z
1	-0.7032	0.1726	0.8532
2	-0.6732	0.2068	0.9950
3	-0.5577	0.2441	0.0065
4	-0.3417	0.2302	0.0833
5	-0.3435	0.1916	0.9740
6	-0.5125	0.1658	0.8574
7	-0.5275	0.1302	0.7430
8	-0.4430	0.1305	0.6373
9	-0.4380	0.0957	0.5488
10	-0.3415	0.0982	0.4567
11	-0.3148	0.0629	0.3670
12	-0.2083	0.0690	0.2872
13	-0.1715	0.0351	0.2040
14	-0.0683	0.0451	0.1245
15	-0.0185	0.0135	0.0388
16	-0.1235	0.1851	0.0347
17	-0.8814	0.1857	0.6298
18	-0.7815	0.1327	0.8767
19	-0.5465	0.0542	0.5383
20	-0.2353	-0.0118	0.2018

G. Description of the Structure

The molecules of DHC are arranged into a structure in such a way that the long conjugated chains are packed together almost unaffected by the cyclohexene rings. As a result the molecules are grouped into what we shall call sections that are separated by the c glide planes; one such section is illustrated in the \bar{b} axis projection of Figure 16. In describing the structure it will be convenient to consider the important features of the intermolecular arrangement in a more simplified form, but reference to Figure 16 must be made occasionally in order to keep the details in proper relation to the overall structure.

Consider as origin a particular symmetry center which is occupied by a molecule. The molecule is essentially plane. Consider next the molecules which are generated from this molecule by the translation $\bar{c} - \bar{a}$; this set of molecules proves to be uniplanar and they populate one of a number of linear plane strips that comprise the structure. The plane of each strip is inclined 8° to \bar{b} . A translation which is almost normal to $\bar{c} - \bar{a}$, namely at 87.1° to it, is $\bar{c} + \bar{a}$; for \bar{a} and \bar{c} are almost equal, $8.14_5^\circ \text{ \AA.}$ and $8.46_5^\circ \text{ \AA.}$ respectively. Hence a plane strip

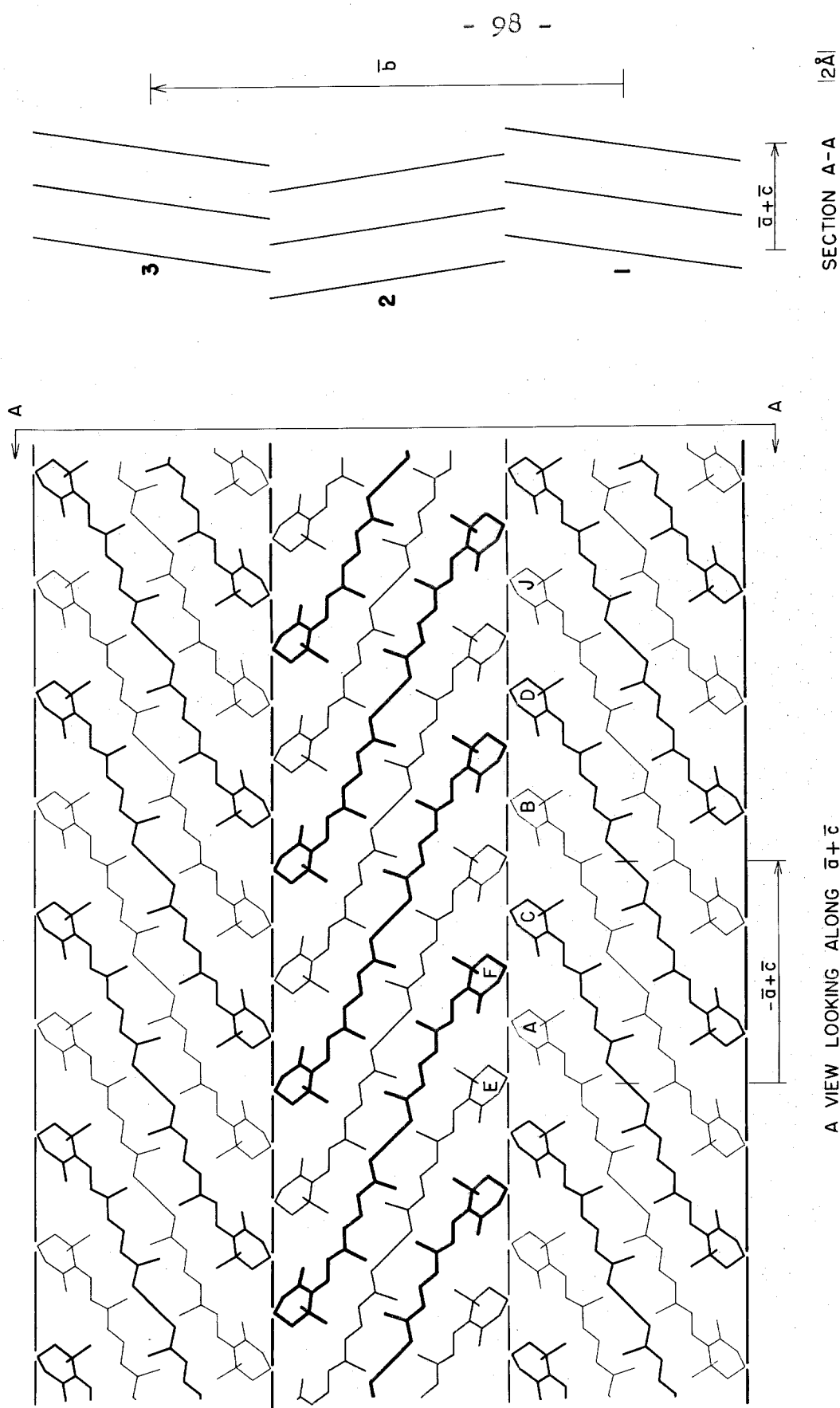


THE B AXIS PROJECTION ONTO THE AC PLANE
OF THOSE MOLECULES LYING BETWEEN $Y = \pm 1/4$
 \vec{E} IS THE DIRECTION OF MAXIMUM POLARIZABILITY

Figure 16.

is repeated by $\bar{c} + \bar{a}$ to form an echelon of parallel strips, separated by 7.25 \AA , in which the molecules are essentially side by side. The diagonals, $\bar{c} - \bar{a}$ equal to 14.95 \AA , and $\bar{c} + \bar{a}$ equal to 7.25 \AA , bound, however, a centered cell in the basal plane. Therefore the echelon really has strips spaced every 3.61 \AA , but the molecules of adjacent strips are displaced along the length of the strip by $(\bar{c} - \bar{a})/2$ or 7.47 \AA . One echelon composes the section of the structure which lies between $y = \frac{1}{4}$ and $y = -\frac{1}{4}$.

A simplified drawing of the DHC molecules in three sections of the structure is shown in Figure 17. The glide planes at $y = \pm\frac{1}{4}$ divide the structure into sections and also offset the plane strips as illustrated in the end view on the right. Molecules C and D, and all others related by the translations along $\bar{c} - \bar{a}$ are contained in one plane strip. In a projection along $\bar{c} + \bar{a}$ we will see the molecules of only two adjacent plane strips, since $\bar{c} + \bar{a}$ is the translation which relates the molecules of every other plane strip. Molecules A and B are thus part of the strip which is immediately behind the one containing molecules C and D. Every molecule has four nearest neighbors in adjacent strips, and these are arranged in what we might call a two-dimensional close-packed array. The four molecules closest to B are C and D, and the two molecules derived from them by the translation $\bar{c} + \bar{a}$. Two strips related



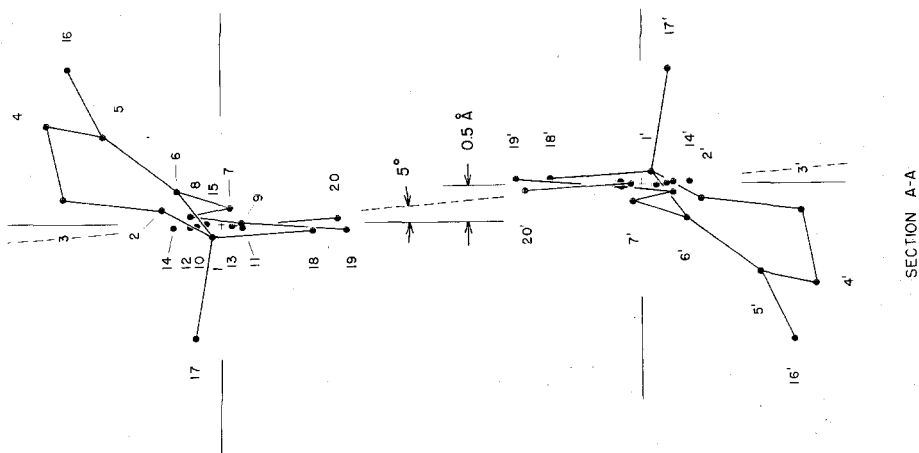
A SIMPLIFIED DRAWING OF DHC MOLECULES ILLUSTRATING THE CLOSE-PACKED PLANE STRIPS AND THE OFFSET CORRUGATED LAYERS THAT COMPRISE THE STRUCTURE.

Figure 17.

by the c glide are offset by the translation of $\bar{c}/2$, but can be regarded as forming a corrugated layer extending in the \bar{b} direction. The angle at the dihedral of two adjacent strips of one such layer is 164° . There are actually two ways in which the strips may be grouped into layers, one of which is illustrated in Figure 17 by the numbering 1, 2, 3. The general features of the structure may thus be quickly summarized as follows. The molecules are arranged into straight plane strips which extend throughout the crystal in the direction $\bar{c} - \bar{a}$. These strips form an offset corrugated layer in the direction of the \bar{b} axis and are closely packed side by side in the direction $\bar{c} + \bar{a}$.

In describing the detailed arrangement of the molecules it will be convenient to consider in turn the intermolecular configuration within one plane strip, the relative positions of molecules in two adjacent strips, and the packing of the ring structures at the dihedrals formed by the \bar{c} glide planes. On the detailed diagrams that follow to illustrate these points molecules are lettered in accordance with Figure 17. Frequent reference will be made to this figure so that the isolated features of the packing can be related to the structure as a whole.

Two molecules from one of the plane strips are shown in Figure 18. The strip is formed by the back to back packing of molecules. That is, the methyl groups of the



TWO ADJACENT MOLECULES IN ONE PLANE STRIP FROM A CORRUGATED LAYER. THE PLANE STRIP LIES ALONG THE DIRECTION $\bar{c}-\bar{a}$.

Figure 18.

positive half of one molecule are interleaved with those of the negative half of the molecule derived from the first by the translation $\bar{c} - \bar{a}$. Positive and negative are used here in reference to the y parameter, but also refer to the ends with unprimed and primed atoms respectively. The two half molecules contained in each unit cell of the \bar{b} axis projection of Figure 16 form one such coupled pair. This coupling is repeated so that the positive half of the second molecule is meshed with the negative half of the third, the positive half of the third with the negative half of the fourth, and so on to form a strip that extends throughout the crystal as shown in Figure 17. The packing distances between the molecules, 3.7, 3.8, 3.9, 4.1, and 4.4 Å., are quite acceptable values, and the half molecules fill space efficiently. The extent to which the atoms of one molecule lie in a single plane is illustrated in section A-A of Figure 18. All chain atoms from 9 to 9', fourteen in all, are coplanar within ± 0.05 Å., and the six methyl groups 18, 19, 20, 18', 19', and 20' are coplanar within ± 0.10 Å. The A-A section also shows that the cyclohexene ring is puckered and twisted out of the plane by rotation around the 7-6 single bond; these two features of the structure will be discussed in more detail later.

The plane of the continuous strip which we have previously described is defined by the vector $\bar{c} - \bar{a}$ and a

vector along the mean length of the molecule, viz., the molecular axis, which is inclined 27° to $\bar{c} - \bar{a}$. The planar molecules of DHC related by the translation $\bar{c} - \bar{a}$ are not contained exactly in the plane of the strip but are rotated by 5° about the molecular axis. This rotation offsets the planes of the molecules by 0.5 \AA . as shown in Figure 18.

The relative positions of molecules in two adjacent and parallel plane strips are illustrated in Figure 19. The molecule C is derived from A by the translation $-\bar{a}$ and this same symmetry operation carries B to D. Molecules A and B are from one plane strip and C and D are from the layer just above. Note that this drawing is projected along the normal to the plane of the molecule; it may be compared with Figure 17 which is projected along $\bar{c} + \bar{a}$. The molecule C above the pair A, B projects nearer to B in the left portion of Figure 19 consistent with the fact that B is 0.5 \AA . further away, as shown in section A-A. The general features of the packing are such that the methyl groups 20 and 18 of C are directed symmetrically into the pockets of molecule B. The effective thickness of the conjugated chains for packing purposes is 3.6 \AA . The two distances, 19-14, and 20-20' between molecules A, C and B, D respectively, are both 3.5 \AA ., which is somewhat short. Lipson and Cochran (120) report unbonded carbon-

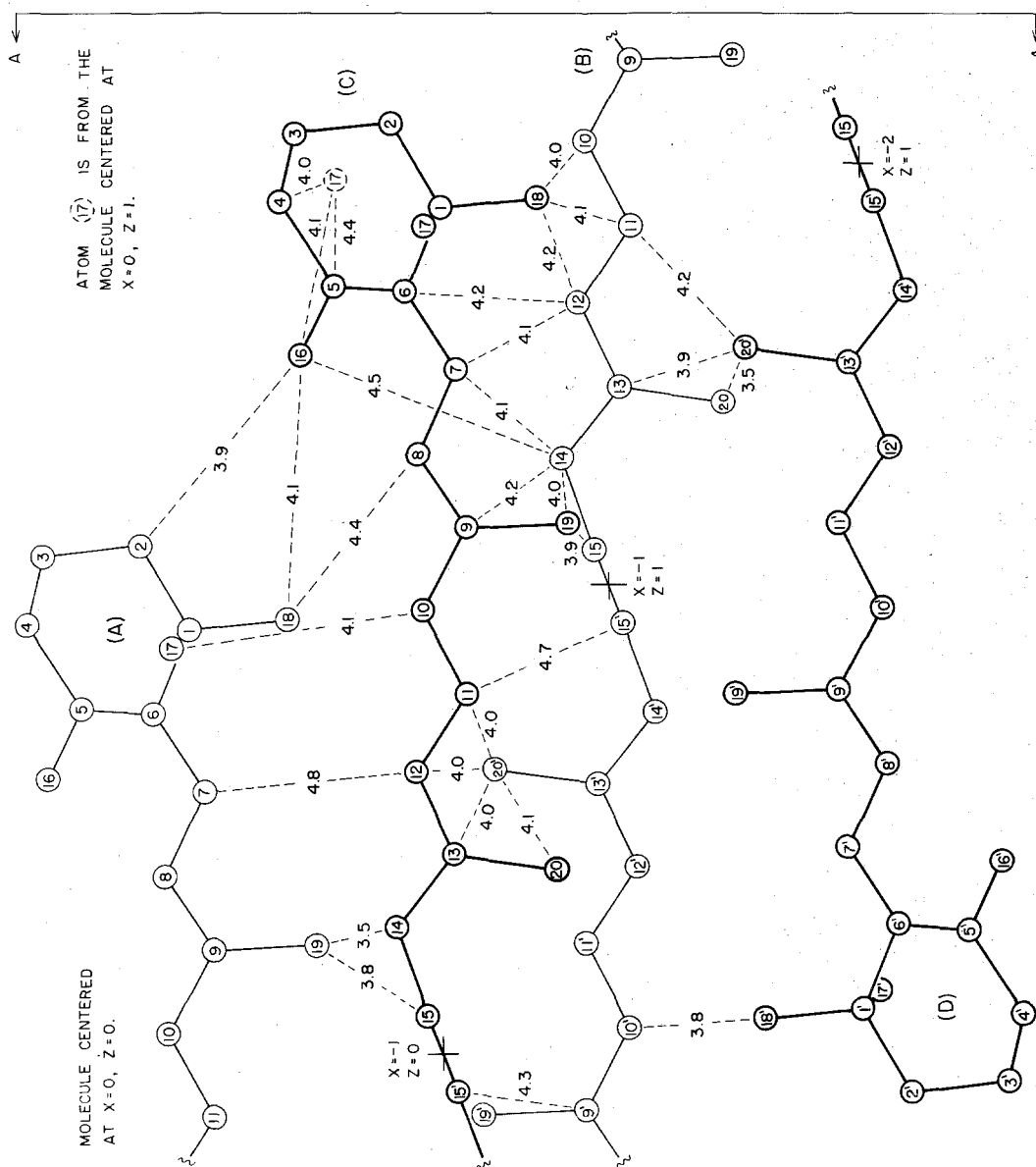


Figure 19.

carbon distances of 3.4 to 3.8 Å., although no references are given for the data. If the hydrogen atoms of the 20 and 20' methyl groups are staggered, the C-H and H-H distances become respectively 3.1 Å. and 2.6 Å. These are not intolerable values for unbonded contacts. Similar distances will be found for the C-H and H-H contacts associated with the 19-14 interaction if the hydrogens are staggered. The situation with this pair of atoms is somewhat more favorable, however, since atom 14 has only a single hydrogen and it does not lie in the direction of the methyl group even in projection. A more detailed consideration of these distances will not be significant until the structure is further refined.

The eighteen atoms of molecule B, shown in Figure 18, comprise the central portion of one molecule of DHC. This group of atoms is boxed in place by the molecules which are its six nearest neighbors. Two are from the same strip, one of which, molecule A, is shown; two are from the layer above, molecules C and D; and two more, not shown, are from the layer below. The missing molecules can be derived from those shown by inversion through the center of molecule B. A comparison with Figure 17 may also prove helpful. The packing of the conjugated chains is illustrated in the simplified drawing of Figure 20. Here we have deleted all ring atoms and methyl groups, and have projected the remaining

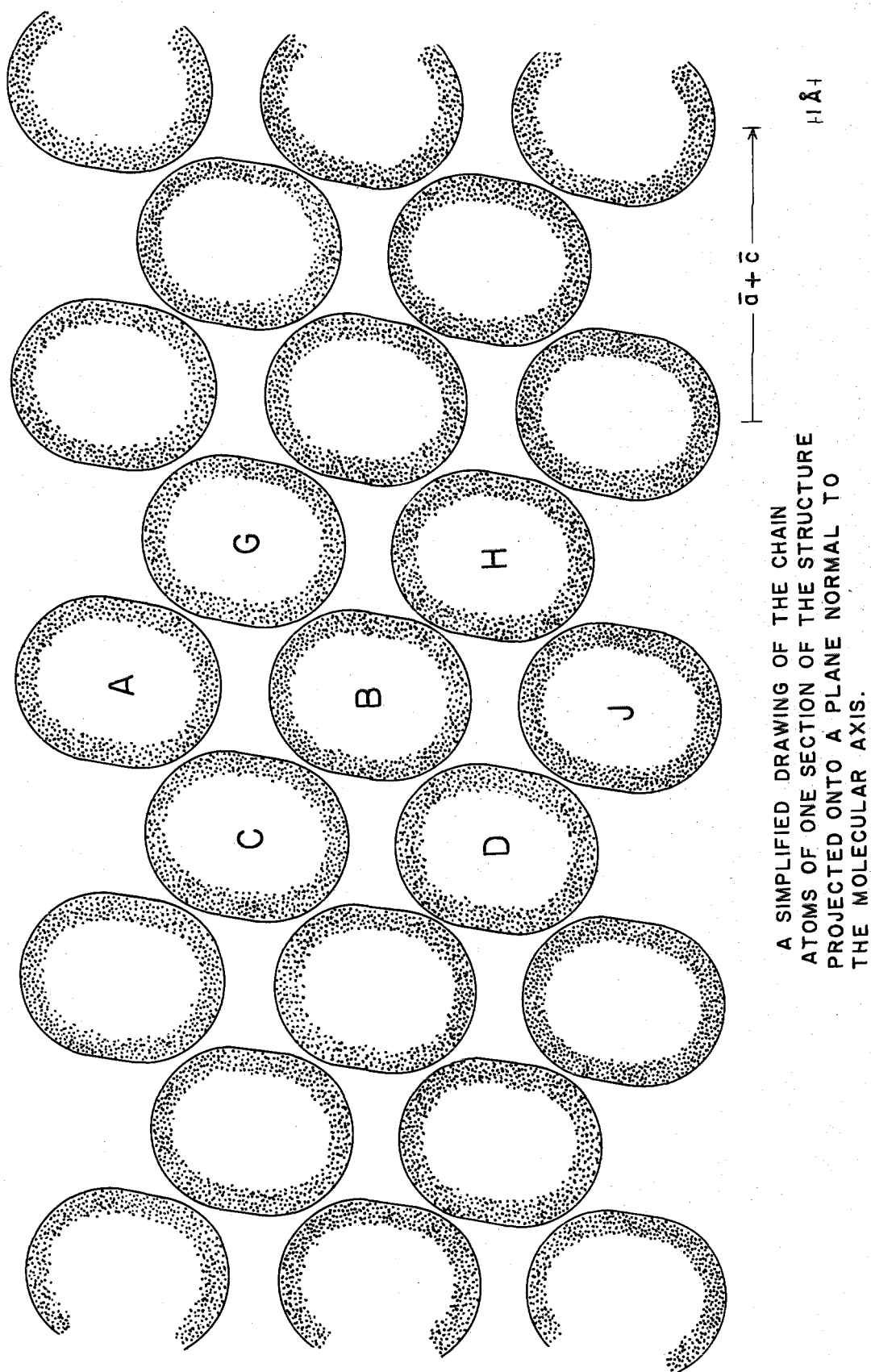


Figure 20.

chain atoms along the molecular axis onto a plane normal thereto. The ellipses have been drawn using van der Waals radii for carbon atoms. This figure is merely a simplified version of the A-A section of Figure 19, only with more molecules shown. The six nearest neighbors of molecule B are labeled. This figure is an end view of what is almost a two-dimensional close packed array of chains. If we consider the chain structure of each molecule to extend so that it includes atoms 6, 1, and 2 of the cyclohexene ring, then molecule A ends at about the center of molecule B; see Figures 17 and 19. This is of course where molecule J begins. All of the molecules in horizontal rows, related by the translation $\bar{c} + \bar{a}$, are essentially side by side. Thus Figure 20 should really be staircased out of the paper as we proceed down the page from row A to C to B --- J, with each successive row being about $7 \overset{\circ}{\text{\AA}}$ further out of the paper. This figure should therefore extend continuously in both dimensions, but in going from A to B to J we are working through the structure in the direction $\bar{c} - \bar{a}$, and by every fourth row we have traversed the length of one molecule, about $28 \overset{\circ}{\text{\AA}}$. The spaces in the figure are of course occupied by the meshed methyl groups, but the almost linear chains, by themselves, form a compact structure with the chains displaced along their length sufficiently to leave room for the bulky cyclohexene rings to fit at the ends; the central portion of each molecule is

tightly boxed by its neighbors.

Figure 19 shows, in a qualitative way, why the ring structure is not coplanar with the chain. Molecules A and B form a compact strip extending beneath molecule C. Molecule B extends under atoms 19 and 18 but molecule A ends at about atom 9 of C. The chain and ring structure simply twist down into the remaining space, bringing atom 16 into contact with 18 and 2 of A, and into contact with atom 17 of the layer beneath, molecule G of Figure 20. This is also illustrated in the A-A section of Figure 18, page 100, by the distortion of the chain from atom 9 to 8 to 7 to 6. Packing then causes the ring structure to twist out of plane even though the conjugation would be stronger if atoms 8, 7, 6, and 5 were coplanar. This rotation of the ring about the 6-7 single bond also allows atom 18 of C to maintain suitable packing distances from 10, 11, and 12 of molecule B, and similarly 17 of A from 10 and 12 of C. The molecules could not pack in their present orientations with the cyclohexene ring in any other configuration.

Figure 21 shows the packing of the rings at the dihedrals of adjacent corrugated layers. Molecules E and F are related to A and C respectively by the c glide in the direction $-\bar{c}/2$. The distances for the packing vectors are all sufficiently long and need no particular comment. The glide reflection carrying E to A, when applied to A, leads

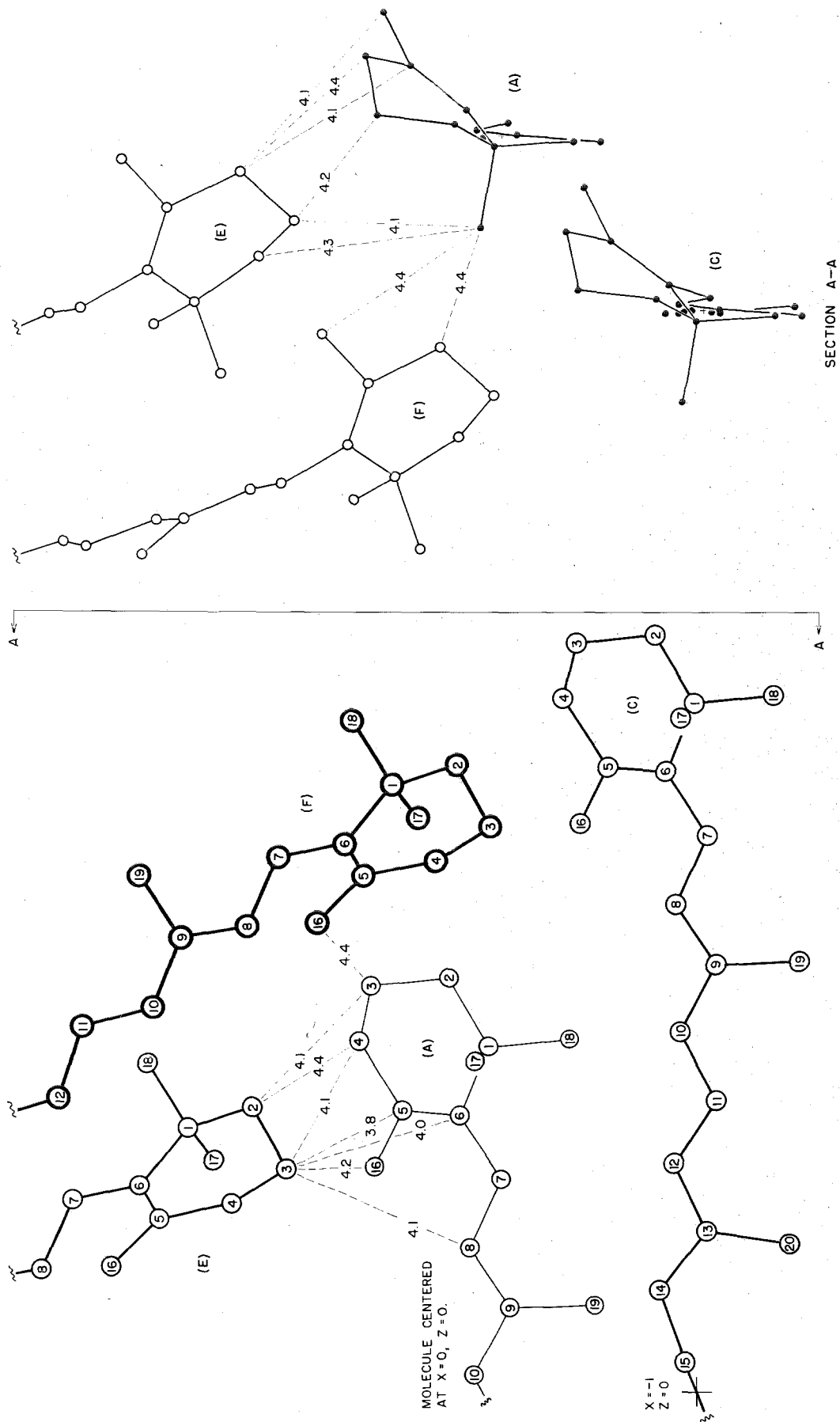


Figure 21.

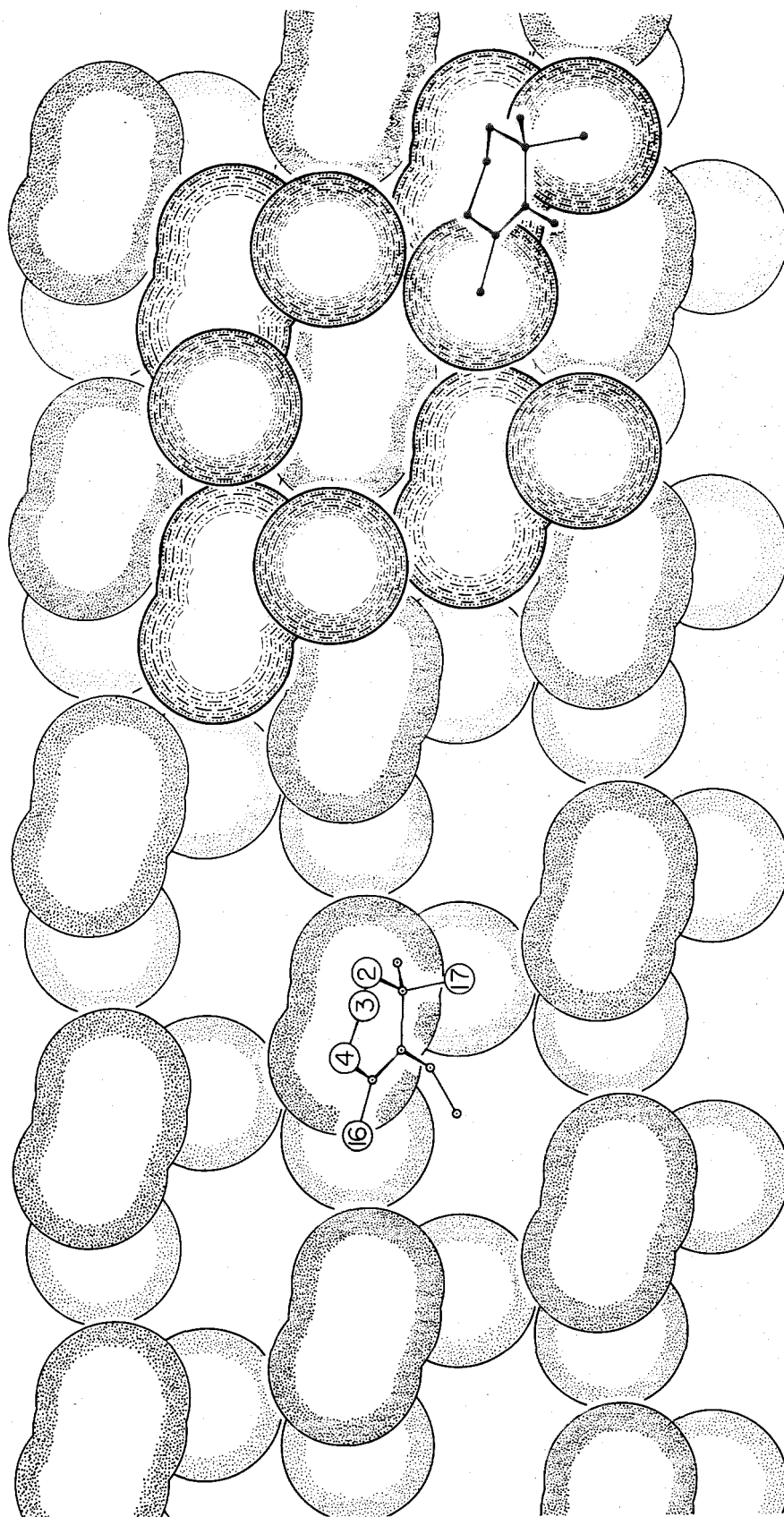
to another molecule, not shown in Figure 21, related to E by the \bar{c} translation. This molecule would lie almost behind F in the left hand figure, since it is derived from F by the translation $\bar{c} + \bar{a}$, and would overlap molecule A in the projection of section A-A. The distances from atoms 2, 3, etc. of E to the various atoms of A have exact counterparts in distances from 2, 3, etc. of A to the corresponding atoms of the molecule derived from E by the \bar{c} translation. We have only shown enough molecules here to display uniquely all of the interatomic distances.

The reason for the single configuration of the cyclohexene ring is illustrated in Figure 21. The crystal structure of DHC might have shown a statistical distribution between the two possible puckered forms of the ring. That is, atom 3 of molecule E might have been displaced to the other side of the ring, were it not that the proximity of atoms 4, 5, 6, 16, and 17 of A prevent the ring from assuming this configuration.

The lattice parameters a , c , and α_2 for the unit cell of DHC are such that they form a pseudo-hexagonal lattice. That is, a and c are almost equal, 8.145 Å. and 8.465 Å. respectively, with α_2 nearly 120° , namely $128^\circ 18.8'$. This means that each of the cyclohexene rings has six nearest neighbors at the same y parameter that are almost symmetrically disposed, as shown in Figure 16, page 96. Since

these rings are packed together with those related by the c glide plane we shall consider this arrangement in more detail. Figure 22 shows a projection along $-\bar{b}$ of the cyclohexene rings of two adjacent sections of the structure related by the c glide plane at $y = \frac{1}{4}$. The molecules are drawn with van der Waals radii and only the numbered atoms, 2, 3, 4, 16, and 17, have been illustrated. The six nearest neighbors around the molecule with the numbered atoms are obvious. The rings are oriented so that their length lies along the x axis leaving four pockets for the rings of the layer above. The arrangement of the four molecules into these pockets is illustrated in the right portion of Figure 22. The rings of the two hexagonal layers related by the c glide plane are not superimposed in cubic or hexagonal closest packing but instead the two layers are merged together to form a centered hexagonal network. The atoms 2, 3, and 4 have nearly the same y coordinate in both layers, and the compact array which these groups of atoms form is apparent in the right hand part of the figure. The methyl groups 16 and 17 are oriented into the pockets between the groups of atoms of this centered hexagonal network.

It is perhaps remarkable that the molecules of DHC should turn out to form a structure in the way that they do; the conjugated chains are placed back to back to elimi-



Z
X

THE B-AXIS PROJECTION OF
THE RINGS FROM TWO
SECTIONS OF THE STRUCTURE

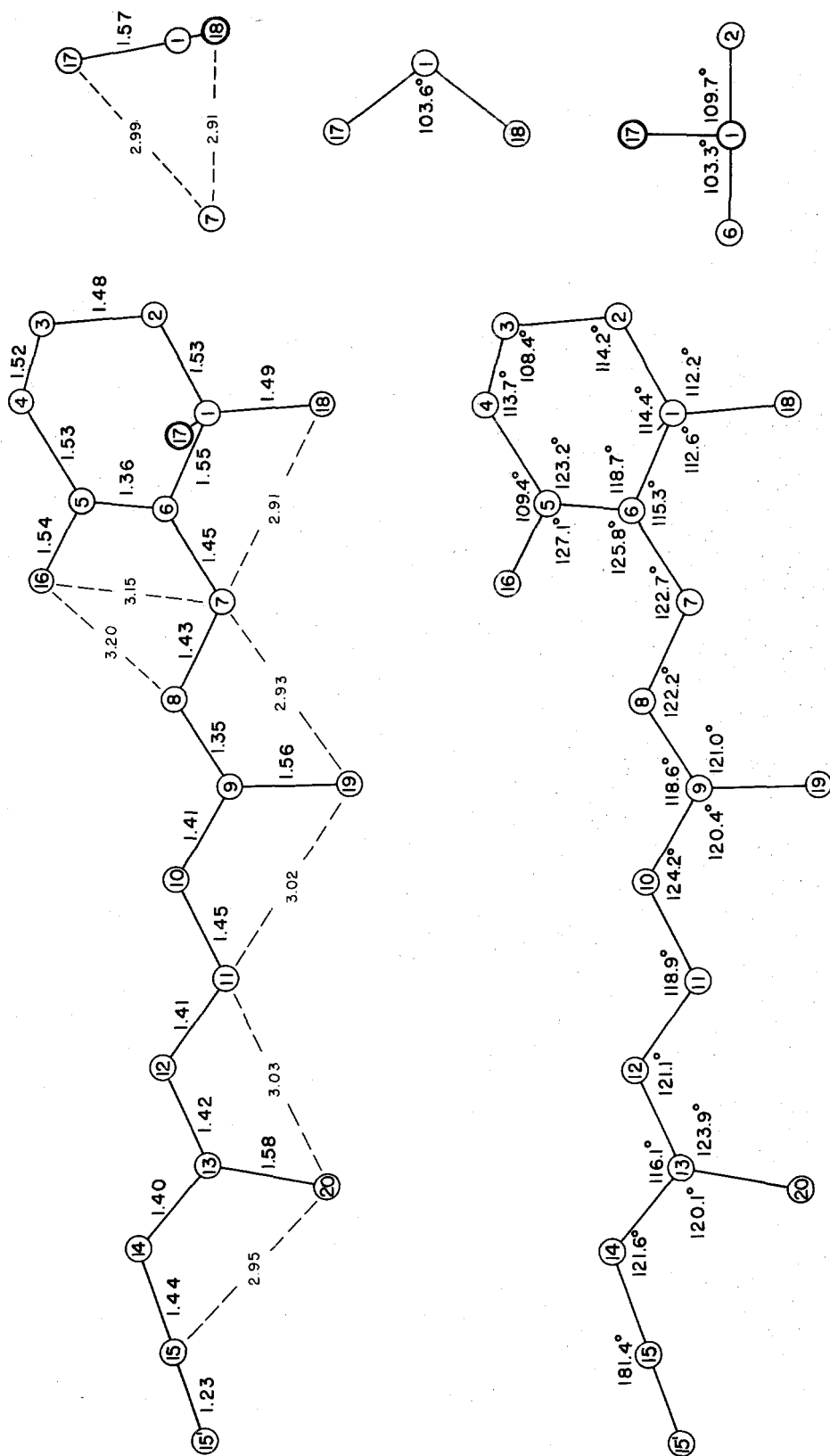
Figure 22.

nate the effect of the protruding methyl groups and form a compact layer 3.6 Å. thick; the layers are ordered into an echelon with the closely packed chains arranged so that there is room at the ends for the cyclohexene rings; the rings from two echelons are merged end to end so that the sections are bonded into a complete structure. After the structure is solved it is easy to point out that the chains are not shaped at all like the bulky cyclohexene rings and space is more efficiently used if the molecules are placed side by side with the rings interwoven into the spaces at the ends of the chains and with each other. It is only unfortunate that not enough is known about the configuration of molecules and the forces of bonding to allow such predictions to be made in advance instead of after the structure is solved.

A description of the bond lengths and bond angles of the DHC molecule, shown in Figure 23, can best be included in the following section of discussion and will accordingly not be given here.

H. Discussion of the Structure

The dimensions and bond angles of the DHC molecule are shown in Figure 23. As stated in a previous section, and as the following discussion will indicate, the structure of DHC is not well refined, but several features of the intermolecular configuration deserve comment. The ten carbon-carbon single bonds, including five in the cyclohexene ring, range in length from 1.48 Å. to 1.58 Å. with an average deviation of 0.025 Å. from the expected bond length of 1.54 Å. The bond lengths along the conjugated chain may be compared with the theoretical values obtained by a molecular orbital treatment of an infinite conjugated chain (106). The observed and calculated distances and the difference $R_o - R_c$ are listed on the following page. The average difference for the eleven tabulated interactions is 0.031 Å. The 9-8 and 8-7 distances are apparently wrong, especially the 1.35 Å. 9-8 single bond. If we neglect the 9-8 and 8-7 bonds there is a significant trend in the observed values as compared with the calculated; namely, they are all longer. Short bond lengths may be a typical result of quantum mechanical calculations on conjugated systems since both butadiene and cyclooctatetraene are also predicted to have shorter bond lengths than those determined experimentally. For butadiene the calculated



Inter- action	Bond Length		$R_o - R_c$
	Observed	Calculated	
15'-15	1.23	1.24 [*]	0.01
15-14	1.44	1.39	0.05
14-13	1.40	1.39	0.01
13-12	1.42	1.40	0.02
12-11	1.41	1.38	0.03
11-10	1.45	1.41	0.04
10-9	1.41	1.38	0.03
9-8	1.35	1.42	-0.07
8-7	1.43	1.36	0.07
7-6	1.45	1.46 [*]	-0.01
6-5	1.36	1.36 [*]	0.00

values are 1.345 Å. and 1.432 Å. (106), while the experimental bond lengths are 1.360 Å. and 1.465 Å. (115) respectively. For cyclooctatetraene the calculated and observed bond lengths are 1.400 Å. (106) and 1.425 Å. (115) respectively. The average deviation for all twenty-

*These values have been assumed by the author. Pauling (96) has given a curve for calculating bond length as a function of partial double-bond character, based on the values of the pure single bond, the pure double bond, the 50% double bond of benzene, and the 1/3 double bond of graphite. This curve cannot be satisfactorily extrapolated to the triple bond distance of 1.20 Å., and the 1.24 Å. value for the 15-15' bond has been assumed. Quantum-mechanical calculations do not apply to the 8-7-6-5 group since the atoms are not coplanar. The distances have arbitrarily been assigned the experimental values for butadiene (115). These experimental values may not be a good choice, but we do not have distances for an exactly similar structure, and bond lengths for other compounds would be no more applicable to the present molecule than those of butadiene.

one bonds of DHC is $0.028 \overset{\circ}{\text{\AA}}$. As stated in a previous section the author does not believe that the atomic positions are more accurate on the average than $0.03 \overset{\circ}{\text{\AA}}$, with a probable maximum error of $0.10 \overset{\circ}{\text{\AA}}$. These limits are consistent with the deviations found for the bond lengths.

Bond angles are, in general, more flexible than bond lengths, and the angles found in Figure 23 are consistent with the accuracy of the other parameters. The angles along the chain may be compared with the theoretically predicted value of $125^{\circ} 16'$ (82, 96). The four angles along the chain on the side of the methyl groups, neglecting the 7-6-1 angle, have an average magnitude of 122.3° . The three similar angles on the opposite side of the planar chain, neglecting the 8-7-6 angle, average to 117.9° . The difference between these two values is significant and will almost certainly remain after refinement of the structure. It is partly due to the meshing of the methyl groups of two molecules, but the author believes that it is principally due to the asymmetry of the two sides of the planar chain of the molecule. Models show that the methyl groups and the hydrogen atoms on the alternate carbon atoms are somewhat crowded. This results in slight deviations from planarity and causes an in-plane bending of the molecule. The deviation from planarity is indicated in the A-A section of Figure 18, page 100, by the fact that the methyl

groups 18, 19, and 20 are staggered slightly, especially 19 and 20. The in-plane bending is obvious from the values of bond angles and is shown by the fact that the atoms 14, 12, 10, 8, and 6 do not project along a straight line in Figure 23. The fact that the bond angle 8-7-6 is not small like the others on that side of the chain supports the view that the bending is due to the molecular asymmetry. Methyl group 16 is in contact with atoms 8 and 7, and this tends to counteract any influence that the groups 18, 17, and 19 would have in interacting with atom 7 to decrease the 8-7-6 angle. The average bond angle along the chain, including the 8-7-6 angle, is 120.7° . This value is considerably smaller than the $125^{\circ} 16'$ predicted by theory. However, the angle found for isobutene and for tetramethylethylene is $124^{\circ} 20'$ (96), the angle found in butadiene is 122° (115), and that found for cyclooctatetraene is 120° (115); these compounds all have bond angles less than the predicted value. The 120.7° found for DHC must be considered within the limits expected for a highly conjugated molecule, especially since benzene, which is forced by symmetry to have 120° bond angles, has such a large resonance energy.

The other angles of the molecule, with a few exceptions, are quite acceptable. The 14-13-20 angle is less than the 12-13-20 angle, consistent with the unsymmetrical environment presented by atom 11 and the triple-bonded atom pair

15,15'. The two angles 10-9-19 and 8-9-19 are almost identical. The angles for the methyl groups 17 and 18 vary from 103.3° to 112.6° , but the environments for the two groups are by no means equivalent and the angular discrepancies are not extreme. It is difficult to predict the angular configuration for the cyclohexene ring with the methyl groups 17, 18, and 16, and the carbon atom 7, especially since no experimental data are available, even for cyclohexene. The group of atoms 16, 5, 4, 6, 7, and 1 are expected to be planar because of the 5-6 double bond. The angles around atom five and six total 359.7° and 359.8° respectively and this group of atoms are essentially planar. The two angles in the ring, 4-5-6 and 5-6-1 are both smaller than the expected value of 125° and both are less than the 16-5-6 and 7-6-5 angles as a result of the ring formation. The other bond angles in the ring would be expected to have values between 109° and 120° , but nearer to the lower value; the average is 112.7° .

The entire molecule has dimensions and angles that are consistent with experimental values and with theory, considering the state of refinement.

In the final analysis a correct molecular structure will explain any unusual physical properties such as cleavage, optical absorption, density, melting point, etc., in so far as these properties can be related to the molecular

or crystal structure; will have dimensions reasonably consistent with our knowledge of structure derived from experiment and theory; will make efficient use of space in intermolecular bonding; and will account for the intensities of the observed X-ray reflections. Each of these criteria for evaluating a molecular structure will be considered briefly in the following paragraphs.

The molecules of DHC, containing only carbon and hydrogen, must be bonded together in the crystal by van der Waals interactions. Some electrostatic attraction may be present as a contribution from resonance hybrids of the long conjugated structure; however, the resulting net charge on any atom should be very nearly zero and the ionic structures cannot contribute a great deal to intermolecular forces. The melting point of DHC is not unusually high, $155-56^{\circ}$ C., as compared with the values of 150° C. and $178-80^{\circ}$ C. for the mono-cis and all-trans β -carotenes respectively (64). Similarly the density is not out of line with those of related compounds, as shown on the following page. The molecules of these compounds are all conjugated and with the exception of methyl bixin all contain rings and are hydrocarbons. The densities are all about 10% higher than the values found for DHC and β -carotene. Coronene has a density considerably higher than the others shown; this is consistent with the very

Compound	Density gm./cm. ³
DHC (calculated -20° C.)	1.03
β -carotene (110)	1.00
diphenylbutadiene (107)	1.138
diphenylhexatriene (107)	1.139
diphenyloctatetraene (107)	1.144
diphenyldecapentaene (107)	1.152
diphenyldodecahexaene (107)	1.135
diphenyltetradecaheptaene (107)	1.130
diphenyldiacetylene (121)	1.163
anthracene (122)	1.25
phenanthrene (122)	1.179
hexamethylbenzene (123)	1.061
coronene (117)	1.377
methylbixin (108, 109)	1.10

efficient packing possible for molecules that are highly symmetric. The low values of density for DHC and β -carotene are probably due to the fact that the molecules are rough in shape and cannot pack very efficiently; the chains have protruding methyl groups and the puckered cyclohexene rings have three methyls projecting in different directions. Methyl bixin has methyl groups along the chain, while hexamethylbenzene has methyl groups all around the ring; both of these substances have slightly lower densities than the other compounds. The crystals of

DHC are not particularly hard, nor do they exhibit any marked tendency to cleave in a particular direction. The structure suggests that the crystals might have a cleavage plane either parallel to the thin flat plates, (010), or between two of the corrugated layers of Figure 17, page 98, although no evidence has been found for either. The general physical properties of DHC are not extreme and almost any intermolecular arrangement, that is in other respects satisfactory, must be considered acceptable.

The preceding section describes the intermolecular vectors that are found in the crystals of DHC and points out several unique features of the way in which the molecules are ordered into a structure. The arrangement of molecules requires the cyclohexene ring to be rotated around the 7-6 single bond so that the plane of the ring makes an angle of 39° with the conjugated chain; as a consequence there is a loss in resonance energy for this bond. It is likely that the 7-6 single bond is far enough removed from the center of the strongly conjugated DHC molecule so that rotation is possible in solution. Two potential wells would be expected in the barrier for rotation about this bond, or more correctly three. Two are cis around the 7-6 bond and one is the trans form; see Figure 14, page 82; atoms 8-7-6-5 of all three would be nearly planar and conjugation would be preserved. The trans form has the methyl groups 17 and 18 equally spaced

about atom 8, while the cis forms, one of which is shown in Figure 23, have atom 16 on the side of the molecule next to atom 8 but displaced slightly above or below the plane of the chain in order to increase the 8-16 distance. The cis form is therefore slightly distorted from complete planarity and might be less stable than the trans configuration. The trans form faces only one possible objection. Models show that this arrangement requires a quite close fit between methyl groups 17 and 18 and atom 8. The in-plane bending found for DHC would tend to mesh the two methyl groups even more tightly around atom 8; as a result atom 2 would be forced into the plane of the cyclohexene ring so that five atoms, 2, 1, 6, 5, and 4, would all be essentially coplanar. This configuration would not distort very easily either for packing or to reduce strain in the ring, since rotation around bonds 7-6 and 1-6 is virtually impossible. Thus what the trans form gains in resonance energy may in part be lost in strain in the ring and in close intramolecular contacts. The effect of the trans orientation on packing cannot be readily estimated since such a structure is impossible for the intermolecular arrangement found in DHC. The cis form of the molecule, on the other hand, is free to rotate around the 1-6 bond and the cyclohexene ring is probably strain free. The cis form found in DHC is sufficiently far, 39° , from planarity around the 7-6 bond so that there is almost no conjugation, and under these circumstances the ring orienta-

tion which occurs in the crystal is largely determined by the intermolecular arrangement. The cis configuration found for the cyclohexene ring of DHC has resulted in a loss of conjugation energy but we have gained a strain free ring, a less hindered molecule, and more efficient packing.

The first part of this section discusses the molecular dimensions and bond angles of 15,15'-dehydro- β -carotene. These parameters are useful as criteria for evaluating a structure only when limits of error are presented, and limits of error are not very meaningful unless the structure is well refined. The bond lengths and angles reported are acceptable in view of the probable error in atomic positions that has been given.

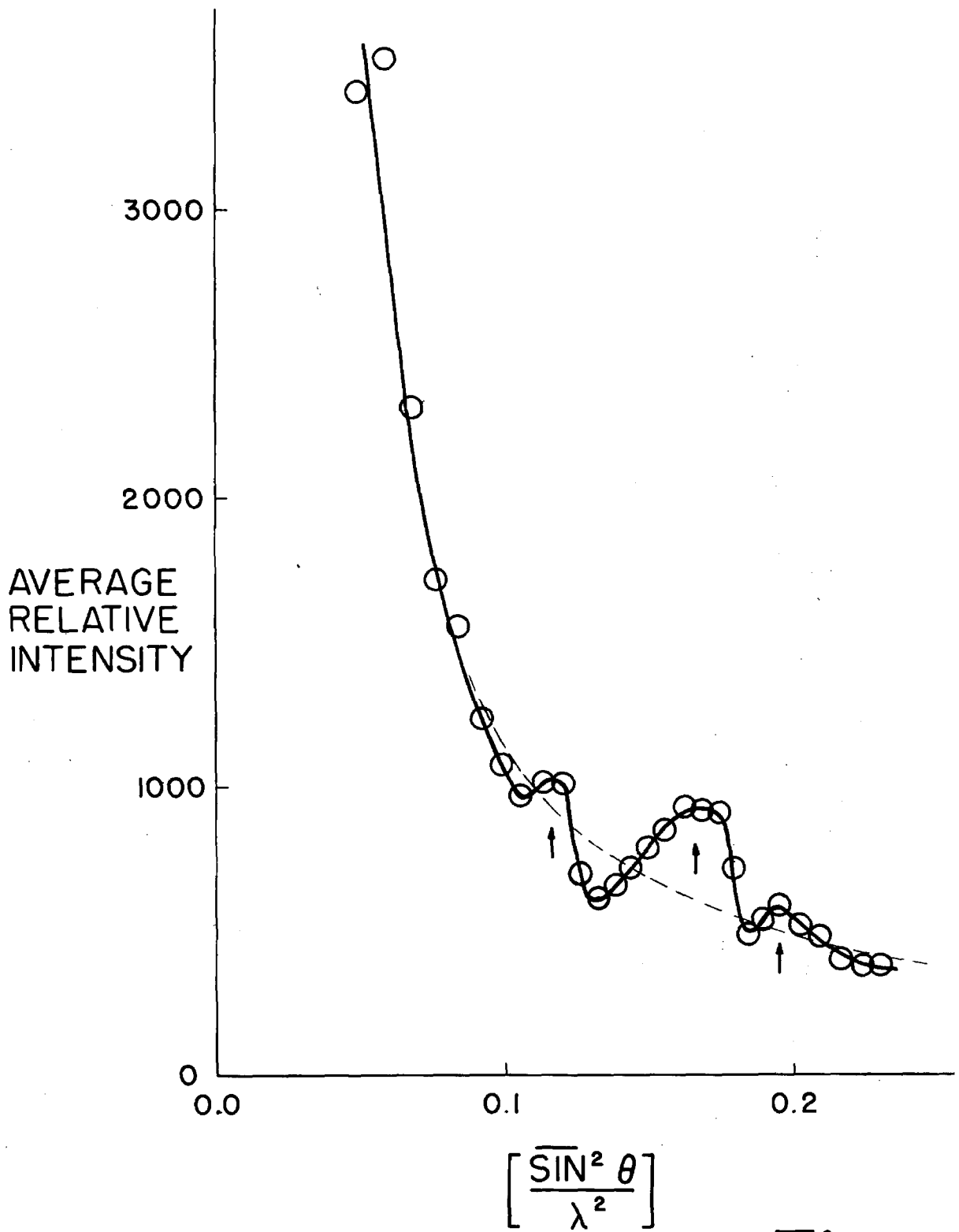
The crystals of DHC were examined under a polarizing microscope and were found to be pleochroic and strongly absorbing in one direction. The crystals were examined with light incident only normal to the face (010); the flat plates are too thin to view in other directions. The \vec{E} vector for maximum absorption of plane polarized light lies approximately along the direction $[10\bar{1}]$. This absorption axis or that which lies along \bar{b} must be the direction of maximum polarizability for the crystals. Since the structure has the molecules inclined only 27° to the ac plane, the direction of high optical absorbance in the ac

plane must be presumed to be the direction of maximum polarizability. The \bar{E} vector shown in the \bar{b} axis projection of Figure 16, page 96, is drawn in the direction of maximum absorption. This figure shows that \bar{E} lies in the direction of the projected molecules and very close to the projection of the double bonds, which are nearly parallel to (010). The molecules related by the c glide at $y = \frac{1}{4}$ would project exactly the same except that they would be translated by $\bar{c}/2$. The orientation of the molecules as illustrated in Figure 16 certainly provide an adequate explanation for the strong pleochroism and for the direction of the strong absorbance.

A satisfactory test of a structure with observed X-ray data requires an adequate explanation of the failure of Wilson's statistics, suitable agreement of atomic interactions with the three-dimensional Patterson which represents all of the data in composite form, as well as agreement between observed and calculated structure factors. The observed and calculated structure factors listed in the appendix and the overall R factor of 25.7% both indicate a satisfactory structure. The R factor is really a rather misleading quantity and a detailed consideration of the agreement between individual observed and calculated structure factors is more significant. This is especially true of structures such as DHC, since large R factors are

likely to occur with hypersymmetric molecules, as pointed out by Rogers and Wilson (124), and by Douglas and Woolfson (125). The R factors usually drop rapidly with refinement, however, as exemplified by the large decrease that followed the three-dimensional Fourier refinement of DHC. Further rapid decreases in R will probably accompany the three-dimensional least-squares refinements that will be used in the next stage of the structural analysis of DHC.

Wilson's statistical arguments are based on the premise that there are a large number of atoms of approximately equal scattering power located randomly in the unit cell (10, 11, 12). DHC has eighty carbon atoms in the unit cell but they are by no means randomly distributed in space; rather they are contained in planes, and, what is perhaps more important, there is a periodic occurrence of atoms every 1.2 to 1.3 Å. along the mean direction of a chain which extends for a total of 24 atoms if we include three from each of the rings. A plot of the values of $\sin^2\theta/\lambda^2$ vs. \bar{I} for the same groups of reflections used in the application of Wilson's method (see Figure 9, page 63) is shown in Figure 24. Each plotted value represents the mean of one hundred reflections. The three peaks of the curve are associated with the regions of negative slope in the Wilson plot and occur at $\sin^2\theta/\lambda^2$ values corresponding to spacings of 1.47 Å., 1.22 Å., and 1.13 Å. Parry has shown a similar plot for the compound



PLOT OF AVERAGE RELATIVE INTENSITY VS. $\left[\frac{\sin^2 \theta}{\lambda^2} \right]$ FOR TWO OVERLAPPING GROUPS OF REFLECTIONS.

FIGURE 24.

uracil, which has a large peak at a $\sin^2\theta$ value corresponding to a spacing of 1.2 \AA . (126). He has explained his results qualitatively by pointing out that the structure is essentially a layer structure and that the atoms fall onto a plane hexagonal net which has a Fourier transform with strong peaks corresponding to a spacing of 1.2 \AA . The explanation given by Parry may be in part valid for DHC since the chain of atoms contains many parts of a benzene ring, or more properly of an anthracene or naphthalene type structure. Four members of a six-membered ring occur six times in the half molecule, excluding the ring itself. However, one is not a layer structure as is uracil, since there are two molecular planes intersecting at an angle of 156° .* The more important factor here is probably the linearly periodic chain structure. Knott has reported the molecular transforms of benzene, naphthalene, and of a planar aliphatic chain (127). All of these structures give strong peaks in reciprocal space corresponding to spacings of about $1.2 - 1.3 \text{ \AA}$, although the transform of the aliphatic chain is not as easy to interpret as are those of benzene and naphthalene. There seems to be ample justification in the above arguments for the occurrence of the strong peak at 1.22 \AA . However, one

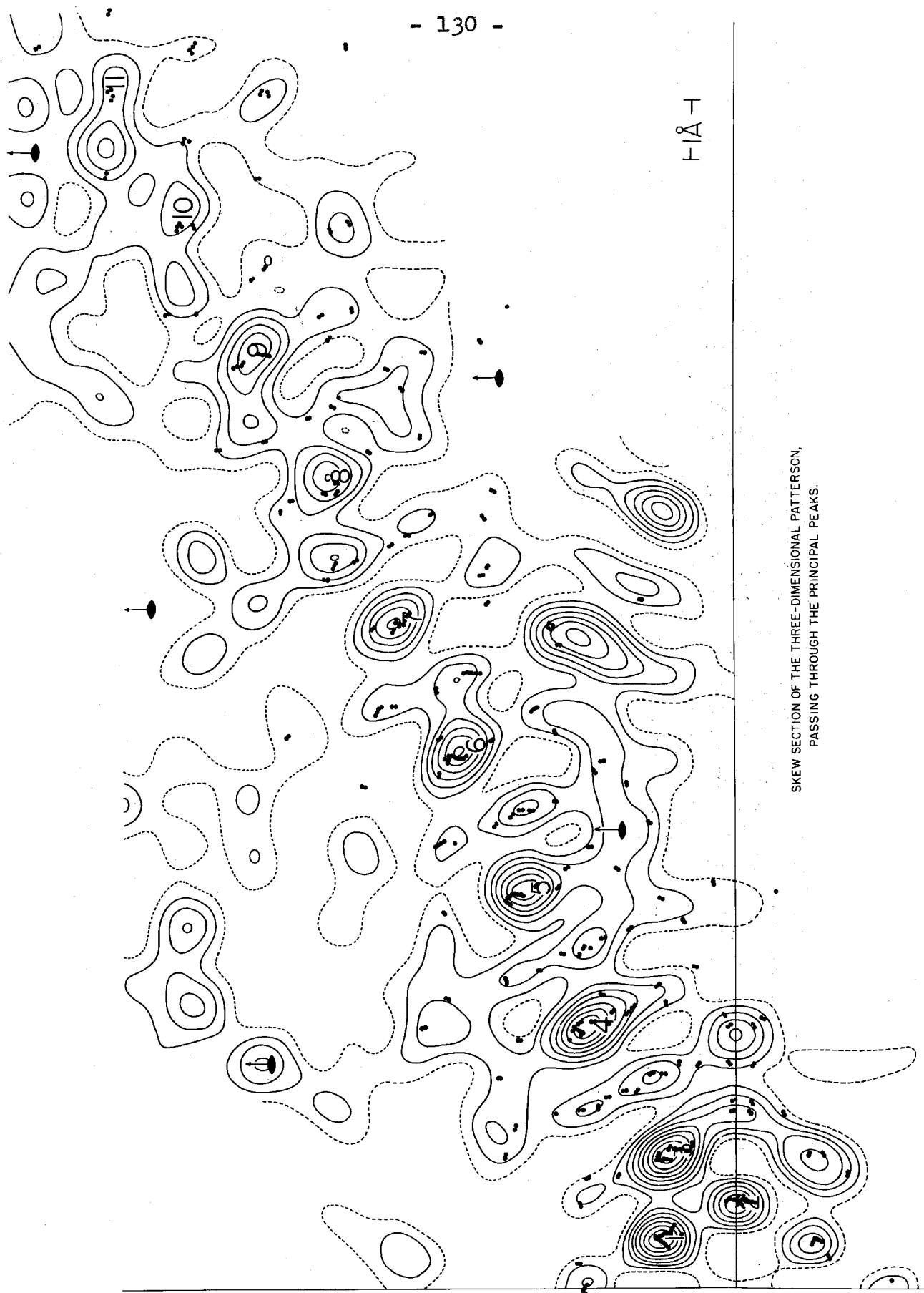
* Note that this is different from the angle at the dihedral of two strips of the structure, 164° ; this arises because the molecules are rotated about their axes by 5° in forming the strips, and are not completely coplanar.

must be a little skeptical of arguments based solely on a molecular transform because this is not the only factor that must be considered in dealing with intensity distributions. For example β -carotene probably gives a transform much like that of DHC, yet the strongest $|F|$ obtained for β -carotene was only 84 electrons out of 592, while DHC has a strongest $|F|$ of 116 out of 588.* The difference lies not so much in the molecular transform of the two molecules as in the arrangement of the molecules into a lattice; that is, in the sampling of the molecular transforms brought about by the packing of the molecules into a periodic structure. There appears to be no obvious explanation for the peaks at 1.47 \AA and 1.13 \AA ; they are much less pronounced than the 1.22 \AA peak, however, and the hypersymmetry of the molecule could well account for them. The molecules of DHC being centered and almost planar have approximately a two-fold rotation axis, or a mirror plane not required by the space group. Perhaps further study of the indices of the reflections in the regions of $\sin\theta$ corresponding to these smaller peaks may give some clue as to what features of the structure cause them, although this information will probably not be of great value.

*The author believes that the value of 116 for a strongest reflection may in fact be low; the very strong reflections of DHC have been difficult to estimate and have large deviations; reference to the appendix will show that the calculated values for the strongest reflections are larger than the observed by 26 to 28 electrons, without the inclusion of hydrogens.

Figure 25 shows the intramolecular interactions from the planar portion of one molecule of DHC superimposed on the section of the three-dimensional Patterson presented in Figure 11, page 71. The degree of agreement is satisfactory, not only in the principal peaks but in many of the details of the Patterson between the principal peaks. For example the pattern of the interactions contained in the elongated peak 4. It is the in-plane bending of the molecule described in the first part of this section that brings about the agreement of the interactions and the Patterson. That the row of peaks 3, 4, 5, ... lie on an unbroken straight line results from the fact that the backbone of the molecule is curved; specifically from the fact that the vectors between atoms 8 and 10, and between atoms 9 and 13 pass almost through the center of symmetry; see Figure 23. Therefore the interactions between atoms 8-8', 8-10', 9-13', etc., which connect atoms across the step due to the triple bond, lie along the molecular axis, since the mean direction of vectors 8-10 and 9-13 is roughly that of the molecular chain.

In the previous paragraphs we have examined some of the criteria which can be used to evaluate a molecular structure. We have found that the dimensions of the molecule are consistent with our knowledge of bond lengths and angles; and that the molecules are arranged into an



SKIEW SECTION OF THE THREE-DIMENSIONAL PATTERSON,
PASSING THROUGH THE PRINCIPAL PEAKS.

Figure 25.

acceptably packed structure. The orientation of the molecules explains the observed dichroism and high optical absorbance. The structure gives good agreement between observed and calculated structure factors; it explains the failure of Wilson's statistics; and its intramolecular interactions are in good agreement with all of the intensity data as exemplified by the three-dimensional Patterson. The entire structure analysis is satisfactory and needs only further refinement to give bond lengths and angles that will be useful in other work of this type.

In concluding the discussion of the crystal structure determination of DHC we shall consider briefly some of the trial and error methods used in the preliminary investigation. In a sense the structure of DHC was really solved with a single zone of data, the $hk\bar{h}$ data. It was the author's intention, after the abandonment of trial and error methods described in Section B, to obtain the best possible set of zero-layer Weissenberg photographs around the $\bar{c} + \bar{a}$ axis, using copper $K\alpha$ X-radiation, long exposures, and the lowest temperature possible, because it was felt that a solution to the structure could be worked out with these data. The use of the intensities obtained in this way, which would have been greater in number than the data actually employed, would almost certainly have proved successful, although the structure could not have been attacked

with the assurance given by the three-dimensional Patterson. It is the author's conviction that the structure could have been solved with zero-layer data around \bar{a} , \bar{b} , and \bar{c} ; this is not to say completely refined, but at least to the extent of a tenable trial structure. Certain improvements would, however, have been essential. First, the models used, especially the wire frame type, must be flexible so that bond lengths and angles can be varied somewhat; those used by the author were rigid. The wire frame models need to be of sufficiently large scale so that measuring errors are not too severe; about 1" per \AA is felt to be the minimum acceptable scale. Second, some quick way must be found to project the models onto a plane of interest. The method used by the author was projection by parallel light. This is satisfactory if the light source is big enough for models of a scale of 1" per \AA . Third, and most important, a quick way must be available to determine the magnitude of structure factors. The author calculated F's by hand from explicit coordinates. This is too time consuming especially since most of the trial structures will prove to be wrong. IBM equipment can be used for rapid calculation of structure factors but this involves measurements of coordinates and the hand punching of these data into cards. The best and quickest way is with structure factor maps drawn to scale. If optical projections are used one simply needs to indicate atomic

coordinates by crosses on celluloid sheets. These sheets can then be superimposed over the scale-drawn structure factor maps for quick estimates. This method is somewhat analogous to the mapping refinement carried out on the DHC structure. It may be that these scale drawn structure factor maps for the various projections of any space group can be obtained optically or electronically by distortion of orthogonal nets. Such maps prove very useful not only in trial structure work but in refinement as well. With the advent of rapid computing equipment these trial and error methods have largely been neglected. However, a three-dimensional Patterson, even with the high powered methods of superposition, does not necessarily give a structure. Expensive computing equipment can perhaps be combined with relatively inexpensive trial and error methods of solution and refinement, without much loss of time and with considerable economic and pedagogical gain.

I. Appendix I--Structure-Factor Data

Table III. The observed and calculated structure factors for 15,15'-dehydro- β -carotene. The asterisk, *, indicates reflections for which F_c has changed sign as a result of refinement by the three-dimensional Fourier. The F_o values followed by the symbol #, are the estimated maximum possible values for unobserved reflections.

$\lambda = 0$	h	k	$ F_o $	F_c	$ \Delta F $
	0	2	3.38	7.22	3.84
		4	9.36	-1.02	8.34
		6	30.72	24.96	5.76
		8	35.72	-38.15	2.43
		10	5.69	-4.51	1.18
	0	12	11.75	-6.89	4.86
		14	29.30	-22.27	7.03
		16	48.36	46.68	1.68
		18	12.19	-6.62	5.57
		20	3.36#	-3.57	0.21
	0	22	25.21	23.01	2.20
		24	2.81#	-3.66	0.85
		26	22.92	-22.56	0.36
	1	0	83.85	-88.10	4.25
		1	15.02	10.98	4.04*
		2	46.03	60.99	14.96
		3	53.03	57.24	4.21
		4	55.11	62.15	7.04
	1	5	62.30	70.44	8.14
		6	62.30	57.34	4.96
		7	7.49	-7.68	0.19
		8	35.20	-29.36	5.84
		9	28.32	-29.76	1.44
	1	10	34.42	19.66	14.76
		11	21.51	-12.10	9.41
		12	6.69	-6.22	0.47
		13	6.29	-3.31	2.98
		14	4.35#	-5.86	1.51

$\lambda = 0$	h	k	$ F_o $	F_c	$ \Delta F $
1	1	15	11.62	-9.07	2.55
		16	6.16	-2.03	4.13
		17	13.58	-12.61	0.97
		18	7.26	-7.94	0.68
		19	17.98	-10.07	7.91
1	1	20	7.06	-6.38	0.68
		21	6.53	-5.15	1.38
		22	4.63	2.76	1.87
		23	5.51	7.72	2.21
		24	9.39	-10.34	0.95
1	1	25	28.21	-29.80	1.59
		26	22.49	21.88	0.61
		27	2.02#	0.53	1.49*
2	2	0	2.93	1.41	1.52*
		1	17.67	-9.53	8.14
		2	3.07#	1.19	1.88
		3	18.11	-9.26	8.85*
		4	21.80	-12.94	8.86
2	2	5	30.42	28.13	2.29
		6	7.56	-0.81	6.75
		7	44.58	46.87	2.29
		8	26.35	29.27	2.92
		9	21.34	24.20	2.86
2	2	10	25.16	-22.16	3.00
		11	10.48	-11.45	0.97
		12	4.51#	-1.36	3.15
		13	4.65#	-6.02	1.37
		14	20.15	-17.49	2.66
2	2	15	14.54	-9.77	4.77
		16	4.96#	-0.04	4.92
		17	9.49	-7.64	1.85
		18	4.94#	1.51	3.43
		19	4.84#	-0.62	4.22*
2	2	20	12.61	11.31	1.30
		21	4.44#	3.05	1.39
		22	13.05	7.65	5.40
		23	22.99	-24.19	1.20
		24	13.72	12.37	1.35
2	25	6.55	10.38	3.83	

$\lambda = 0$	h	k	$ F_o $	F_c	$ \Delta F $
3	3	0	17.01	-7.99	9.02
		1	16.23	10.69	5.54
		2	18.05	-11.19	6.86*
		3	25.12	15.18	8.94
		4	25.22	27.07	1.85
	3	5	31.23	-21.56	9.67
		6	19.09	-11.59	7.50
		7	7.88	4.96	2.92
		8	14.94	-9.18	5.76
		9	11.96	8.10	3.86*
3	10	10	30.61	30.41	0.20
		11	29.93	30.13	0.20
		12	11.62	5.86	5.76
		13	9.61	10.29	0.68
		14	10.77	8.73	2.04
	3	15	10.94	10.66	0.28
		16	6.57	-12.26	5.69
		17	5.91	-2.15	3.76*
		18	8.79	12.10	3.31
		19	5.65	-2.26	3.39
3	20	20	9.72	10.94	1.22
		21	13.67	-10.04	3.63
		22	10.34	-5.81	4.53
		23	10.38	12.56	2.18
	4	0	6.79	5.70	1.09*
		1	6.17	9.90	3.73
		2	20.26	24.64	4.38
		3	8.50	-0.08	8.42*
		4	11.86	-5.92	5.94*
4	5	5	24.24	18.78	5.46
		6	7.78	10.70	2.92
		7	5.34	-3.20	2.14
		8	23.21	25.27	2.06
		9	8.35	16.82	8.47
	4	10	19.24	-15.82	3.42
		11	7.67	-9.92	2.25
		12	7.36	7.77	0.41
		13	5.27	-4.85	0.42
		14	22.33	18.62	3.71

$\lambda = 0$	h	k	$ F_0 $	F_c	$ \Delta F $
	4	15	8.08	-12.66	4.58
		16	8.71	3.64	5.07*
		17	8.25	5.14	3.11
		18	11.04	9.21	1.83
		19	1.90#	1.42	0.48
	4	20	14.04	-7.59	6.45
		21	15.82	9.88	5.94
		22	6.99	-9.08	2.09
		23	12.04	15.23	3.19
		24	11.22	12.57	1.35
	4	25	2.66#	2.74	0.08
		26	1.61#	-13.55	11.94
	5	0	21.29	-12.20	9.09*
		1	10.36	-15.61	5.25
		2	21.70	19.51	2.19
		3	7.26	3.26	4.00
		4	9.44	6.34	3.10*
	5	5	7.02	-7.67	0.65
		6	11.49	-9.12	2.37
		7	3.30#	-1.43	1.87
		8	22.10	21.96	0.14
		9	5.09	-7.33	2.24
	5	10	4.81	0.03	4.78*
		11	2.30#	5.66	3.36
		12	1.55#	-0.59	0.96
		13	6.05	-5.48	0.57
		14	7.94	10.14	2.20
	5	15	9.94	8.05	1.89
		16	8.99	-3.31	5.68*
		17	3.73#	-4.48	0.75
		18	8.47	-8.20	0.27
		19	3.13#	-2.10	1.03
	5	20	4.09	0.16	3.93*
		21	1.97#	-0.47	1.50

$\lambda = 1$	h	k	$ F_o $	F_c	$ \Delta F $
0		1	11.38	8.44	2.94
		2	45.21	49.75	4.54
		3	43.02	-40.57	2.45
		4	78.18	-96.06	17.88
		5	112.10	140.71	28.61
0		6	68.60	-76.12	7.52
		7	24.80	21.48	3.32
		8	36.97	27.00	9.97
		9	17.75	12.21	5.54
		10	18.71	9.83	8.88
0		11	8.41	-6.43	1.98
		12	27.85	25.19	2.66
		13	7.13	-1.14	5.99
		14	7.52	-4.09	3.43
		15	5.07	-5.13	0.06
0		16	14.24	12.63	1.61
		17	7.94	6.37	1.57
		18	22.80	21.51	1.29
		19	22.92	-20.22	2.70
		20	5.50	-2.34	3.16
0		21	6.99	-3.68	3.31
		22	9.13	-7.54	1.59
		23	2.93#	0.29	2.64*
		24	31.56	24.16	7.40
		25	22.66	19.36	3.30
0		26	19.62	17.16	2.46
		27	1.38#	1.57	0.19
		28	7.01	-6.56	0.45
		29	4.06	0.92	3.14*
		30	3.87#	-3.40	0.47
0		31	11.48	-12.50	1.02
		32	2.41#	2.24	0.17
1		1	116.20	142.73	26.53
		2	61.05	-76.11	15.06
		3	52.48	51.64	0.84
		4	34.08	-34.97	0.89
		5	17.74	-19.56	1.82

$\lambda = 1$	h	k	$ F_o $	F_c	$ \Delta F $
	1	6	52.21	45.03	7.18
		7	13.56	1.19	12.37
		8	17.32	-15.76	1.56
		9	14.44	-19.23	4.79
		10	22.81	-17.93	4.88
	1	11	9.17	-4.96	4.21
		12	17.35	13.66	3.69
		13	4.84	-9.46	4.62
		14	4.60	0.30	4.30*
		15	6.93	11.04	4.11
	1	16	10.30	-10.27	0.03
		17	10.67	12.67	2.00
		18	10.89	9.26	1.63
		19	5.38	0.34	5.04*
		20	13.32	-15.54	2.22
	1	21	7.49	7.15	0.34
		22	22.95	20.09	2.86
		23	11.38	11.13	0.25
		24	20.35	-14.04	6.31
		25	19.93	-21.49	1.56
	1	26	12.53	-16.88	4.35
		27	4.72#	-4.03	0.69
		28	26.75	28.36	1.61
		29	3.92#	0.31	3.61
		30	6.74	-7.58	0.84
	1	31	8.61	5.78	2.83
	2	1	18.79	13.92	4.87
		2	65.97	62.22	3.75
		3	26.43	31.51	5.08
		4	22.61	13.01	9.60
		5	14.15	11.26	2.89
	2	6	5.32	-0.08	5.24
		7	21.33	7.83	13.50*
		8	4.84#	-12.12	7.28
		9	11.37	-12.11	0.74
		10	17.11	-17.62	0.51
	2	11	6.69	8.53	1.84
		12	5.53	4.21	1.32
		13	4.83	-5.19	0.36
		14	11.06	-8.23	2.83
		15	6.79	-5.70	1.09

$\lambda = 1$	h	k	$ F_o $	F_c	$ \Delta F $
	2	16	6.43	-6.58	0.15
		17	5.36#	-3.05	2.31
		18	7.97	-5.40	2.57
		19	6.43	-5.69	0.74
		20	7.80	-5.74	2.06
	2	21	6.58	0.99	5.59
		22	9.17	-7.30	1.87
		23	4.79	-6.82	2.03
		24	5.68	-0.98	4.70
		25	11.80	7.23	4.57
	2	26	7.84	-6.10	1.74
		27	7.66	10.19	2.53
		28	16.35	-17.35	1.00
		29	4.14	0.10	4.04*
		30	1.22#	-2.47	1.25
	3	1	17.17	-4.83	12.34*
		2	12.25	-4.93	7.32*
		3	4.76#	-5.54	0.78
		4	7.75	1.05	6.70
		5	29.87	31.56	1.69
	3	6	34.94	37.71	2.77
		7	17.89	-17.72	0.17
		8	21.84	18.53	3.31
		9	8.83	1.94	6.89
		10	16.16	-16.47	0.31
	3	11	4.86#	-5.53	0.67
		12	9.19	9.41	0.22
		13	16.23	-14.63	1.60
		14	8.56	-12.97	4.41
		15	5.23	1.10	4.13*
	3	16	8.65	-2.11	6.54*
		17	4.98	-0.73	4.25*
		18	3.55#	0.63	2.92
		19	5.98	2.99	2.99
		20	2.53#	0.42	2.11
	3	21	12.28	9.30	2.98
		22	7.11	-2.55	4.56*
		23	4.86	0.63	4.23
		24	7.11	-3.91	3.20
		25	5.34	4.75	0.59
	3	26	8.34	-9.79	1.45
		27	2.53	2.75	0.22*

$\lambda = 1$	h	k	$ F_o $	F_c	$ \Delta F $
4	4	1	6.31	4.73	1.58
		2	18.21	15.68	2.53
		3	14.77	-1.17	13.60*
		4	8.19	-6.13	2.06
		5	8.11	-4.54	3.57*
	4	6	13.29	-11.89	1.40
		7	10.18	10.08	0.10
		8	9.02	8.52	0.50
		9	4.31#	2.73	1.58
		10	18.23	21.17	2.94
4	4	11	8.01	9.82	1.81
		12	3.58#	0.04	3.54*
		13	9.33	6.85	2.48
		14	6.54	10.23	3.69
		15	7.95	-9.59	1.64
4	4	16	6.00	-1.32	4.68
		17	6.66	4.52	2.14*
		18	5.50	10.99	5.49
		19	3.78#	6.64	2.86
		20	13.70	-12.99	0.71
4	4	21	4.56	-0.08	4.48
		22	3.52	-0.82	2.70
		23	1.79#	4.50	2.71
5	5	1	4.35#	4.88	0.53
		2	16.14	-11.60	4.54
		3	15.06	13.32	1.74
		4	18.94	20.22	1.28
		5	4.27#	-2.29	1.98
5	5	6	4.20#	0.68	3.52*
		7	5.67	11.48	5.81
		8	5.55	-2.08	3.47*
		9	3.95#	3.17	0.78
		10	5.58	6.14	0.56
5	5	11	3.70#	-2.97	0.73
		12	6.31	-6.37	0.06
		13	5.84	4.11	1.73
		14	3.07#	-6.05	2.98
		15	9.62	10.67	1.05
5	5	16	3.10	3.56	0.46
		17	1.14#	2.87	1.73

$\ell = 2$	h	k	$ F_0 $	F_c	$ \Delta F $
0	0	0	57.61	54.77	2.84
		1	12.32	-3.82	8.50*
		2	55.40	-52.36	3.04
		3	19.25	12.85	6.40
		4	23.29	27.33	4.04
	0	5	39.83	-35.64	4.19
		6	22.07	-27.22	5.15
		7	12.40	1.78	10.62
		8	22.79	-16.77	6.02
		9	16.33	-18.39	2.06
	0	10	32.08	36.92	4.84
		11	25.96	-30.49	4.53
		12	11.28	9.82	1.46
		13	6.85	5.57	1.28
		14	23.83	-21.48	2.36
	0	15	15.59	15.56	0.03
		16	4.51	-0.42	4.09
		17	3.36#	4.14	0.78
		18	8.68	-4.16	4.52
		19	26.63	22.64	3.99
0	0	20	33.93	31.92	2.01
		21	15.90	16.51	0.61
		22	2.81#	5.96	3.15
		23	14.70	-13.58	1.12
		24	9.48	-12.40	2.92
	0	25	9.50	6.22	3.28
		26	5.69	-7.15	1.46
		27	17.36	-13.82	3.54
		28	11.90	-8.31	3.59
		29	5.95	-7.48	1.53
	0	30	8.57	-8.94	0.37
		31	6.05	7.45	1.40
1	0	0	18.37	2.58	15.79*
		1	6.69	-0.78	5.91*
		2	6.09	-0.67	5.42*
		3	13.56	-2.65	10.91*
		4	7.75	-13.23	5.48
	1	5	23.19	-25.43	2.24
		6	57.59	66.34	8.75
		7	43.47	-49.32	5.85
		8	39.33	45.00	5.67
		9	4.60#	3.15	1.45

$l = 2$	h	k	$ F_o $	F_c	$ \Delta F $
1	1	10	17.29	-4.77	12.52*
		11	18.79	17.52	1.27
		12	16.51	-10.06	6.45
		13	11.14	7.30	3.84
		14	9.12	5.79	3.33
1	1	15	6.05	7.77	1.72
		16	4.98#	0.05	4.93*
		17	10.07	11.33	1.26
		18	4.72#	-0.27	4.45*
		19	7.27	0.30	6.97
1	1	20	28.01	-30.84	2.83
		21	3.87#	-6.45	2.58
		22	19.75	16.54	3.21
		23	23.94	24.69	0.75
		24	13.39	13.95	0.56
1	1	25	5.86#	2.58	3.28
		26	5.44#	-1.67	3.77
		27	13.10	6.07	7.03
		28	4.37#	-4.41	0.04
		29	5.11	-8.72	3.61
1	30		1.95#	0.94	1.01
2	0	0	23.75	22.97	0.78
		1	22.32	-19.72	2.60
		2	53.26	54.98	1.72
		3	36.76	-49.26	12.50
		4	28.38	30.62	2.24
2	5	5	7.66	-3.79	3.87
		6	15.29	-10.70	4.59
		7	9.41	5.77	3.64
		8	15.64	-7.34	8.30
		9	9.32	-1.54	7.78
2	10	10	14.24	-14.55	0.31
		11	6.99	-8.65	1.66
		12	15.68	7.61	8.07*
		13	5.32#	3.87	1.45
		14	5.84	-3.44	2.40
2	15	15	4.99#	0.67	4.32*
		16	4.76#	4.47	0.29
		17	4.48#	-7.46	2.98
		18	9.95	3.59	6.36*
		19	5.18	0.46	4.72*

$\lambda = 2$	h	k	$ F_0 $	F_c	$ \Delta F $
	2	20	11.15	15.14	3.99
		21	5.89	7.91	2.02
		22	10.72	-7.79	2.93*
		23	14.42	-14.12	0.30
		24	5.14#	-3.66	1.48
	2	25	4.65#	-3.42	1.23
		26	4.04#	-3.80	0.24
		27	5.22	3.67	1.55
	3	0	26.53	29.45	2.92
		1	11.55	10.29	1.26
		2	16.57	11.23	5.34
		3	23.91	18.27	5.64
		4	4.67#	1.15	3.52
	3	5	10.61	-7.70	2.91
		6	6.88	-6.49	0.39
		7	8.98	7.40	1.58
		8	10.71	2.22	8.49*
		9	21.29	-26.52	5.23
	3	10	5.46	6.69	1.23
		11	6.11	8.34	2.23
		12	13.68	-13.56	0.12
		13	3.52#	-0.71	2.81*
		14	8.49	7.90	0.59
	3	15	6.05	-9.09	3.04
		16	2.26#	-8.09	5.83
		17	5.97#	3.53	2.44
		18	9.46	-3.78	5.68*
		19	10.02	-7.68	2.34
	3	20	5.07#	-0.11	4.96
		21	4.67#	-7.10	2.43
		22	4.16#	-2.62	1.54
		23	5.89	4.87	1.02
		24	2.32#	2.73	0.41
	4	0	20.66	-19.73	0.93
		1	18.47	19.19	0.72
		2	3.49#	4.64	1.15
		3	3.38#	-1.50	1.88
		4	14.81	17.42	2.61

$\lambda = 2$	h	k	$ F_o $	F_c	$ \Delta F $
4	4	5	2.88#	7.24	4.36
		6	2.41#	-1.85	0.56*
		7	16.03	13.31	2.72
		8	4.42#	-3.09	1.33
		9	5.41	4.59	0.82
4	4	10	7.65	-11.98	4.33
		11	6.28	-11.13	4.85
		12	3.97#	2.75	1.22*
		13	4.99	8.47	3.48
		14	3.59#	-3.90	0.31
4	4	15	11.11	-11.73	0.62
		16	8.76	-7.73	1.03
		17	5.23	4.06	1.17
		18	8.53	9.74	1.21
5	5	0	2.88#	7.01	4.13
		1	8.26	-6.06	2.20
		2	2.81#	4.55	1.74
		3	2.74#	3.04	0.30
		4	11.22	-9.88	1.34
5	5	5	2.53#	-2.34	0.19
		6	2.37#	5.92	3.55
		7	2.12#	-0.82	1.30
		8	1.61#	8.92	7.31

$\lambda = 3$	h	k	$ F_0 $	F_c	$ \Delta F $
	0	1	13.99	-14.43	0.44
		2	16.75	14.91	1.84
		3	17.93	-23.00	5.07
		4	14.45	-5.67	8.78*
		5	26.02	23.68	2.34
	0	6	3.03#	-4.38	1.35
		7	23.46	-25.85	2.39
		8	6.28	6.95	0.67
		9	10.28	13.10	2.82
		10	30.03	-24.37	5.66
	0	11	3.30#	5.11	1.81
		12	6.31	1.86	4.45
		13	5.01	-3.66	1.35
		14	8.85	-13.61	4.76
		15	42.60	41.44	1.16
	0	16	3.24	1.25	1.99
		17	4.46	5.70	1.24
		18	9.14	-7.98	1.16
		19	16.90	-21.44	4.54
		20	2.63#	-4.76	2.13
	0	21	4.76	0.59	4.17*
		22	11.97	-10.92	1.05
		23	21.36	-20.79	0.57
		24	6.21#	-5.29	0.92
		25	5.87#	0.17	5.70*
	0	26	5.18#	-4.70	0.48
		27	4.65#	6.62	1.97
		28	7.72	-7.50	0.22
		29	4.31	-2.78	1.53
	1	1	12.28	9.40	2.88
		2	16.79	9.96	6.83
		3	26.17	-22.12	4.05
		4	18.11	-8.79	9.32
		5	7.22	5.16	2.06
	1	6	11.33	-11.30	0.03
		7	5.01#	-4.90	0.11
		8	5.01#	4.56	0.45
		9	5.74	-11.14	5.40
		10	8.12	-5.80	2.32
	1	11	19.52	23.44	3.92
		12	13.16	-15.58	2.42
		13	4.76#	5.89	1.13
		14	13.51	-7.54	5.97*
		15	16.87	-16.74	0.13

$\ell = 3$	h	k	$ F_o $	F_c	$ \Delta F $
	1	16	9.97	8.64	1.33
		17	11.89	14.94	3.05
		18	28.62	33.16	4.54
		19	7.04	6.37	0.67
		20	2.70#	1.35	1.35
	1	21	1.79#	5.01	3.22
		22	5.82#	-2.26	3.56
		23	8.35	2.58	5.77*
		24	5.05#	-0.53	4.52
		25	14.48	-16.78	2.30
	1	26	6.93	-8.14	1.21
		27	2.97#	-2.58	0.39
	2	1	5.28#	1.65	3.63
		2	9.58	-8.13	1.45
		3	5.25#	-9.75	4.50
		4	5.22#	-0.26	4.96*
		5	13.00	8.83	4.17
	2	6	10.24	-7.55	2.69
		7	24.97	34.33	9.36
		8	19.40	-26.39	6.99
		9	5.63	16.94	11.31
		10	7.49	-1.84	5.65*
	2	11	4.42#	8.49	4.07
		12	9.13	3.58	5.55*
		13	11.63	-11.99	0.36
		14	19.54	20.25	0.71
		15	3.13#	7.13	3.95
	2	16	7.77	0.02	7.75
		17	1.14#	-0.74	0.40*
		18	10.82	-9.17	1.65
		19	13.42	-20.68	7.26
		20	11.15	8.50	2.65*
	2	21	6.79	8.46	1.67
		22	10.90	11.20	0.30
		23	10.34	9.61	0.73
		24	5.91	2.56	3.35
	3	1	15.66	13.03	2.63
		2	12.67	-15.37	2.70
		3	12.42	15.52	3.10
		4	10.71	-16.89	6.18
		5	14.74	21.34	6.60

$\ell = 3$	n	k	$ F_o $	F_c	$ \Delta F $
	3	6	9.54	-10.30	0.76
		7	6.03	-8.18	2.15
		8	7.16	2.50	4.66*
		9	8.49	-7.98	0.51
		10	8.73	-0.86	7.87
	3	11	5.71#	-1.01	4.70
		12	5.53#	4.23	1.30
		13	5.32#	-1.33	3.99*
		14	10.94	-12.65	1.71
		15	4.79#	4.09	0.70*
	3	16	9.88	6.87	3.01
		17	4.06#	-0.73	3.33
		18	3.52#	-1.95	1.57
		19	2.74#	10.28	7.54
	4	1	7.72	9.30	1.58
		2	6.03	-0.54	5.49
		3	12.63	12.43	0.20
		4	3.15#	-1.63	1.52
		5	8.88	-12.88	4.00
	4	6	8.15	2.00	6.15*
		7	4.86	-3.63	1.23
		8	2.03#	-3.08	1.05
		9	6.31	8.31	2.00
		10	7.54	-8.44	0.90*
	4	11	1.14#	-7.31	6.17

$\ell = 4$	h	k	$ F_o $	F_c	$ \Delta F $
	0	0	3.33#	3.70	0.37
		1	17.51	-14.83	2.68
		2	6.40	1.16	5.24*
		3	3.36#	-2.75	0.61
		4	15.15	20.72	5.57
	0	5	12.93	-13.71	0.78
		6	14.52	-14.06	0.46
		7	8.94	-8.14	0.80
		8	11.00	7.48	3.52
		9	6.80	2.02	4.78*
	0	10	28.32	22.61	5.71
		11	18.60	14.19	4.41
		12	3.92	1.01	2.91
		13	9.80	-9.68	0.12
		14	6.60	1.71	4.89*
	0	15	4.22	-5.28	1.06
		16	6.72	0.05	6.67*
		17	5.98	-5.50	0.48
		18	14.58	-13.76	0.82
		19	17.66	-21.11	3.45
	0	20	16.43	14.76	1.67
		21	7.08	-8.82	1.74
		22	12.21	-10.68	1.53
		23	13.58	-12.39	1.19
		24	5.32	-2.81	2.51
	0	25	5.91	-5.74	0.17
		26	1.90#	-0.25	1.65
	1	0	8.84	-14.84	6.00
		1	14.02	9.63	4.39
		2	6.20	-5.42	0.78
		3	3.95#	6.57	2.62
		4	3.97#	-5.62	1.65
	1	5	7.08	-10.05	2.97
		6	3.99#	0.79	3.20
		7	5.55	6.91	1.36
		8	4.01#	-3.14	0.87
		9	11.56	-7.23	4.33
	1	10	9.53	-2.97	6.56*
		11	5.44	-7.59	2.15
		12	11.95	11.54	0.41
		13	7.02	11.30	4.28
		14	13.71	14.94	1.23

$\ell = 4$	h	k	$ F_o $	F_c	$ \Delta F $
1	1	15	7.40	-9.05	1.65
		16	1.52#	-0.94	0.58*
		17	3.55#	-8.17	4.62
		18	12.74	8.97	3.77
		19	5.74	-4.78	0.96
1	1	20	13.40	-17.26	3.86
		21	9.50	-12.42	2.92
		22	6.35	-5.98	0.37
		23	1.95#	1.94	0.01
2	2	0	2.63#	9.63	7.00
		1	7.29	11.87	4.58
		2	3.21#	-3.68	0.47
		3	7.51	-7.25	0.26
		4	9.78	-7.82	1.96
2	2	5	3.13#	0.80	2.33*
		6	2.61#	-0.04	2.57*
		7	2.30#	-2.25	0.05*
		8	6.32	0.92	5.40*
		9	3.59#	3.68	0.09
2	2	10	3.52#	-1.65	1.87*
		11	10.34	-4.57	5.77
		12	3.33#	4.94	1.61
		13	9.35	-13.14	3.79
		14	3.03#	-1.27	1.76
2	2	15	2.88#	-1.56	1.32
		16	10.22	17.36	7.14
		17	13.09	18.50	5.41
		18	2.07#	-2.17	0.10*
		19	1.52#	11.12	9.60
3	3	0	4.44	3.20	1.24
		1	2.74#	-2.35	0.39
		2	4.20	-5.79	1.59
		3	2.70#	-0.78	1.92*
		4	2.63#	-0.82	1.81
3	3	5	2.61#	-4.80	2.19
		6	11.84	15.04	3.20
		7	2.41#	3.96	1.55*
		8	2.26#	4.43	2.17
		9	13.00	-23.62	10.62
3	3	10	9.46	19.31	9.85
		11	1.45#	2.33	0.88*

$\lambda = 5$	h	k	$ F_o $	F_c	$ \Delta F $
0	0	1	9.83	5.22	4.61
		2	12.34	-10.04	2.30
		3	2.77#	0.60	2.17
		4	18.69	23.11	4.42
		5	20.57	22.36	1.79
	0	6	4.98	5.30	0.32
		7	3.79	1.84	1.95
		8	7.29	-6.87	0.42
		9	5.76	5.90	0.14*
		10	5.97	2.39	3.58*
0	C	11	11.40	12.58	1.18
		12	8.96	-11.28	2.32
		13	12.68	-9.81	2.87
		14	9.95	-15.25	5.30
		15	9.08	4.15	4.93*
	0	16	6.41	1.88	4.53
		17	3.07#	-4.86	1.79
		18	11.56	-13.83	2.27
		19	3.33	-3.03	0.30*
		20	2.45#	1.61	0.84
0	0	21	4.48	2.10	2.38*
		22	3.13	5.68	2.55
	1	1	2.17#	-0.66	1.51
		2	3.46#	-4.26	0.80
		3	3.46#	5.82	2.36
		4	5.95	-3.18	2.77*
		5	3.41#	-0.70	2.71
	1	6	8.22	-12.39	4.17
		7	3.33#	2.37	0.96*
		8	9.65	11.02	1.37
		9	8.65	8.25	0.40
		10	3.13#	0.41	2.72
1	1	11	6.90	2.18	4.72*
		12	2.93#	-4.31	1.38
		13	7.02	2.59	4.43*
		14	2.66#	-0.94	1.72
		15	6.83	-6.48	0.35
	1	16	4.51	-9.40	4.89
		17	1.90#	-1.67	0.23
		18	1.22#	-8.15	6.93

$\ell = 5$	h	k	$ F_o $	F_c	$ \Delta F $
	2	1	2.49#	-4.65	2.16
		2	2.45#	4.47	2.02
		3	2.41#	-5.25	2.84
		4	2.74	1.61	1.13*
		5	2.30#	-1.77	0.53*
	2	6	3.95	-1.54	2.41*
		7	2.07#	-1.76	0.31*
		8	5.25	-6.57	1.32
		9	1.73#	-2.48	0.75
		10	1.30#	8.59	7.29

$\lambda = -1$	h	k	$ F_o $	F_c	$ \Delta F $
1	1	1	26.21	-21.71	4.50
		2	25.18	28.16	2.98
		3	46.03	51.05	5.02
		4	19.40	-21.00	1.60
		5	69.01	-77.76	8.75
1	1	6	37.23	33.90	3.33
		7	20.99	22.19	1.20
		8	52.02	57.47	5.45
		9	13.79	24.98	11.19
		10	3.41#	10.25	6.84
1	1	11	12.65	0.48	12.17
		12	6.83	7.00	0.17
		13	20.33	-21.05	0.72
		14	20.71	-20.47	0.24
		15	7.97	3.39	4.58
1	1	16	21.93	-18.84	3.09
		17	30.27	-20.56	9.71
		18	10.10	9.44	0.66
		19	24.57	22.34	2.23
		20	25.85	-23.04	2.81
1	1	21	22.79	16.75	6.04
		22	10.75	-7.71	3.04
		23	12.48	9.72	2.76
		24	4.09#	-1.98	2.11
		25	10.15	-10.78	0.63
1	1	26	7.96	5.07	2.89
		27	9.19	-7.75	1.44
		28	15.16	17.88	2.72
		29	16.23	-14.57	1.66
		30	7.01	-7.31	0.30
1	1	31	3.36#	-1.86	1.50
		32	7.01	6.11	0.90
2	2	1	46.93	-39.18	7.75
		2	23.33	15.87	7.46
		3	33.63	31.69	1.94
		4	27.56	-20.28	7.28
		5	17.00	-8.15	8.85
2	2	6	21.21	18.03	3.18
		7	3.55	2.14	1.41
		8	9.00	4.05	4.95
		9	5.68	-2.48	3.20
		10	10.03	-5.30	4.73

$\lambda = -1$	h	k	$ F_o $	F_c	$ \Delta F $
2	11		20.86	12.23	8.63
	12		61.36	58.98	2.38
	13		43.97	41.60	2.37
	14		20.86	15.27	5.59
	15		18.61	-18.96	0.35
2	16		5.32#	-1.51	3.81
	17		22.79	14.56	8.23
	18		18.57	-10.70	7.87
	19		18.42	16.33	2.09
	20		5.39#	-2.49	2.90
2	21		20.94	-13.68	7.26
	22		9.62	10.13	0.51
	23		18.73	-15.21	3.52
	24		18.15	18.69	0.54
	25		4.98	1.36	3.62
2	26		5.05	5.25	0.20
	27		6.41	-4.93	1.48
	28		7.33	2.52	4.81
	29		4.01#	1.34	2.67*
	30		14.83	15.62	0.79
2	31		7.64	-5.58	2.06
3	1		32.72	30.29	2.43
	2		50.76	46.02	4.74
	3		10.36	-0.84	9.52*
	4		21.79	-13.98	7.81
	5		29.34	30.52	1.18
3	6		21.33	17.48	3.85
	7		6.68	-4.22	2.46
	8		25.16	23.42	1.74
	9		25.93	23.74	2.19
	10		7.59	3.16	4.43
3	11		5.20	1.09	4.11
	12		18.94	-9.19	9.75
	13		14.33	11.77	2.56
	14		28.41	-25.82	2.59
	15		33.38	24.93	8.45
3	16		5.76	1.14	4.62*
	17		5.44	2.34	3.10
	18		30.88	22.61	8.27
	19		9.86	-4.94	4.92
	20		10.81	5.02	5.79

$\lambda = -1$	h	k	$ F_o $	F_c	$ \Delta F $
3	21		5.58	-6.56	0.98
	22		6.58	10.46	3.88
	23		3.24#	-1.55	1.69
	24		15.21	20.50	5.29
	25		4.86#	-2.64	2.22
3	26		8.67	5.86	2.81
	27		9.47	-7.37	2.10
	28		4.63	7.08	2.45
	29		3.13#	-1.11	2.02
	30		2.21#	-6.57	4.36
4	1		7.52	12.01	4.49
	2		14.29	-10.64	3.65
	3		20.18	14.88	5.30
	4		3.46#	-4.25	0.79
	5		6.69	-7.20	0.51
4	6		5.74	-2.77	2.97
	7		29.17	30.64	1.47
	8		21.42	-13.92	7.50
	9		16.78	6.60	10.18*
	10		4.27#	0.32	3.95
4	11		15.28	6.10	9.18
	12		5.07	4.24	0.83*
	13		11.22	8.41	2.81
	14		7.72	2.73	4.99
	15		7.45	2.26	5.19
4	16		10.17	3.22	6.95
	17		11.50	-8.37	3.13
	18		7.05	9.20	2.15
	19		4.65	-1.90	2.75
	20		13.51	-18.94	5.43
4	21		9.33	-10.87	1.54
	22		15.10	9.59	5.51
	23		4.39#	0.81	3.58
	24		10.77	-7.87	2.90
	25		3.58#	0.82	2.76
4	26		4.06	-2.82	1.24*
	27		2.57#	-3.31	0.74

$\lambda = -1$	h	k	$ F_o $	F_c	$ \Delta F $
5	1		6.58	-1.30	5.28*
	2		4.17#	1.07	3.10*
	3		16.16	10.54	5.62
	4		10.84	13.70	2.86
	5		11.86	-9.00	2.86
5	6		5.20	9.16	3.96
	7		4.46#	-1.46	3.00
	8		13.54	10.33	3.21
	9		9.02	8.36	0.66
	10		11.19	-11.34	0.15
5	11		9.54	-4.24	5.30
	12		4.09#	-0.72	3.37
	13		5.82	-0.27	5.55
	14		3.46#	-1.24	2.22*
	15		6.68	-0.75	5.93
5	16		2.32#	-2.56	0.24*
	17		4.39#	-1.93	2.46
	18		8.27	-11.09	2.82
	19		7.71	-7.41	0.30
	20		15.49	17.98	2.49
5	21		5.44	4.25	1.19
	22		9.20	-8.26	0.94
	23		4.37	-6.86	2.49
	24		1.73#	0.71	1.02
6	1		4.51	-1.04	3.47*
	2		3.44	3.00	0.44
	3		19.20	-19.31	0.11
	4		10.23	8.11	2.12
	5		19.66	20.02	0.36
6	6		4.90#	3.94	0.96
	7		8.42	-2.52	5.90*
	8		4.86	-3.06	1.80
	9		6.77	-3.44	3.33
	10		12.34	12.11	0.23
6	11		11.81	9.12	2.69
	12		4.17#	1.04	3.13
	13		5.81	-4.92	0.89
	14		12.09	12.66	0.57
	15		6.11	-2.35	3.76*

$\ell = -1$	h	k	$ F_o $	F_c	$ \Delta F $
	6	16	3.15#	2.94	0.21
		17	4.37	2.46	1.91
		18	2.02#	2.12	0.10
	7	1	5.05	-10.15	5.10
		2	6.12	-9.23	3.11
		3	2.53#	3.57	1.04
		4	2.37#	3.00	0.63
		5	2.21#	3.58	1.37
	7	6	1.90#	-1.47	0.43*

$\ell = -2$	h	k	$ F_o $	F_c	$ \Delta F $
	1	0	68.23	-77.33	9.10
		1	32.90	33.92	1.02
		2	21.02	21.42	0.40
		3	8.32	-9.03	0.71
		4	32.98	-28.84	4.14
	1	5	34.31	-36.62	2.31
		6	32.42	26.92	5.50
		7	58.58	65.62	7.04
		8	25.57	-20.94	4.63
		9	34.19	-32.23	1.96
	1	10	20.51	16.20	4.31
		11	22.00	14.04	7.96
		12	4.20#	5.00	0.80
		13	65.67	62.04	3.63
		14	33.22	23.20	10.02
	1	15	21.76	-14.12	7.64
		16	26.98	23.50	3.48
		17	4.98#	-4.24	0.74
		18	5.01#	0.92	4.09
		19	4.99#	4.32	0.67
	1	20	13.30	-11.45	1.85
		21	4.72#	1.33	3.39*
		22	14.09	-12.68	1.41
		23	18.71	24.33	5.62
		24	13.35	-12.32	1.03
	1	25	3.21#	-1.53	1.68
		26	2.49#	4.17	1.68
		27	13.18	12.22	0.96
		28	5.53#	1.19	4.34
		29	10.61	7.02	3.59
	1	30	5.76	-6.80	1.04
		31	3.59#	-0.97	2.62
		32	1.45#	6.06	4.61
	2	0	37.39	38.36	0.97
		1	38.86	34.84	4.02
		2	7.08	6.61	0.47
		3	26.28	18.86	7.42
		4	44.71	38.11	6.60
	2	5	16.58	12.63	3.95
		6	3.15#	-0.12	3.03*
		7	26.95	20.38	6.57
		8	11.46	11.42	0.04
		9	20.20	16.26	3.94

$\lambda = -2$	h	k	$ F_o $	F_c	$ \Delta F $
	2	10	4.98	2.64	2.34
		11	4.35#	0.09	4.26
		12	59.49	50.25	9.24
		13	42.24	-28.17	14.07
		14	5.03#	-4.07	0.96
	2	15	18.11	-15.99	2.12
		16	5.36#	5.59	0.23
		17	40.04	36.39	3.65
		18	17.00	6.88	10.12
		19	18.49	11.88	6.61
	2	20	10.29	-10.37	0.08
		21	12.19	13.10	0.91
		22	5.73	-2.45	3.28
		23	11.38	12.10	0.72
		24	8.97	-7.83	1.14
	2	25	19.07	24.59	5.52
		26	6.43	-3.08	3.35
		27	5.84#	-5.11	0.73
		28	5.39#	0.64	4.75
		29	10.06	9.16	0.90
	2	30	6.41	-4.81	1.60
		31	3.33#	-3.31	0.02
	3	0	63.80	57.53	6.27
		1	4.56#	-1.37	3.19*
		2	15.15	-8.35	6.80
		3	2.02#	-1.88	0.14
		4	9.99	10.20	0.21
	3	5	25.01	-19.26	5.75
		6	34.51	36.05	1.54
		7	18.66	-14.96	3.70
		8	25.83	11.29	14.54
		9	19.20	-1.46	17.74
	3	10	42.78	33.78	9.00
		11	4.16#	5.28	1.12
		12	15.24	-8.75	6.49
		13	4.54#	-2.34	2.20
		14	6.69	10.12	3.43
	3	15	31.42	25.80	5.62
		16	5.76	1.19	4.57
		17	9.02	-4.62	4.40
		18	13.40	-11.79	1.61
		19	8.35	7.39	0.96

$l = -2$	h	k	$ F_o $	F_c	$ \Delta F $
	3	20	7.38	-8.50	1.12
		21	4.24#	-9.48	5.24
		22	6.66	-3.30	3.36
		23	3.46#	-2.19	1.27
		24	2.90#	-2.11	0.79
	3	25	8.23	-5.40	2.83
		26	5.76#	-0.71	5.05
		27	8.97	7.82	1.15
		28	6.47	-0.68	5.79
		29	6.64	-4.35	2.29
	3	30	7.89	7.64	0.25
	4	0	33.82	-20.89	12.93
		1	11.39	-13.61	2.22
		2	41.62	25.37	16.25
		3	2.32#	9.82	7.50
		4	12.89	-14.72	1.83
	4	5	43.50	40.54	2.96
		6	11.43	-6.77	4.66
		7	17.26	-9.88	7.38
		8	25.56	22.01	3.55
		9	16.74	8.82	7.92
	4	10	10.45	-5.22	5.23
		11	5.97	-9.79	3.82
		12	12.99	-7.15	5.84
		13	4.39#	1.63	2.76
		14	6.61	6.95	0.34
	4	15	9.46	-9.05	0.41
		16	7.71	-4.60	3.11
		17	8.50	1.78	6.72
		18	9.96	-9.06	0.90
		19	11.26	-7.72	3.54
	4	20	5.46	2.72	2.74
		21	10.33	11.59	1.26
		22	7.18	-5.90	1.28
		23	4.46#	0.87	3.59
		24	6.80	1.15	5.65
	4	25	6.99	-7.51	0.52
		26	4.92	-7.73	2.81
		27	3.13#	-0.79	2.34
		28	2.45#	-0.10	2.35

$\lambda = -2$	h	k	$ F_o $	F_c	$ \Delta F $
5	5	0	39.67	-32.22	7.45
		1	12.74	-10.54	2.20
		2	13.30	-9.16	4.14
		3	14.22	14.40	0.18
		4	10.58	10.32	0.26
	5	5	17.11	-9.33	7.78
		6	9.61	-4.96	4.65
		7	12.60	9.63	2.97
		8	16.43	14.07	2.36
		9	6.71	8.36	1.65
	5	10	16.13	-10.61	5.52
		11	6.11	7.82	1.71
		12	9.17	6.41	2.76
		13	14.67	9.17	5.50
		14	4.67#	-0.92	3.75*
	5	15	22.58	23.69	1.11
		16	7.72	-6.40	1.32
		17	13.31	-11.72	1.59
		18	6.33	5.71	0.62
		19	14.59	13.28	1.31
	5	20	7.66	-4.34	3.32
		21	4.04#	4.57	0.53
		22	3.78#	-2.56	1.22
		23	12.71	-13.71	1.00
		24	3.03#	0.22	2.81*
	5	25	10.89	13.42	2.53
6	6	0	5.05	3.52	1.53
		1	10.88	-9.82	1.06
		2	10.77	-10.55	0.22
		3	14.43	-18.32	3.89
		4	4.92#	-3.00	1.92
	6	5	14.60	15.79	1.19
		6	4.65#	8.31	3.66
		7	12.11	-5.88	6.23*
		8	12.32	-2.42	9.90*
		9	17.80	18.36	0.56
	6	10	15.18	21.59	6.41
		11	8.68	8.20	0.48
		12	6.05#	8.93	2.88
		13	7.89	2.55	5.34
		14	5.67#	3.73	1.94

$\ell = -2$	h	k	$ F_o $	F_c	$ \Delta F $
	6	15	9.10	9.39	0.29
		16	6.03	-4.84	1.19
		17	7.20	4.04	3.16
		18	6.24	2.87	3.37
		19	3.97#	1.68	2.29*
	6	20	3.36#	-0.69	2.67
		21	2.21#	8.23	6.02
	7	0	5.05#	3.78	1.27*
		1	6.80	5.04	1.76*
		2	10.30	12.27	1.97
		3	9.56	9.76	0.20
		4	4.90#	2.75	2.15
	7	5	13.05	-17.72	4.67
		6	6.63	-8.49	1.86
		7	8.40	-10.71	2.31
		8	4.37#	0.70	3.67*
		9	4.17#	-0.16	4.01
	7	10	6.03	-3.45	2.58*
		11	3.62#	5.58	1.96
		12	3.21#	6.04	2.83
		13	2.49#	4.45	1.96

$\ell = -3$	h	k	$ F_o $	F_c	$ \Delta F $
	1	1	12.19	10.08	2.11
		2	30.58	31.83	1.25
		3	25.91	22.34	3.57
		4	3.33#	2.46	0.87
		5	3.55#	3.57	0.02
	1	6	20.72	13.27	7.45
		7	11.30	12.82	1.52
		8	41.77	35.53	6.24
		9	5.13	-13.09	7.96
		10	44.84	-31.84	13.00
	1	11	54.91	47.83	7.08
		12	4.76#	3.99	0.77
		13	16.83	9.26	7.57
		14	7.36	-6.36	1.00
		15	7.75	-7.42	0.33
	1	16	5.01#	4.80	0.21
		17	4.98#	-4.74	0.24
		18	24.52	25.93	1.41
		19	15.05	10.59	4.46
		20	21.45	16.51	4.94
	1	21	12.12	-10.69	1.43
		22	7.80	10.67	2.87
		23	5.30	-4.53	0.77
		24	15.79	16.00	0.21
		25	11.46	-5.38	6.08
	1	26	5.71#	6.23	0.52
		27	5.27#	2.91	2.36
		28	7.23	5.06	2.17
		29	5.81	-5.13	0.68
		30	3.13#	-1.83	1.30
	2	1	6.31	6.49	0.18
		2	3.58#	-2.85	0.73
		3	36.84	33.60	3.24
		4	2.85#	-6.80	3.95
		5	3.15#	3.11	0.04
	2	6	34.41	-24.61	9.80
		7	37.92	33.26	4.66
		8	34.13	-18.93	15.20
		9	43.98	38.40	5.58
		10	31.36	22.55	8.81

$\ell = -3$	n	k	$ F_0 $	F_c	$ \Delta F $
	2	11	19.66	-14.05	5.61
		12	5.59	2.90	2.69
		13	25.11	26.08	0.97
		14	8.27	4.91	3.36
		15	20.61	-17.47	3.14
	2	16	25.75	24.68	1.07
		17	11.52	5.52	6.00
		18	5.42#	3.25	2.17
		19	12.28	-11.45	0.83
		20	5.03#	-2.80	2.23
	2	21	4.88#	-7.63	2.75
		22	4.35#	-6.17	1.82
		23	3.87#	-0.08	3.79*
		24	3.30#	-2.55	0.75
		25	2.30#	-2.12	0.18
	2	26	5.82#	2.17	3.65
		27	5.41#	-3.92	1.49
		28	7.48	-5.87	1.61
		29	7.77	9.00	1.23
		30	6.96	11.19	4.23
	3	1	13.18	11.82	1.36
		2	23.70	12.29	11.41
		3	11.56	-10.98	0.58
		4	17.47	23.06	5.59
		5	6.31	-5.21	1.10
	3	6	20.06	13.87	6.19
		7	16.05	13.40	2.65
		8	3.82#	-1.90	1.92
		9	19.01	17.87	1.14
		10	13.71	8.88	4.83
	3	11	20.32	-19.41	0.91
		12	16.93	-13.38	3.55
		13	7.94	-0.22	7.72
		14	7.16	3.22	3.94
		15	14.28	13.63	0.65
	3	16	6.35	-5.71	0.64
		17	23.87	-20.16	3.71
		18	7.77	-5.68	2.09
		19	7.70	7.06	0.64
		20	7.82	5.79	2.03

$\ell = -3$	h	k	$ F_o $	F_c	$ \Delta F $
3	3	21	8.03	-9.58	1.55
		22	3.65#	2.16	1.49
		23	3.18#	1.99	1.19
		24	2.45#	0.28	2.17
		25	5.92#	3.93	1.99
3	3	26	5.55#	-4.34	1.21
		27	14.06	-16.57	2.51
		28	4.52#	-1.28	3.24
		29	3.79#	5.04	1.25
		30	6.03	-8.84	2.81
4	4	1	54.38	-48.82	5.56
		2	22.05	-19.14	2.91
		3	35.99	31.44	4.55
		4	14.42	-6.30	8.12
		5	24.86	-21.90	2.96
4	4	6	9.52	8.79	0.73
		7	11.44	9.74	1.70
		8	14.12	13.23	0.89
		9	7.55	7.42	0.13
		10	6.93	-1.48	5.45
4	4	11	18.20	-11.81	6.39
		12	28.17	27.90	0.27
		13	4.37#	5.22	0.85
		14	18.99	14.23	4.76
		15	8.98	3.26	5.72
4	4	16	11.73	4.70	7.03
		17	15.70	-11.97	3.73
		18	14.15	12.58	1.57
		19	7.97	9.60	1.63
		20	4.88#	-4.26	0.62
4	4	21	4.79#	-4.99	0.20
		22	6.12	6.47	0.35
		23	4.48#	-5.11	0.63
		24	4.99	-6.87	1.88
		25	3.95#	4.31	0.36
4	4	26	3.58#	-2.20	1.38
		27	3.15#	1.76	1.39
		28	2.53#	4.66	2.13

$\lambda = -3$	h	k	$ F_o $	F_c	$ \Delta F $
5	5	1	9.14	5.72	3.42
		2	3.85	-3.73	0.12
		3	16.07	-13.02	3.05
		4	11.67	-12.12	0.45
		5	12.86	-13.76	0.90
	5	6	3.15#	1.26	1.89*
		7	3.41#	6.27	2.86
		8	15.29	14.82	0.47
		9	3.85#	12.41	8.56
		10	7.02	7.40	0.38
	5	11	10.86	11.12	0.26
		12	14.75	14.57	0.18
		13	23.08	22.88	0.20
		14	12.86	12.95	0.09
		15	24.11	-15.32	8.79
	5	16	4.98	8.18	3.20
		17	14.77	10.45	4.32
		18	4.63#	-0.53	4.00*
		19	4.54#	-2.38	2.16
		20	21.55	18.65	2.90
	5	21	4.22#	-4.91	0.69
		22	3.97#	-2.52	1.45
		23	3.67#	2.44	1.23
		24	10.18	9.40	0.78
		25	6.51	-3.24	3.27
	5	26	7.14	7.74	0.60
6	6	1	8.14	7.90	0.24
		2	6.77#	3.37	3.40*
		3	6.77#	8.79	2.02
		4	6.77#	2.46	4.31
		5	23.90	22.00	1.90
	6	6	18.55	-12.59	5.96
		7	21.00	-21.24	0.24
		8	23.09	-23.34	0.25
		9	10.23	-13.84	3.61
		10	18.08	13.07	5.01
	6	11	11.79	13.62	1.83
		12	6.40#	-1.45	4.95*
		13	6.24#	-2.08	4.15
		14	6.09#	9.26	3.17
		15	20.39	17.94	2.45

$\lambda = -3$	h	k	$ F_o $	F_c	$ \Delta F $
	6	16	17.10	13.70	3.40
		17	5.41#	6.38	0.97
		18	11.29	9.75	1.54
		19	4.72#	7.75	3.03
		20	4.29#	-3.72	0.57
	6	21	3.73#	-0.79	2.94
		22	11.55	10.86	0.69
	7	1	8.44	4.96	3.48
		2	5.80#	-0.14	5.66*
		3	9.34	-9.85	0.51
		4	5.71#	-4.18	1.53
		5	5.63#	-0.79	4.84
	7	6	5.56#	-0.53	5.03
		7	16.42	13.64	2.78
		8	10.01	9.27	0.74
		9	5.16#	3.40	1.76
		10	17.26	-15.57	1.69
	7	11	4.79#	-4.63	0.16
		12	4.54#	-6.97	2.43
		13	10.98	-8.81	2.17
		14	9.06	-8.10	0.96
		15	3.41#	3.60	0.19
	7	16	2.74#	5.49	2.75

$\ell = -4$	h	k	$ F_o $	F_c	$ \Delta F $
1	1	0	4.24	-6.09	1.85
		1	13.89	7.37	6.52
		2	21.57	21.95	0.38
		3	2.61#	2.97	0.36
		4	2.66#	-2.10	0.56
	1	5	36.80	-40.51	3.71
		6	41.24	37.06	4.18
		7	17.50	15.56	1.94
		8	11.61	8.87	2.74
		9	19.20	-15.22	3.98
	1	10	3.38#	6.82	3.44
		11	14.54	15.93	1.39
		12	16.98	13.17	3.81
		13	17.70	18.63	0.93
		14	7.33	-2.63	4.70
	1	15	5.80	-4.53	1.27*
		16	14.78	-13.10	1.68
		17	20.32	25.81	5.49
		18	17.05	8.80	8.25
		19	3.73#	0.09	3.64
	1	20	12.93	-10.10	2.83
		21	9.95	-11.72	1.77
		22	4.17	-5.65	1.48
		23	5.16	7.29	2.13
		24	5.42	3.11	2.31
	1	25	4.74	-7.20	2.46
		26	2.74#	-2.62	0.12
		27	2.32#	-1.53	0.79
		28	1.67#	-0.83	0.84
2	0	0	17.47	-3.39	14.08*
		1	32.26	35.41	3.15
		2	5.81	3.52	2.29
		3	13.10	2.28	10.82*
		4	16.60	10.90	5.70
	2	5	14.68	12.68	2.00
		6	24.51	-21.22	3.29
		7	4.60	1.99	2.61
		8	37.99	39.60	1.61
		9	13.30	4.87	8.43

$\lambda = -4$	h	k	$ F_o $	F_c	$ \Delta F $
	2	10	21.32	-20.40	0.92
		11	10.29	6.25	4.04
		12	3.38#	-1.97	1.41
		13	17.76	-7.93	9.83
		14	7.87	5.99	1.88
	2	15	3.78#	-9.59	5.81
		16	6.53	-2.29	4.24
		17	9.47	10.22	0.75
		18	7.92	-1.05	6.87*
		19	5.28	-7.79	2.51
	2	20	7.88	-8.04	0.16
		21	3.70#	1.42	2.28
		22	3.13#	5.02	1.89
		23	4.86	3.07	1.79
		24	3.52#	-0.13	3.39*
	2	25	3.30#	2.23	1.07
		26	5.92	-6.62	0.70
		27	5.95	-6.18	0.23
		28	2.26#	-2.20	0.06
		29	1.38#	-4.94	3.56
	3	0	14.88	-15.27	0.39
		1	23.76	-25.11	1.35
		2	28.29	-21.00	7.29
		3	34.06	-29.40	4.66
		4	14.98	-15.50	0.52
	3	5	2.26#	1.89	0.37
		6	14.58	10.06	4.52
		7	24.53	19.24	5.29
		8	8.41	-7.25	1.16
		9	2.93#	-3.96	1.03
	3	10	9.56	9.45	0.11
		11	16.75	17.40	0.65
		12	21.78	-15.39	6.39
		13	24.11	19.14	4.97
		14	11.91	10.65	1.26
	3	15	18.85	18.35	0.50
		16	3.90#	-2.03	1.87
		17	5.32	-2.64	2.68
		18	7.65	-6.22	1.43
		19	10.51	11.03	0.52

$\lambda = -4$	h	k	$ F_o $	F_c	$ \Delta F $
	3	20	6.82	7.61	0.79
		21	3.36#	-1.82	1.54
		22	9.61	-9.58	0.03
		23	1.73#	2.72	0.99
		24	6.03	6.28	0.25
	3	25	12.51	-14.98	2.47
		26	3.00#	0.84	2.16
		27	7.55	5.80	1.75
		28	6.94	-3.31	3.63
		29	1.05#	5.23	4.18
	4	0	8.73	-7.43	1.30
		1	9.41	10.82	1.41
		2	13.20	8.42	4.78
		3	2.77#	4.52	1.75
		4	14.68	-13.16	1.52
	4	5	16.70	-14.42	2.28
		6	18.96	-19.04	0.08
		7	3.13#	1.26	1.87
		8	3.24#	0.70	2.54
		9	13.88	12.81	1.07
	4	10	15.46	17.87	2.41
		11	6.55	6.61	0.06
		12	12.69	13.21	0.52
		13	28.09	31.06	2.97
		14	3.87#	3.20	0.67
	4	15	6.82	-2.53	4.29
		16	3.99#	4.74	0.75
		17	17.80	17.85	0.05
		18	7.33	-3.37	3.96
		19	5.20	4.80	0.40
	4	20	3.90#	2.02	1.88
		21	12.32	9.25	3.07
		22	3.65#	2.07	1.58
		23	9.45	6.34	3.11
		24	9.56	-8.33	1.23
	4	25	14.73	13.84	0.89
		26	6.32	-2.03	4.29
		27	2.17#	1.66	0.51
		28	1.22#	1.99	0.77

$\lambda = -4$	h	k	$ F_o $	F_c	$ \Delta F $
	5	0	17.00	19.10	2.10
		1	24.90	-19.75	5.15
		2	2.63#	1.00	1.63
		3	6.35	2.22	4.13*
		4	26.38	25.53	0.85
	5	5	6.36	5.37	0.99
		6	9.46	9.74	0.28
		7	22.48	-15.59	6.89
		8	19.32	-20.11	0.79
		9	9.99	-11.87	1.88
	5	10	22.72	-23.40	0.68
		11	5.09	1.22	3.87*
		12	24.73	21.16	3.57
		13	9.43	-2.10	7.33*
		14	7.51	-1.58	5.93
	5	15	30.58	32.45	1.87
		16	10.14	12.45	2.31
		17	5.13	-1.09	4.04
		18	25.72	22.88	2.84
		19	15.93	13.95	1.98
	5	20	14.62	-8.60	6.02
		21	16.48	15.37	1.11
		22	3.36	-4.29	0.93
		23	2.90#	-1.44	1.46
		24	2.61	-4.30	1.69
	5	25	2.17#	-0.65	1.52
		26	1.30#	2.45	1.15
	6	0	13.14	7.82	5.32
		1	3.99#	2.60	1.39
		2	3.99#	-0.46	3.53
		3	3.99#	1.12	2.87
		4	11.57	-7.53	4.04
	6	5	7.61	3.42	4.19
		6	11.90	9.82	2.08
		7	19.57	-20.10	0.53
		8	5.27	1.70	3.57*
		9	22.84	21.92	0.92
	6	10	24.15	23.44	0.71
		11	12.12	-11.17	0.95
		12	24.77	-21.74	3.03
		13	25.53	-27.46	1.93
		14	6.71	-5.96	0.75

$\lambda = -4$	h	k	$ F_o $	F_c	$ \Delta F $
6	15		3.65#	3.85	0.20
	16		5.63	-2.62	3.01
	17		17.87	16.41	1.46
	18		23.90	-17.96	5.94
	19		10.85	11.70	0.85
6	20		11.79	7.97	3.82
	21		2.41#	2.28	0.13
	22		11.56	11.13	0.43
	23		0.89#	-5.05	4.16
7	0		5.78	6.94	1.16
	1		9.96	-8.69	1.27
	2		3.70#	-1.28	2.42
	3		3.67#	4.54	0.87
	4		3.65#	1.81	1.84
7	5		7.38	-6.04	1.34
	6		3.58#	-1.57	2.01
	7		3.52#	2.42	1.10
	8		7.30	-3.65	3.65*
	9		9.61	-8.19	1.42
7	10		17.04	-14.68	2.36
	11		10.10	5.71	4.39
	12		7.04	-4.54	2.50
	13		24.08	21.97	2.11
	14		17.36	-15.21	2.15
7	15		4.83	4.29	0.54
	16		5.03	-4.75	0.28
	17		10.77	-9.67	1.10
	18		0.89#	-0.42	0.47
8	0		2.26#	-1.56	0.70*
	1		2.26#	0.99	1.27*
	2		4.01	3.98	0.03
	3		2.17#	-4.50	2.33
	4		6.03	-2.78	3.25*
8	5		5.18	2.66	2.52
	6		1.84#	-0.62	1.22*
	7		8.29	6.54	1.75
	8		1.22#	-0.78	0.44

$\ell = -5$	h	k	$ F_o $	F_c	$ \Delta F $
	1	1	3.07#	4.85	1.78
		2	10.13	10.17	0.04
		3	5.82	-6.29	0.47*
		4	9.57	6.28	3.29
		5	15.73	10.58	5.15
	1	6	3.27#	-0.80	2.47*
		7	5.44	6.83	1.39
		8	6.36	9.43	3.07
		9	13.22	-13.07	0.15
		10	3.52#	-3.30	0.22
	1	11	13.46	10.00	3.46
		12	9.37	12.44	3.07
		13	3.62#	-3.10	0.52
		14	18.30	-20.62	2.32
		15	9.83	-3.57	6.26*
	1	16	12.16	7.68	4.48
		17	2.32#	5.92	3.60
		18	3.41#	5.37	1.96
		19	3.27#	-3.44	0.17
		20	9.02	-11.54	2.52
	1	21	6.41	-1.93	4.48*
		22	6.17	5.78	0.39
		23	2.41#	3.18	0.77
		24	3.46	5.84	2.38
		25	1.05#	-5.23	4.18
	2	1	10.84	-5.94	4.90
		2	18.38	-16.81	1.57
		3	8.64	-9.93	1.29
		4	16.86	-19.29	2.43
		5	25.49	-25.01	0.48
	2	6	5.41	8.33	2.92
		7	9.35	5.66	3.69
		8	6.57	-1.03	5.54
		9	20.40	15.38	5.02
		10	22.41	16.16	6.25
	2	11	27.46	-22.60	4.86
		12	3.44#	3.47	0.03
		13	3.52#	7.23	3.71
		14	20.51	19.37	1.14
		15	7.27	1.59	5.68*

$\lambda = -5$	h	k	$ F_o $	F_c	$ \Delta F $
	2	16	5.92	6.25	0.33
		17	3.62#	4.10	0.48
		18	3.30#	1.04	2.26*
		19	10.02	-10.60	0.58
		20	6.55	6.22	0.33
	2	21	7.23	4.56	2.67
		22	3.07#	-1.14	1.93*
		23	4.14	4.58	0.44
		24	8.71	-11.62	2.91
		25	2.26#	-0.89	1.37*
	2	26	4.20	3.07	1.13*
	3	1	4.81#	-4.48	0.33
		2	1.45#	-3.84	2.39
		3	1.67#	1.56	0.11*
		4	12.85	19.84	6.99
		5	2.17#	-3.97	1.80
	3	6	15.14	-10.76	4.38
		7	20.22	-20.71	0.49
		8	5.38	-7.83	2.45
		9	5.53	-4.25	1.28
		10	9.53	13.43	3.90
	3	11	21.83	17.08	4.75
		12	12.71	9.55	3.16
		13	3.44#	2.56	0.88*
		14	18.04	19.95	1.91
		15	9.89	10.70	0.81
	3	16	9.38	8.88	0.50
		17	12.59	-12.48	0.11
		18	3.55#	1.11	2.44
		19	12.97	16.14	3.17
		20	13.68	15.02	1.34
	3	21	5.78	-3.67	2.11
		22	9.00	5.23	3.77
		23	10.67	-8.95	1.72
		24	13.03	13.70	0.67
		25	2.41#	2.83	0.42
	3	26	3.95	4.13	0.18

$\lambda = -5$	h	k	$ F_o $	F_c	$ \Delta F $
4	4	1	10.00	9.55	0.45
		2	13.30	-13.01	0.29
		3	18.48	18.68	0.20
		4	2.49#	2.31	0.18
		5	5.03	5.66	0.63
4	4	6	2.74#	-4.09	1.35
		7	5.95	5.13	0.82
		8	2.97	7.32	4.35
		9	11.91	-12.56	0.65
		10	19.24	-20.37	1.13
4	4	11	16.98	-18.43	1.45
		12	3.44#	-2.79	0.65
		13	3.52#	3.83	0.31
		14	14.40	17.21	2.81
		15	15.41	10.68	4.73
4	4	16	6.50	10.28	3.78
		17	17.73	17.37	0.36
		18	14.60	15.36	0.76
		19	3.49#	2.07	1.42
		20	19.74	20.86	1.12
4	4	21	4.92	-4.87	0.05
		22	5.16	5.81	0.65
		23	4.79	2.71	2.08
		24	7.31	-8.31	1.00
		25	2.21#	0.96	1.25*
4	26	2.93	3.92	0.99	
5	5	1	3.10#	-3.17	0.07
		2	3.10#	0.14	2.96*
		3	12.39	11.32	1.07
		4	17.73	13.58	4.15
		5	3.24#	-2.27	0.97
5	5	6	16.86	-13.77	3.09
		7	3.36#	4.81	1.45
		8	13.54	-10.61	2.93
		9	13.34	11.52	1.82
		10	29.20	25.11	4.09
5	5	11	8.91	6.10	2.81
		12	27.38	-24.86	2.52
		13	7.80	4.70	3.10
		14	13.65	-14.88	1.23
		15	44.18	-41.03	3.15

$\ell = -5$	h	k	$ F_o $	F_c	$ \Delta F $
	5	16	22.22	17.79	4.43
		17	9.84	-9.32	0.52
		18	3.38	3.21	0.17
		19	8.87	9.13	0.26
		20	4.83	6.23	1.40
	5	21	8.94	7.90	1.04
		22	2.66#	-1.46	1.20
		23	7.09	6.53	0.56
		24	4.11	5.15	1.04
	6	1	9.69	6.10	3.59
		2	3.59#	-1.31	2.28*
		3	3.59#	-1.31	2.28*
		4	9.57	-4.00	5.57
		5	3.62#	-1.46	2.16
	6	6	3.62#	-1.64	1.98
		7	3.62#	-1.01	2.61
		8	3.62#	-2.03	1.59
		9	9.43	-7.28	2.15
		10	3.59#	4.60	1.01
	6	11	27.92	-24.59	3.33
		12	22.79	13.10	9.69
		13	30.21	-26.00	4.21
		14	22.50	20.44	2.06
		15	24.05	20.13	3.92
	6	16	13.94	-9.38	4.56
		17	11.65	-10.16	1.49
		18	13.48	-12.79	0.69
		19	2.66#	-1.22	1.44
		20	5.16	-2.93	2.23
	6	21	2.97	4.46	1.49
		22	1.52#	2.49	0.97
	7	1	4.20	3.61	0.59
		2	3.82	2.23	1.59
		3	10.45	-5.06	5.39
		4	3.79	-3.61	0.18
		5	3.38#	-0.32	3.06*
	7	6	15.33	9.04	6.29
		7	12.52	-8.30	4.22
		8	25.71	22.04	3.67
		9	19.69	-11.93	7.76
		10	3.13#	2.06	1.07

$\lambda = -5$	h	k	$ F_o $	F_c	$ \Delta F $
	7	11	3.00#	-1.25	1.75
		12	9.65	12.97	3.32
		13	6.66	4.30	2.36
		14	15.47	-10.21	5.26
		15	8.94	-6.53	2.41
	7	16	3.65	3.63	0.02
		17	5.69	5.72	0.03
		18	0.89#	11.95	11.06
	8	1	2.41#	5.55	3.14
		2	8.18	8.09	0.09
		3	2.32#	0.79	1.53
		4	8.97	7.20	1.77
		5	6.63	-5.24	1.39
	8	6	17.15	19.63	2.48
		7	3.33	-2.41	0.92
		8	4.11	-1.36	2.75
		9	1.52#	-1.12	0.40
		10	0.89#	-4.29	3.40

$\lambda = -6$	h	k	$ F_o $	F_c	$ \Delta F $
	1	0	5.55	-1.40	4.15*
		1	7.41	-12.39	4.98
		2	3.24#	0.25	2.99
		3	3.18#	1.36	1.82
		4	14.26	-18.01	3.75
	1	5	10.77	-12.04	1.27
		6	8.03	-7.36	0.67
		7	2.63#	-2.83	0.20*
		8	6.93	5.97	0.96
		9	9.05	5.12	3.93*
	2	0	17.54	-20.76	3.22
		1	9.44	13.09	3.65
		2	9.08	7.03	2.05*
		3	9.24	-8.51	0.73
		4	4.58#	4.93	0.35
	2	5	10.52	16.55	6.03
		6	21.69	-22.73	1.04
		7	4.27#	-2.62	1.65
		8	12.27	9.28	2.99
		9	7.99	-7.32	0.67
	2	10	13.56	-18.08	4.52
		11	3.44#	-1.18	2.26*
		12	5.23	6.49	1.26
		13	18.05	19.99	1.94
		14	1.55#	12.09	10.54
	3	0	13.13	4.01	9.12*
		1	8.12	-11.97	3.85
		2	11.36	15.57	4.21
		3	4.58#	2.84	1.74
		4	4.54#	3.53	1.01
	3	5	4.63#	-6.75	2.12
		6	11.48	3.62	7.86*
		7	4.34#	6.05	1.71
		8	6.19	-1.08	5.11*
		9	4.09#	-0.62	3.47*
	3	10	4.16	-4.13	0.03
		11	3.75#	-1.95	1.80
		12	13.09	-19.57	6.48
		13	12.67	-8.56	4.11
		14	11.30	9.66	1.64
	3	15	4.34	9.59	5.25

$\ell = -6$	h	k	$ F_0 $	F_c	$ \Delta F $
	4	0	4.34#	-3.41	0.93
		1	4.81#	6.30	1.49
		2	4.83#	1.07	3.76
		3	4.83#	3.77	1.06
		4	10.15	11.28	1.13
	4	5	4.86#	-0.41	4.45
		6	4.88#	3.01	1.87
		7	4.90#	-0.22	4.68
		8	4.92#	0.50	4.42
		9	12.50	-2.47	10.03*
	4	10	15.87	10.13	5.74
		11	8.68	-8.17	0.51
		12	12.70	14.06	1.36
		13	14.70	11.78	2.92
		14	29.69	-25.58	4.11
	4	15	4.63#	-8.11	3.48
		16	29.76	-29.21	0.55
		17	4.35#	1.59	2.76
		18	5.59	5.92	0.33
		19	3.92#	-6.31	2.39
	4	20	7.94	7.56	0.38
		21	11.22	9.35	1.87
		22	8.15	7.73	0.42
		23	2.37#	4.75	2.38
	5	0	6.03	6.76	0.73
		1	4.52#	-0.16	4.36*
		2	5.38	3.76	1.62
		3	4.56#	-1.24	3.32
		4	4.58#	-0.79	3.79*
	5	5	4.60#	-3.11	1.49
		6	4.63#	-4.52	0.11
		7	17.66	-9.65	8.01
		8	4.67#	2.84	1.83
		9	23.33	12.66	10.67
	5	10	37.60	-31.68	5.92
		11	34.13	25.87	8.26
		12	28.70	-23.01	5.69
		13	9.76	-10.43	0.67
		14	4.51#	0.71	3.80

$\ell = -6$	h	k	$ F_o $	F_c	$ \Delta F $
	5	15	8.75	7.61	1.14
		16	12.77	14.06	1.29
		17	4.09#	-3.06	1.03
		18	3.90#	-4.04	0.14
		19	11.54	-10.09	1.45
	5	20	9.50	-7.51	1.99
		21	13.05	-10.89	2.16
		22	5.14	7.25	2.11
	6	0	13.03	9.46	3.57

$\ell = -7$	h	k	$ F_o $	F_c	$ \Delta F $
	3	1	4.86	1.38	3.48*
		2	7.91	-4.61	3.30*
		3	5.68	-0.55	5.13*
		4	10.62	11.11	0.49
		5	7.48	10.02	2.54
	3	6	1.67#	-1.15	0.52
	4	1	4.04#	5.65	1.61
		2	4.76#	-0.18	4.58
		3	4.74#	-3.38	1.36
		4	4.72#	0.29	4.43
		5	12.92	9.77	3.15
	4	6	12.82	-13.84	1.02
		7	14.04	-10.13	3.91
		8	16.26	12.81	3.45
		9	28.02	-23.34	4.68
		10	25.52	23.84	1.68
	4	11	16.29	-11.89	4.40
		12	4.16#	-4.31	0.15
		13	3.99#	-2.47	1.52
		14	6.51	-7.51	1.00
		15	6.19	-2.31	3.88*
	4	16	3.38#	3.24	0.14
		17	9.29	12.25	2.96
		18	2.70#	0.57	2.13
		19	2.12#	-3.86	1.74
	5	1	4.35	0.71	3.64*
		2	4.90	-3.77	1.13*
		3	4.60#	-2.53	2.07
		4	20.90	17.27	3.63
		5	31.10	-24.74	6.36
	5	6	26.43	19.80	6.63
		7	13.16	-8.01	5.15
		8	4.72	2.49	2.23
		9	5.41	4.70	0.71
		10	7.80	8.98	1.18

$\lambda = -7$	h	k	$ F_c $	F_c	$ \Delta F $
	5	11	4.94	-2.05	2.89*
		12	4.34	-6.74	2.40
		13	3.92#	-0.19	3.73*
		14	7.27	5.98	1.29
		15	3.52#	2.71	0.81
	5	16	3.27#	1.74	1.53
		17	4.46	-3.50	0.96
		18	3.65	-6.80	3.15
		19	1.61#	-6.63	5.02

$\lambda = -8$	h	k	$ F_o $	F_c	$ \Delta F $
	4	0	12.14	5.82	6.32
		1	6.12	2.66	3.46*
		2	3.58#	-6.43	2.85
		3	12.48	12.18	0.30
		4	15.72	-17.40	1.68
	4	5	14.13	18.82	4.69
		6	12.39	-10.86	1.53
		7	3.18#	-3.85	0.67
		8	3.07#	6.69	3.62
		9	8.24	9.10	0.86
	4	10	2.66#	-1.93	0.73*
		11	2.37#	-1.34	1.03
		12	1.84#	-0.99	0.85
	5	0	24.28	-25.36	1.08
		1	7.80	8.10	0.30
		2	3.67#	-1.92	1.75
		3	8.63	6.07	2.56
		4	3.59#	2.24	1.35
	5	5	7.44	4.57	2.87
		6	3.44#	-2.37	1.07
		7	8.80	9.72	0.92
		8	5.46	7.40	1.94
		9	3.07#	-1.01	2.06*
	5	10	3.13#	-5.57	2.44
		11	2.61#	3.05	0.44
		12	2.26#	-0.78	1.48
		13	1.38#	-0.05	1.33

J. Appendix II--IBM Calculations

IBM equipment was used throughout the two-dimensional refinement described in Section E, page 77, and some of the techniques used in these calculations will be outlined below since they can be generally applied. Most of these procedures have been extended by the author to three-dimensional work without appreciable change. We shall describe an operation that involves the calculation of structure factors, the calculation of the normal equations of a least-squares refinement, and the calculation of parameters for an iteration of this process.

In all, three separate decks of cards are used, the D deck, the A deck, and the S deck. The D deck contains atom serial numbers and atomic parameters, one card for each of the twenty atoms of the asymmetric unit. The A, or detail deck, contains indices of all reflections and atom numbers, one card per atom per reflection. The S, or sum deck, has one card per reflection with the appropriate indices. The detail cards contain, in addition to indices and atom numbers, the product $(\text{wt.})^{\frac{1}{2}}(8\pi f_C)[\exp(-B\sin^2\theta/\lambda^2)]$ for use in least-squares calculations. The S deck contains F_O , $f_C[\exp(-B\sin^2\theta/\lambda^2)]$, and $(\text{wt.})^{\frac{1}{2}}$ for use in calculating structure factors and in least-squares procedures. The S and D deck contain y punches for picking up appropriate

selectors for read-in, read-out, calculate, and punch operations. Both the S cards and the A cards contain a y punch for reflections with $k + \ell$ even for selecting the appropriate trigonometric functions and making the proper negative multiplications. The A deck, the S deck, and the D deck also contain suitable code punches to indicate the stage of refinement in operation.

The use of these decks in a typical calculation proceeds as follows. Parameters are hand punched into the D deck. The A cards are sorted on atom number and collated with the D deck with the coordinate cards in front. The merged decks are passed through the 604 and suitable arguments for the trigonometric functions are calculated. The structure factors for DHC are of the form,

$$F(hk\ell) = 4f_C[\exp(-B\sin^2\theta/\lambda^2)] \sum_1^{20} \left\{ \begin{array}{l} \sin \\ \cos \end{array} \right\} 2\pi(hx_1 + \ell z_1) \left\{ \begin{array}{l} \sin \\ \cos \end{array} \right\} 2\pi(ky_1)$$

\sin for $k + \ell$ odd
 \cos for $k + \ell$ even

The arguments for use in the sine-cosine boards available must be of the form, $4(hx)^*$, where $(hx)^*$ has been reduced to a positive number less than one as follows,

if $hx + \ell z = n.abc$ $(hx)^* = 0.abc$	if $ky = -n.abc$ $(hx)^* = 1-0.abc$
--	--

The operation with the 604 consists of reading the parameters from the D card which is in front of all detail cards for this atom, and then calculating the arguments of the form indicated for each of the A cards. The D deck is punch suppressed in these operations. The D cards are removed by hand or by sorting. The A cards are then passed through the 604 for calculation of sines and cosines for both arguments at once.* The detail cards are then sorted in order of indices and collated with the S deck with the S cards following the detail cards of the same index. The merged cards are run through the 604 and the product of either sin-sin or cos-cos is made and the sum carried for each detail card. When an S card is read several things occur. First, F_o , $(wt.)^{\frac{1}{2}}$, and $4f_c[\exp(-B\sin^2\theta/\lambda^2)]$ are read and calculate selectors are picked up. The calculate time of the S card is used to calculate F_c , ΔF , and $\Delta F(wt.)^{\frac{1}{2}}$, with F_o being given the sign of F_c in calculating ΔF .** The merged S and D decks are fed in reverse

*It is convenient here to work the cards in blocks, for instance those with even or odd $k +$. Then one block is sorted in order of index before calculation of sines and cosines and while the other group is being run through the 604.

**Efficient use of storage space through punch selectors is necessary here. In some cases two passes through the 604 may be required, if for instance there are more than two or three kinds of atoms in the structure.

order, through the reproducer, and $\Delta F(\text{wt.})^{\frac{1}{2}}$ is transferred by gang punching from the sum or S cards to the corresponding detail or A deck. The sum cards are then sorted from the detail deck and the A cards are sorted on atom number. The A and the D decks are merged, with the D cards following the corresponding detail cards. These merged decks are then passed through the 604, and the coefficients of the normal equations are calculated by summing over the detail cards; these coefficients are then punched into the parameter or D deck. For two-dimensional least-squares calculations the $x_i - y_i$ cross term may be retained or neglected as seems desirable. For three-dimensional work all off diagonal terms are usually neglected except the $x_i - z_i$ term of monoclinic crystals. The D cards are then sorted from the A deck and correction terms for the parameters are calculated, and new parameter cards are prepared from the D deck. Note that this operation leaves the A deck in proper order for the recalculation of the arguments of the trigonometric functions and the next step of a cyclic process of successive least-squares evaluations.

The S deck containing both F_o , F_c and ΔF is used for calculating R factors, and for tabulation of these values. The procedure outlined above is particularly useful in large calculations. There is just enough space in the detail cards to allow two complete structure-factor calcu-

lations and least-squares reductions. In a large operation this is of considerable importance, since 500 reflections require, in the case of DHC, 10,000 cards in the detail deck.

In order to facilitate the calculation of the two-dimensional Fourier series used in the refinement described in Section E, a special deck of master cards was used, which we shall call the M-D (Master-Detail) deck. The M-D cards are simply detail cards for a normal M card summation over y in 120ths, except that no signs are included for the observed structure factors. The M-D cards are prepared in a straightforward but fairly lengthy operation that requires the use of all of the M deck, including the alternates, since the summation is in 120ths. The M-D deck is then sorted in correct order for the summation over y.

In the calculation of a two-dimensional Fourier series the M-D cards are reproduced to give a set of detail cards, the B deck. The B deck is then collated with the S or sum deck, which contains the F_o values for a particular trial structure, with the S cards in front of the corresponding B cards.* The merged decks are run through the reproducer and the signs of the calculated structure factors are transferred from the S deck to the B deck in a gang punch

*For this procedure the S deck must contain not only the normal indices but also the special ones required for the M card system, since the detail cards do not have the normal indices.

operation. The S cards are sorted from the B deck, and the B cards are then collated with control cards, while in the same operation the alternate detail cards are removed. The B cards are then ready for the summation over y.

The M-D cards are reproduced and the above procedure repeated for each different combination of structure-factor signs for which a Fourier is desired. This method saved considerable time in the refinement of the projected structure of DHC. A complete two-dimensional Fourier could be run in about three hours using the M-D system as outlined.

III

REFERENCES

1. van der Wyk, A. J. A., Misch, L.; Compt. Rend. Soc. Phys. et Hist. Nat. Geneve, 55, 96 (1938).
2. Romers, C.; Acta Cryst., 6, 429 (1953).
3. Ayerst, E. M., Duke, J. R. C.; Acta Cryst., 7, 588 (1954).
4. Cox, E. G., Dougill, M. W., Jeffrey, G. A.; J. Chem. Soc. (1952), 4854.
5. Hendricks, S. B.; Z. Kryst., 91, 48 (1935).
6. Ahmed, F. R., Cruickshank, D. W. J.; Acta Cryst., 6, 385 (1953).
7. Jeffrey, G. A., Parry, G. S.; J. Chem. Soc. (1952), 4864.
8. Jeffrey, G. A., Parry, G. S.; Nature, 169, 1105 (1952).
9. Patterson, A. L.; Z. Kryst., 90, 517 (1935).
10. Wilson, A. J. C.; Acta Cryst., 2, 318 (1949).
11. Howells, E. R., Phillips, D. C., Rogers, D.; Acta Cryst., 3, 210 (1950).
12. Wilson, A. J. C.; Nature, 150, 152 (1942).
13. "Internat. Tabellen z. Bestimmung v. Kryst.", Vol. 2, 571, Gebrüder Borntraeger, Berlin (1935).
14. Giebe, E., Scheibe, A.; Z. Physik, 33, 760 (1925).

15. Howells, E. R., Phillips, D. C., Rogers, D.; Research
(London), 2, 338 (1949).
16. Wiebenga, E. H., Moerman, N. F.; Z. Krist., 99, 217
(1938).
17. Wiebenga, E. H.; J. Am. Chem. Soc., 74, 6156 (1952).
18. Vaughan, P., Donohue, J.; Acta Cryst., 5, 530 (1952).
19. Donohue, J.; J. Phys. Chem., 56, 502 (1952).
20. Pauling, L., Corey, R. B.; Proc. Nat. Acad. Sci., 37,
241 (1951).
21. Elliot, A.; J. Chem. Phys., 20, 756 (1952).
22. Newman, R., Badger, R. M.; J. Chem. Phys., 19, 1147
(1951).
23. Carpenter, G. B., Donohue, J.; J. Am. Chem. Soc., 72,
2315 (1950).
24. Karrer, P., Jucker, E.; "Carotinoide," Verlag Birk-
häuser, Basel (1948).
25. Zechmeister, L.; "Carotinoide," Verlag von Julius
Springer, Berlin (1934).
26. Zechmeister, L.; Chemical Reviews, 34, 267 (1944).
27. Fox, D. L.; Fortschritte der Chemie Organischer
Naturstoffe, 5, 20 (1948).
28. Karrer, P.; Fortschritte der Chemie Organischer
Naturstoffe, 5, 1 (1948).

29. Zechmeister, L.; Harvey Lectures XLVII, Academic Press Inc., New York (1952).
30. Chem. & Eng. News, Reports on Nomenclature, 24, 1235 (1946).
31. Zechmeister, L.; Chem. & Eng. News, 25, 463 (1947).
32. Dyson, G. M.; Chem. & Eng. News, 25, 1766 (1947).
33. Karrer, P., Eugster, C. H.; Compt. Rend., 230, 1920 (1950).
34. Karrer, P., Eugster, C. H.; Helv. Chim. Acta, 33, 443 (1950).
35. Karrer, P., Eugster, C. H.; Helv. Chim. Acta, 33, 1172 (1950).
36. Karrer, P., Eugster, C. H., Tobler, E.; Helv. Chim. Acta, 33, 1349 (1950).
37. Karrer, P., Eugster, C. H.; Helv. Chim. Acta, 33, 1433 (1950).
38. Karrer, P., Eugster, C. H.; Helv. Chim. Acta, 33, 1952 (1950).
39. Karrer, P., Eugster, C. H.; Helv. Chim. Acta, 34, 28 (1951).
40. Karrer, P., Eugster, C. H., Faust, M.; Helv. Chim. Acta, 34, 823 (1951).
41. Karrer, P., Eugster, C. H.; Helv. Chim. Acta, 34, 1805 (1951).

42. Eugster, C. H., Garbers, C., Karrer, P.; Helv. Chim. Acta, 35, 1179 (1952).
43. Garbers, C. F., Eugster, C. H., Karrer, P.; Helv. Chim. Acta, 35, 1850 (1952).
44. Garbers, C. F., Eugster, C. H., Karrer, P.; Helv. Chim. Acta, 36, 562 (1953).
45. Garbers, C. F., Karrer, P.; Helv. Chim. Acta, 36, 828 (1953).
46. Eugster, C. H., Garbers, C. F., Karrer, P.; Helv. Chim. Acta, 36, 1378 (1953).
47. Garbers, C. F., Eugster, C. H., Karrer, P.; Helv. Chim. Acta, 36, 1783 (1953).
48. Pictet, G., Karrer, P.; Helv. Chim. Acta, 37, 1721 (1954).
49. Inhoffen, H. H., Bohlmann, F.; Fortschritte der Chemischen Forschung, 1, 175 (1949).
50. Inhoffen, H. H., Bohlmann, F., Bartram, K.; Ann., 561, 13 (1948).
51. Inhoffen, H. H., Pommer, H., Bohlmann, F.; Ann., 561, 26 (1948).
52. Inhoffen, H. H., Bohlmann, F., Bohlmann, M.; Ann., 565, 35 (1949).
53. Inhoffen, H. H., Bohlmann, F.; Ann., 565, 41 (1949).
54. Inhoffen, H. H., Pommer, H., Meth, E. G.; Ann., 565, 45 (1949).

55. Inhoffen, H. H., Bohlmann, F., Bohlmann, M.; Ann., 568, 47 (1950).
56. Inhoffen, H. H., Pommer, H., Winkelmann, K.; Ann., 568, 174 (1950).
57. Inhoffen, H. H., Pommer, H., Meth, E. G.; Chem. Ztg., 74, 211 (1950).
58. Inhoffen, H. H., Pommer, H., Meth, E. G.; Ann., 569, 74 (1950).
59. Inhoffen, H. H., Bohlmann, F., Rummert, G.; Ann., 569, 226 (1950).
60. Inhoffen, H. H., Bohlmann, F., Bartram, K., Pommer, H.; Chem. Ztg., 74, 285 (1950).
61. Inhoffen, H. H., Pommer, H., Bohlmann, F.; Chem. Ztg., 74, 309 (1950).
62. Inhoffen, H. H., Bohlmann, F., Bartram, K., Pommer, H.; Abhandl. Braunschweig. Wiss. Ges., 2, 75 (1950).
63. Inhoffen, H. H., Pommer, H., Bohlmann, F.; Ann., 569, 237 (1950).
64. Inhoffen, H. H., Bohlmann, F., Bartram, K., Rummert, G., Pommer, H.; Ann., 570, 54 (1950).
65. Inhoffen, H. H., Pommer, H., Westphal, F.; Ann., 570, 69 (1950).
66. Inhoffen, H. H., Bohlmann, F., Linhoff, G.; Ann., 570, 73 (1950).
67. Inhoffen, H. H., Bohlmann, F., Rummert, G.; Ann., 571, 75 (1951).

68. Inhoffen, H. H., Pommer, H., Meth, E. G.; Ann., 572, 151 (1951).
69. Inhoffen, H. H., Bohlmann, F., Aldag, H. J.; Angew. Chem., 63, 146 (1951).
70. Inhoffen, H. H., Bohlmann, F., Aldag, H. J., Bork, S., Leibner, G.; Ann., 573, 1 (1951).
71. Inhoffen, H. H.; Naturwiss., 38, 478 (1951).
72. Inhoffen, H. H., Leibner, G.; Ann., 575, 105 (1952).
73. Inhoffen, H. H., Arend, W.; Ann., 578, 177 (1952).
74. Inhoffen, H. H., Bork, S., Schwieter, U.; Ann., 580, 1 (1953).
75. Inhoffen, H. H., Isler, O., von der Bey, G., Raspé, G., Zeller, P., Ahrens, R.; Ann., 580, 7 (1953).
76. Inhoffen, H. H., von der Bey, G.; Ann., 583, 100 (1954).
77. Inhoffen, H. H., Siemer, H., Möhle, K. D.; Ann., 585, 126 (1954).
78. Inhoffen, H. H., Krause, H. J., Bork, S.; Ann., 585, 132 (1954).
79. Inhoffen, H. H., Schwieter, U., Raspé, G.; Ann., 588, 117 (1954).
80. Inhoffen, H. H., Siemer, H.; Fortschritte der Chemie Organischer Naturstoffe, 9, 1 (1952).
81. Polgár, A., Zechmeister, L.; J. Am. Chem. Soc., 64, 1856 (1942).

82. Pauling, L.; Fortschritte der Chemie Organischer
Naturstoffe, 3, 203 (1939).
83. Oroshnik, W., Karmas, G., Mebane, A. D.; J. Am. Chem.
Soc., 74, 295 (1952).
84. Karrer, P., Schwyzer, R., Neuwirth, A.; Helv. Chim.
Acta, 31, 1210 (1948).
85. Elvidge, J. A., Linstead, R. P., Sims, P., Orkin, B. A.;
J. Chem. Soc. (1950), 2235.
86. Elvidge, J. A., Linstead, R. P., Sims, P.; J. Chem.
Soc. (1951), 3386.
87. Elvidge, J. A., Linstead, R. P., Sims, P.; J. Chem.
Soc. (1951), 3398.
88. Pauling, L.; Helv. Chim. Acta, 32, 2241 (1949).
89. Wallcave, L.; "Thesis", California Institute of
Technology (1953).
90. Zechmeister, L., Polgár, A.; J. Am. Chem. Soc., 65,
1522 (1943).
91. Zechmeister, L., LeRosen, A. L., Schroeder, W. A.,
Polgár, A., Pauling, L.; J. Am. Chem. Soc., 65, 1940
(1943).
92. Mulliken, R. S.; J. Chem. Phys., 7, 121 (1939).
93. Mulliken, R. S.; J. Chem. Phys., 7, 364 (1939).
94. Pauling, L., Proc. Nat. Acad. Sci., 25, 577 (1939).
95. Lewis, G. N., Calvin, M.; Chem. Rev., 25, 273 (1939).

96. Pauling, L.; "The Nature of the Chemical Bond,"
Cornell Univ. Press, Ithica, New York (1948).
97. Pauling, L., Sherman, J.; J. Chem. Phys., 1, 606
(1933).
98. Pauling, L., Sherman, J.; J. Chem. Phys., 1, 679
(1933).
99. Wheland, G. W.; J. Chem. Phys., 2, 474 (1934).
100. Lennard-Jones, J. E.; Proc. Roy. Soc., A-158, 280
(1937).
101. Lennard-Jones, J. E., Turkevich, J.; Proc. Roy. Soc.,
A-158, 297 (1937).
102. Penney, W. G.; Proc. Roy. Soc., A-158, 306 (1937).
103. Penney, W. G., Kynch, G. J.; Proc. Roy. Soc., A-164,
409 (1938).
104. Coulson, C. A.; Proc. Roy. Soc., A-169, 413 (1939).
105. Coulson, C. A.; J. Chem. Phys., 7, 1069 (1939).
106. Lennard-Jones, J. E., Coulson, C. A.; Trans. Faraday
Soc., 35, 311 (1939).
107. Hengstenberg, J., Kuhn, R.; Z. Krist., 75, 301 (1930).
108. Hengstenberg, J., Kuhn, R.; Z. Krist., 76, 174 (1931).
109. Waldmann, H., Brandenberger, E.; Z. Krist., 82, 77
(1932).
110. Taylor, W. H.; Z. Krist., 96, 150 (1937).

111. Lindlar, H.; Helv. Chim. Acta, 35, 446 (1952).
112. Oroshnik, W., Karmas, G., Mebane, A. D.; J. Am. Chem. Soc., 74, 3807 (1952).
113. Campbell, K. N., Campbell, B. K.; Chem. Revs. 31, 148 (1942).
114. MacGillivray, C. H., Kreuger, A., Eichhorn, E. L.; Proc. Koninkl. Ned. Akad. Wetenschap., B54, No. 5 (1951).
115. Allen, P. W., Sutton, L. E.; Acta Cryst., 3, 46 (1950).
116. Hoerni, J. A., Ibers, J. A.; Acta Cryst., 7, 744 (1954).
117. Lonsdale, K.; Proc. Roy. Soc., A-123, 494 (1929).
118. Robertson, J. M., White, J. G.; J. Chem. Soc. (1945), 607.
119. James, R. W.; "The Optical Principles of the Diffraction of X-Rays," G. Bell and Sons Ltd., London (1950).
120. Lipson, H., Cochran, W.; "The Determination of Crystal Structures," G. Bell and Sons Ltd., London (1953).
121. Wiebenga, E. H.; Z. Krist., 102, 193 (1940).
122. Lange, N. A.; "Handbook of Chemistry," pages 378 and 580, Handbook Publishers, Inc., Sandusky, Ohio (1949).
123. Brockway, L. O., Robertson, J. M.; J. Chem. Soc. (1939), 1324.

124. Rogers, D., Wilson, A. J. C.; Acta Cryst., 6, 439 (1953).
125. Douglas, A. S., Woolfson, M. M.; Acta Cryst., 7, 517 (1954).
126. Parry, G. S.; Acta Cryst., 7, 313 (1954).
127. Knott, G.; Proc. Phys. Soc., 52, 229 (1940).

IV

PROPOSITIONS

1. The presence or absence of pyroelectric behavior is often of considerable importance in the determination of crystal space groups. It is suggested that measurements of hydrostatic piezoelectricity might provide a more quantitative indication of the symmetry properties of crystals than the methods usually used for this purpose.

2. It is proposed that a suitable electronic device can be constructed to synthesize the visual curves used in electron diffraction structural work. It would be possible to use frequency and amplitude factors obtained either from Fourier integral transforms of visual curves or from proposed trial structures. The effects of small variations in interatomic distances would be quickly and easily observed. (Maxwell R.SI, 11, 47-54, 1940; Shimuza et al, RSI 21, 779, 1950; Pepinsky, JAPP 18, 601, 1947.)

3. The following projects for structural analysis are proposed:

a) Structural investigation of the compounds disiloxane, hexamethyldisiloxane and hexachlorodisiloxane might provide some worthwhile data on the bond angle Si-O-Si in the siloxanes. This value seems to be somewhat in doubt with reported values in the range 125-160 degrees. (Flory

et al, JACS 74, 3364) A value of 150° is reported for this angle in low cristobalite. (Niewenkamp Zeit.Kr. 92, 82, 1935 and 96, 454, 1937) Work on some of the cyclic siloxanes indicates a value of 130° . (Aggarwal and Bauer, J Ch Ph 18, 42, 1951; Harker, Acta Cryst. 1, 34, 1948) Dipole calculations with several assumptions give a value of 160° . (Sauer and Mead, JACS 68, 1794, 1946) On the basis of steric repulsion between methyl groups alone I would favor a value of about 150° for the hexamethyl and hexachloro-compounds. The disiloxane could conceivably have any value in the above range. The bond angle is doubtless fairly flexible because of the high ionic bond character but a study of the above simple compounds would perhaps provide a better answer to the problem.

b) Schomaker, Sheehan and Hedberg have reported a planar structure for the heavy atoms in the compound $(\text{SiH}_3)_3\text{N}$. Electron diffraction studies of similar compounds such as $(\text{SiH}_3)_2\text{NCH}_3$, $\text{SiH}_3\text{N}(\text{CH}_3)_2$, $(\text{Si}(\text{CH}_3)_3)_2\text{NH}$, $(\text{Si}(\text{CH}_3)_3)_2\text{NCH}_3$, $(\text{CH}_3)_2\text{Si}(\text{NHCH}_3)_2$, $(\text{SiCH}_3)_2\text{NH})_3$ and $(\text{Si}(\text{CH}_3)_2\text{NH})_4$ might give further information concerning the Si-N bond and the effects of steric repulsion on the N-Si-N bond angle.

c) Sulfur analogs of a few of the siloxanes have been prepared by the action of silver sulfide on the alkyl-chlorosilanes (Nat. 165, 685, 1950). The compound hexamethylthiosiloxane prepared in this way should be compared with its oxygen counterpart in light of the difference in

structure found for SiO_2 and SiS_2 . The bond angle Si-S-Si found in SiS_2 could hardly be expected to prevail in this compound and a value of about 125° might be reasonable.

The bond length would probably remain about the same

2.14 Å. (Str. Ber. Vol. 3, 286)

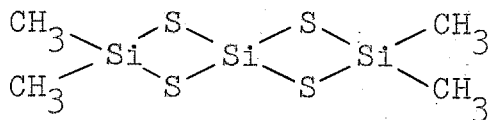
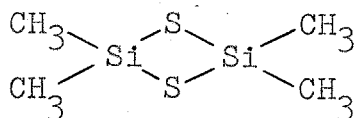
d) Gem dithiols have recently been prepared for the first time by the action of H_2S on aldehydes and ketones at high pressure (JACS 74, 3982, 1952). At least three of the compounds reported methyldithiol, 2,2-propanedithiol, and 1,1-propanedithiol should be quite suitable for electron diffraction work. Perhaps these structures would provide some additional support for the rather large discrepancy (8°) in the bond angle S-C-S found in thioformaldehyde (106.5) and trithioacetaldehyde (114.5). (Acta Cryst. 3, 46-72, 1950) The increase no doubt due in large measure to steric interaction which would be largely absent in the methyl compound and present in the other two compounds.

e) The structure reported (Thesis of Dr. Marsh) for 1,4-diselenane indicates an Se-C bond distance of 2.01 Å. and an angle C-Se-C of 98.6 degrees. Steric repulsion between selenium atoms is suggested as a possible explanation for the long Se-C distance. This report represents the first data for a single bond of this type and further work might prove of some significance. Similar repulsion effects would be expected in the liquid compounds selenocyclobutane,

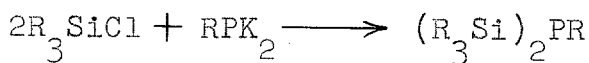
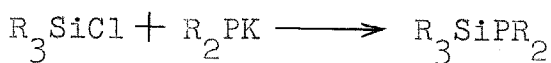
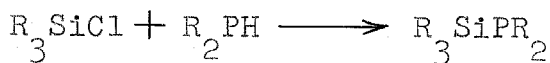
selenocyclopentane and selenocyclohexane. The crystalline compound 2,6-diselenospiro-4-heptane should also provide an interesting project for structural analysis. It is isomorphous with the sulfur analog and it might be possible to make use of heavy atom techniques in the determination of the structure. The crystals are monoclinic however and unless the selenium (sulfur) atoms are in special positions the heavy atom method would be of limited value.

(J Ch Soc. 1929, 1096; 1929, 2197; 1930, 1496; Rec. T R Ch. 56, 492, 1937)

4. The methods used to prepare the thiosiloxanes of 3c should be applied to a dichlorosilane and its mixtures with silicon tetrachloride in an effort to prepare terminated compounds involving the linkages found in SiS_2 . For example



5. It may be possible to prepare the phosphorous analogs of some of the silazines by one of the following reactions. Such compounds are as yet unreported.

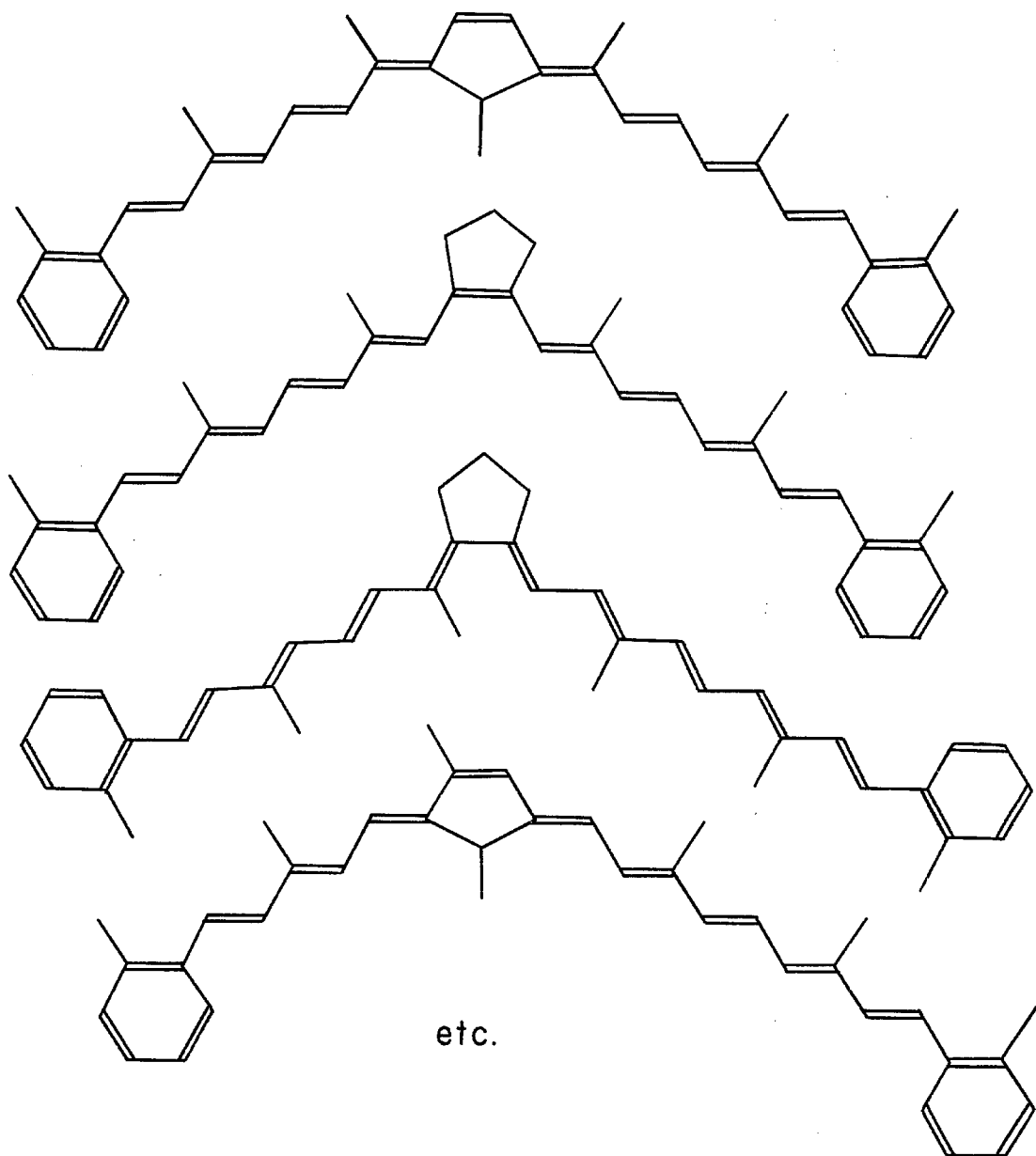
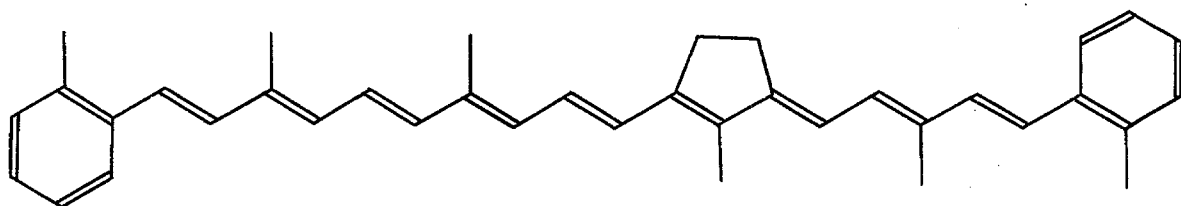
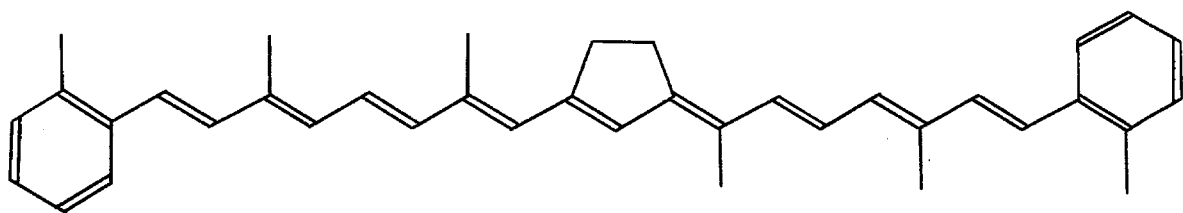


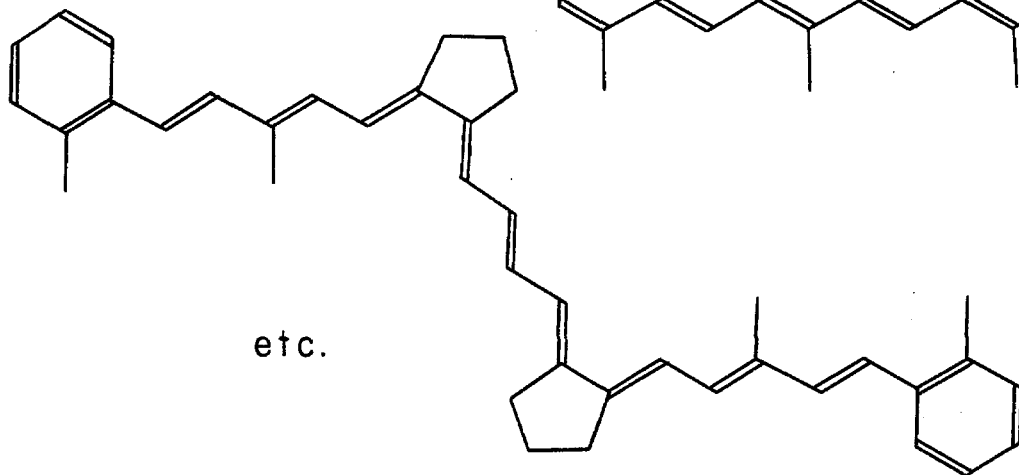
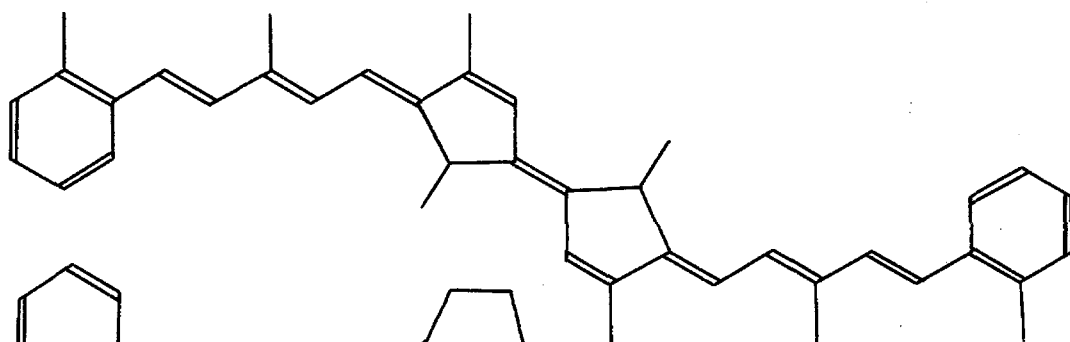
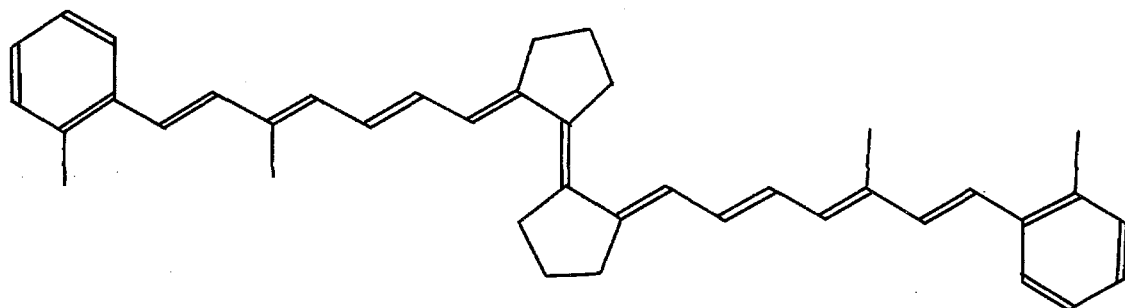
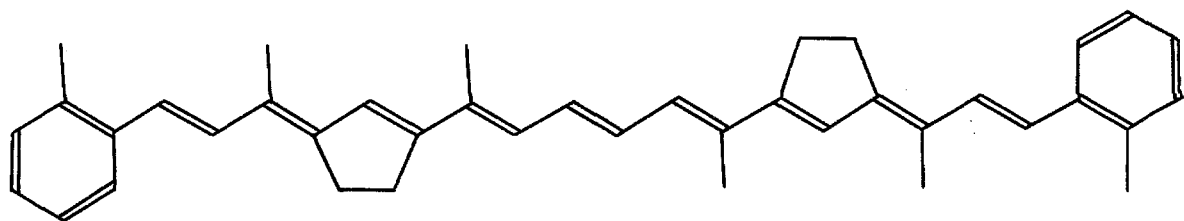
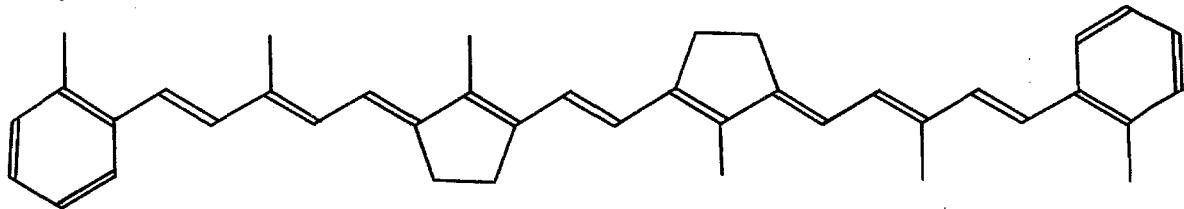
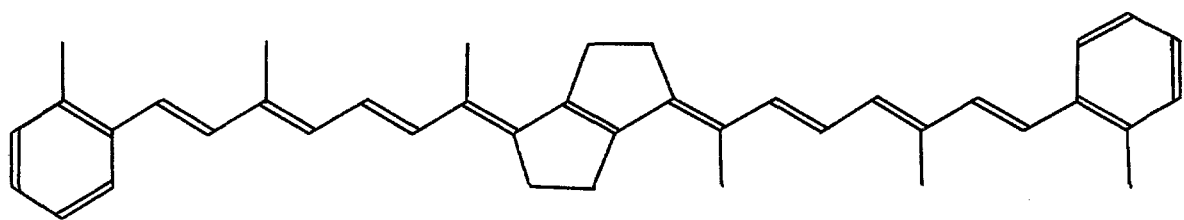
6. Some further insight into the structure of conjugated linear systems could be obtained from a study of the compounds shown on the following pages. These molecules have both trans and cis forms, and some of the latter are cis about single as well as double bonds. The spectral study of these controlled isomers should be helpful in assigning structures to some of the isomeric carotenes and related substances.

7. A modification of the 'M' cards used in Fourier and Patterson summations would make operations with them easier, safer, and in the long run more reliable.

8. Three changes and additions to the 'M' card procedure as outlined by R. A. Pasternak are advocated.

9. The principle of operation and some details of design are proposed for a simple electro-mechanical machine for evaluating bond lengths and bond angles.





etc.

10. Some effort should be directed toward the design and development of a suitable printer that will eliminate the hand plotting of Fourier and Patterson data as obtained from present day computing equipment. Rough design specifications are proposed along with some suggestion as to details of construction.

11. It has been reported (private communication to the author) that the coefficient of friction between fibrous cellulose and solid H_2O is inversely proportional to the force applied normal to the surface, and varies inversely with the size of the crystallites of the solid water. An extensive experimental investigation of this postulate seems advisable.